U.S. Department of Transportation

Slab Track Field Test and Demonstration Program for Shared Freight and High-Speed Passenger Service

Office of Research
and Development
Washington, DC 20590

DOT/FRA/ORD-10/10

Final Report
August 2010

NOTICE

This document is disseminated under the sponsorship of the Department of Transportation in the interest of information exchange. The United States Government assumes no liability for its contents or use thereof.

NOTICE

The United States Government does not endorse products or manufacturers. Trade or manufacturers' names appear herein solely because they are considered essential to the objective of this report.

REPORT DOCUMENTATION PAGE

Form Approved
OMB No. 0704-0188

1. AGENCY USE ONLY (Leave blank)	2. REPORT DATE	3. REPORT TYPE AND DATES COVERED
	August 2010	Technical Report

4. TITLE AND SUBTITLE
Slab Track Field Test and Demonstration Program for Shared Freight and High-Speed Passenger Service

5. FUNDING NUMBERS
RR19/HG272

6. AUTHOR(S)
Dingqing Li

7. PERFORMING ORGANIZATION NAME(S) AND ADDRESS(ES)
U.S. Department of Transportation
Research and Innovative Technology Administration
John A. Volpe National Transportation Systems Center
55 Broadway
Cambridge MA 02142-1093

8. PERFORMING ORGANIZATION REPORT NUMBER
DOT-VNTSC-FRA-10-05

9. SPONSORING/MONITORING AGENCY NAME(S) AND ADDRESS(ES)
U.S. Department of Transportation
Federal Railroad Administration
Office of Research and Development
Washington, DC 20590

10. SPONSORING/MONITORING AGENCY REPORT NUMBER
DOT/FRA/ORD-10/10

11. SUPPLEMENTARY NOTES
COTR: Ted Sussman

12a. DISTRIBUTION/AVAILABILITY STATEMENT
This document is available to the public through the FRA Web site at http://www.fra.dot.gov.

12b. DISTRIBUTION CODE

13. ABSTRACT (Maximum 200 words)

Two types of slab tracks were installed on the High Tonnage Loop at the Facility for Accelerated Service Testing. Direct fixation slab track (DFST) and independent dual block track (IDBT) were installed into a 5-degree curve with 4-inch superelevation. The total slab track test section was 500 feet (ft) long, which consisted of 250 ft of IDBT and 250 ft of DFST. This program was conducted to demonstrate the durability of the slab track for 39-ton axle loads while maintaining the track geometry conditions of a Class 9 track. More specifically, the program was carried out to characterize slab track stiffness conditions, to quantify slab track dynamic responses and long-term performance under heavy axel load train operation, and to provide the test data for validating slab track analysis and design methodologies for shared heavy-freight and high-speed train service.

14. SUBJECT TERMS
Slab track, ballasted track, high-speed train, heavy axle load traffic

15. NUMBER OF PAGES
126

16. PRICE CODE

17. SECURITY CLASSIFICATION OF REPORT	18. SECURITY CLASSIFICATION OF THIS PAGE	19. SECURITY CLASSIFICATION OF ABSTRACT	20. LIMITATION OF ABSTRACT
Unclassified	Unclassified	Unclassified	

NSN 7540-01-280-5500
Standard Form 298 (Rev. 2-89)
Prescribed by ANSI Std. 239-18
298-102

METRIC/ENGLISH CONVERSION FACTORS

ENGLISH TO METRIC	METRIC TO ENGLISH
LENGTH (APPROXIMATE)	**LENGTH (APPROXIMATE)**
1 inch (in) = 2.5 centimeters (cm)	1 millimeter (mm) = 0.04 inch (in)
1 foot (ft) = 30 centimeters (cm)	1 centimeter (cm) = 0.4 inch (in)
1 yard (yd) = 0.9 meter (m)	1 meter (m) = 3.3 feet (ft)
1 mile (mi) = 1.6 kilometers (km)	1 meter (m) = 1.1 yards (yd)
	1 kilometer (km) = 0.6 mile (mi)
AREA (APPROXIMATE)	**AREA (APPROXIMATE)**
1 square inch (sq in, in^2) = 6.5 square centimeters (cm^2)	1 square centimeter (cm^2) = 0.16 square inch (sq in, in^2)
1 square foot (sq ft, ft^2) = 0.09 square meter (m^2)	1 square meter (m^2) = 1.2 square yards (sq yd, yd^2)
1 square yard (sq yd, yd^2) = 0.8 square meter (m^2)	1 square kilometer (km^2) = 0.4 square mile (sq mi, mi^2)
1 square mile (sq mi, mi^2) = 2.6 square kilometers (km^2)	10,000 square meters (m^2) = 1 hectare (ha) = 2.5 acres
1 acre = 0.4 hectare (he) = 4,000 square meters (m^2)	
MASS - WEIGHT (APPROXIMATE)	**MASS - WEIGHT (APPROXIMATE)**
1 ounce (oz) = 28 grams (gm)	1 gram (gm) = 0.036 ounce (oz)
1 pound (lb) = 0.45 kilogram (kg)	1 kilogram (kg) = 2.2 pounds (lb)
1 short ton = 2,000 pounds (lb) = 0.9 tonne (t)	1 tonne (t) = 1,000 kilograms (kg) = 1.1 short tons
VOLUME (APPROXIMATE)	**VOLUME (APPROXIMATE)**
1 teaspoon (tsp) = 5 milliliters (ml)	1 milliliter (ml) = 0.03 fluid ounce (fl oz)
1 tablespoon (tbsp) = 15 milliliters (ml)	1 liter (l) = 2.1 pints (pt)
1 fluid ounce (fl oz) = 30 milliliters (ml)	1 liter (l) = 1.06 quarts (qt)
1 cup (c) = 0.24 liter (l)	1 liter (l) = 0.26 gallon (gal)
1 pint (pt) = 0.47 liter (l)	
1 quart (qt) = 0.96 liter (l)	
1 gallon (gal) = 3.8 liters (l)	
1 cubic foot (cu ft, ft^3) = 0.03 cubic meter (m^3)	1 cubic meter (m^3) = 36 cubic feet (cu ft, ft^3)
1 cubic yard (cu yd, yd^3) = 0.76 cubic meter (m^3)	1 cubic meter (m^3) = 1.3 cubic yards (cu yd, yd^3)
TEMPERATURE (EXACT)	**TEMPERATURE (EXACT)**
[(x-32)(5/9)] °F = y °C	[(9/5) y + 32] °C = x °F

QUICK INCH - CENTIMETER LENGTH CONVERSION

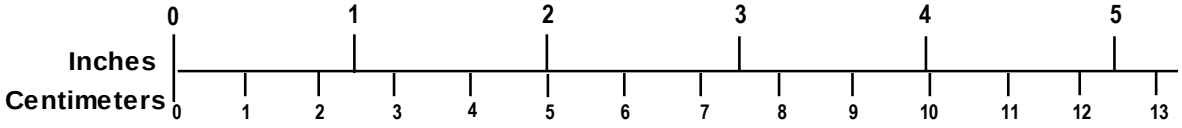

QUICK FAHRENHEIT - CELSIUS TEMPERATURE CONVERSION

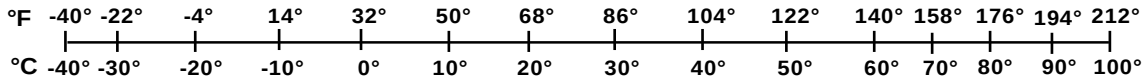

For more exact and or other conversion factors, see NIST Miscellaneous Publication 286, Units of Weights and Measures. Price $2.50 SD Catalog No. C13 10286

Updated 6/17/98

Acknowledgments

This project was jointly funded by the Portland Cement Association (PCA) and the Federal Railroad Administration (FRA) under its Next Generation High-Speed Rail Program. David Bilow of PCA served as the program manager. Donald Plotkin of FRA, Robert McCown, formerly of FRA, and Andrew Sluz and Ted Sussman of the Volpe National Transportation Systems Center provided advice during the test program. Mr. Sluz and Mr. Sussman also served as contracting officer technical representatives for this project.

Guidance and contributions were provided from the expert panel members of the Cooperative Concrete Slab Track Research and Demonstration Program, suppliers, and other PCA and Construction Technology Laboratories personnel, including Steven Chrismer, Nathan Higgins, Richard Lanyi, Mohammad Longi, Nicholas Skoutelas, Jan Zicha, Bernard Sonneville, William Osler, Shiraz Tayabji, Claire Ball, Hamid Lotfi, William Kucera, and Gene Randich.

Transportation Technology Center, Inc. (TTCI), employees Kenneth Laine, Mark White, David Williams, Ira Kalb, Rick Montoya, and Rachel Anaya contributed significantly to the slab track demonstration and testing program. TTCI student intern Matt Aguirre assisted with data reduction and analysis.

Contents

Illustrations

Tables

Executive Summary

Although slab track for high-speed rail (HSR) has been used for decades in Europe and Japan, its use in North America has been limited. With the growth of urban areas and increased congestion on highways and airports, more HSR passenger service may be needed.

In some cases, economic and practical limitations may require passenger and freight trains to share at least some segments of the same tracks and right-of-way (ROW), but conventional track structures may not be adequate for both types of train services. Conventional track structures may not be capable of retaining the tight tolerances required for HSR service while simultaneously withstanding heavy axle load (HAL) freight traffic without incurring excessive rates of track degradation. To address the needs of both types of rail traffic, an alternative track structure may be necessary to ensure adequate stability and reliability.

In 2000, the Portland Cement Association (PCA) initiated a research program entitled Cooperative Slab Track Research and Demonstration Program for Shared Freight and High-Speed Passenger Service. The objective of the program was to advance concrete slab track technology and to demonstrate the capability of slab track to provide a low maintenance and safe track structure for shared HSR and HAL freight on U.S. railroads.

A major part of the cooperative research and demonstration program was the Slab Track Field Testing and Demonstration Program for Shared Freight and High-Speed Passenger Service project, which was carried out from July 2003 to July 2006 by the Transportation Technology Center, Inc. (TTCI), a wholly owned subsidiary of the Association of American Railroads (AAR), in Pueblo, CO. The program was jointly funded by PCA and the Federal Railroad Administration (FRA).

This testing program was undertaken to demonstrate the durability of slab track for 39-ton axle loads while maintaining the track geometry conditions of a Class 9 track. More specifically, the testing program was completed to characterize slab track stiffness conditions, to quantify its dynamic responses and long-term performance under HAL operation, and to provide test data for validating slab track analyses and design methodologies developed for shared HAL freight and HSR service.

In July 2003, two types of slab track—direct fixation slab track (DFST) and independent dual block track (IDBT)—were installed on the High Tonnage Loop (HTL) at the Facility for Accelerated Service Testing (FAST), Transportation Technology Center (TTC), in Pueblo, Colorado. The slab track test section in the HTL is in a 5-degree curve with 4-inch superelevation. The total slab track section is 500 ft long, consisting of 250 ft of IDBT and 250 ft of DFST. The transition from each slab to the ballasted track is in the spiral, from the 5-degree curve to tangent track.

The train at FAST consists of 60–80 39-ton axle load cars and runs on the HTL (2.7 miles (mi)) lap-by-lap at 40 miles per hour (mph). The direction of train traffic is generally 50 percent clockwise (CW) and 50 percent counterclockwise (CCW). In addition, the slab track test section was located in a bypass at FAST, which subjected it to roughly 50 percent of total traffic for the 3 years (yr) of the testing program.

The testing program was concluded in the summer of 2006. For 3 yr, a total of 170 million gross tons (MGT) of HAL traffic was accumulated on the slab track test section, exceeding the target tonnage of 150 MGT. Various measurements were conducted during the 3 yr of testing and monitoring to quantify the slab track responses and performance under HAL train operations. The following sections give the main conclusions drawn from this testing program.

Track Geometry Performance of Slab Track

The slab track test section on the HTL was demonstrated capable of supporting HAL train operations while maintaining the track geometry conditions for Class 9 track. Little track geometry degradation was measured after 3 yr of testing and 170 MGT of accumulated traffic. No track geometry maintenance was required for surface, alignment, gage, or crosslevel of the slab track test section. From the beginning of the testing program until its completion, there was little cumulative settlement and little lateral movement of the slab track.

The surface condition of the slab track was superior to the adjacent ballasted track; however, several spot-tamping operations were done in the transition areas to smooth out cumulative differential track settlement that accumulated in the ballasted transitions.

Slab Track Stiffness Characteristics

When measured after the construction of the slab track test section, the IDBT showed an average track modulus of 3,000 pound/inch/inch (lb/in/in), whereas the DFST showed an average track modulus of 2,100 lb/in/in. These values, especially for the DFST, were lower than originally expected. Extremely resilient rubber boots and pads were used in each slab track design.

During the 3-year period, the increase in track modulus for the DFST was moderate, but the increase for the IDBT was significant. This increase was caused by the gradual deposit of fine sand blowing into spaces between the IDBT components. This was determined during the IDBT inspection in November 2006. This process caused an increase in track modulus by limiting the deflection of the block ties within the rubber boots. Under the action of passing trains, some of the sand in the IDBT was flushed out when mixed with rainwater. This left a fine gray deposit around the block ties. Although the IDBT track modulus increased between 2003 and 2006, the laboratory measured an IDBT pad removed during the inspection, which indicated that the pad stiffness was still within tolerance.

In terms of lateral gage strength, both the IDBT and the DFST slab tracks showed more uniform lateral gage strength or stiffness than the adjacent ballasted track. For the DFST, there was a significant decrease in gage strength in terms of delta gage (delta gage = loaded gage – unloaded gage) measured. From 2 to 169 MGT, delta gage measured under track loading vehicle test loads (33-kilopound vertical wheel load and 18-kilopound lateral wheel load) increased an average of 0.3 to 0.5 in. For the DFST, rubber pads were installed at the rail-slab interface. Extremely resilient pads such as those used in the DFST may be of concern under HAL operations. For the IDBT, little gage strength degradation in terms of delta gage was seen, although unloaded track gage increased an average of 56.8–57.1 in, with the maximum being 57.2 in. Compared with the DFST, the resilience of the rubber boots and pads used in the IDBT

had less influence on gage strength or stiffness because of their location at the tie and slab interface.

Dynamic Wheel/Rail Forces on Slab Track

Because of superior track geometry and resilient pads and boots, the slab track test sections generated lower dynamic vertical and lateral wheel loads than the ballasted track test section of the same curvature and speed superelevation. The maximum vertical load generated in the slab track was 58 kilopounds (kip) as compared with 73 kip generated on the ballasted track with the same curvature and speed superelevation. The maximum lateral wheel load generated in the slab track was 20 kip as compared with 24 kip in the ballasted track. Note, the slab track test section, located in a 5-degree curve with 4-inch superelevation, is underbalanced at the nominal train operating speed of 40 mph on the HTL; for example, higher vertical wheel loads are applied on the high rail than on the low rail.

Slab Track Deflection Response

Slab track deflection occurred primarily between the rail and the concrete slabs due to the resilient pads (DFST) or rubber boots/pads (IDBT). Only a small amount of deformation was recorded from the underlying subbase and subgrade layers.

Higher dynamic wheel loads and lower track stiffnesses correspond to larger rail-to-slab deflections regardless of the slab track type. For the DFST, the maximum vertical rail-to-slab deflection was 0.25 in and the maximum lateral rail-to-slab deflection was 0.1 in, both recorded on the high rail. For the IDBT, the maximum vertical rail-to-slab deflection was 0.15 in and the maximum lateral rail-to-slab deflection was 0.07 in, again measured on the high rail.

For the DFST from 2003 to 2006, little increase in vertical rail-to-slab track deflection was measured. However, an increasing trend was observed of lateral rail-to-slab deflection, which appeared consistent with the trend of decreasing gage strength for the DFST. For the IDBT from year 2003 to 2006, the general trends for both vertical and lateral rail-to-slab deflections measured were decreasing, particularly for the deflections measured on the high rail. These results appear to be consistent with the increase in track stiffness for the IDBT slab track.

Subgrade Pressure and Deformation under Slab Track

The maximum subgrade pressure generated under HAL vehicles was 12 pounds per square inch (psi), well below the compressive strength of the subgrade soil at the test site (above 50 psi). The relatively low subgrade pressure with respect to the soil strength explains the small amount of subgrade deformation generated under the HAL train operation. Under the slab track test section, the maximum deformation recorded in the subbase or subgrade was less than 0.06 in.

Vibration Attenuation

In the slab track test section, vibration attenuation was achieved using rubber pads (DFST) or rubber boots/pads (IDBT). The vibration measurements showed significant vibration attenuation from the rail to the slab regardless of slab track type. Under HAL train operations at 40 mph, the maximum acceleration recorded on the rails ranged between 10 and 25g (absolute value)

whereas the maximum acceleration recorded on the slab ranged between 0.4 and 2g (absolute value). On average, attenuation was achieved by a factor of 20.

Vibration measured on the rails showed no obvious trend between the transitions and the slab tracks as well as between high and low rails. Analysis of vibration attenuation in frequency domain showed the attenuation of vibration energy across the entire spectrum.

Slab Track Construction

Design of slab track must adequately account for geologic variations that affect the support of the structure. Neither slab track nor ballasted track can bridge or span variations in track support like that of a bridge. State of the art ballasted track design procedures require similar data on local soil conditions and geology, so this should not be viewed as an additional cost of slab track over ballasted track, but rather the cost of building a structure to reduce life-cycle cost by reducing future maintenance expense. In a similar manner, the subgrade stabilization completed as part of this test should also be conducted for the construction of a state of the art ballasted track.

Slab track construction challenges range from tight tolerances of 1/8 in required to achieve the desired track Class 9 compliance, to environmental challenges associated with expansion/contraction of the rail. Rail bracing to fight rail movement from expansion and contraction was found to be a critical element during the construction of the slab track. Adequate bracing was found to be the only way to maintain rail position. An attempt to use white paint to reduce the thermal gain of the rail was not found to be effective.

Other Performance Parameters

No rail defect was recorded in the slab track test section for a total of 170 MGT of HAL traffic, nor was any weld defect or failure reported for the 14 thermite welds used. For comparison purposes, the average weld life in similar 5-degree curves of the HTL is approximately 80 MGT. In addition, only a small amount of rail wear and no corrugation were observed in the test sections.

Recommendations

The slab track test section remains in the HTL, and it is planned to remain in track until a reason to remove the slab exists, such as a new test, performance problems, or any other concern. As the slab track test section continues to be subjected to HAL train operations, it is recommended that its performance monitoring continue in terms of track geometry conditions. Future gage strength testing is also recommended to determine if gage strength of the DFST may further degrade under HAL. Testing of rubber boots or pads in either IDBT or DFST slab for a possible temperature increase under train operation or a change of resilient property over time may provide further insight regarding their eventual life under HAL train operation. Finally, the recommendation is that a test section of slab track be installed in revenue service with shared heavy freight and HSR operations.

1. Introduction

1.1 Background

Although slab track for HSR has been used for decades in Europe and Japan, its use in the United States has been limited. Additional HSR passenger service may be needed in North America as urban areas grow and congestion on highways and airports increases. In some cases, economic and practical limitations may require passenger and freight trains to share at least some segments of the same tracks and ROW. Conventional track structures, however, may not be adequate for both types of train services.

Conventional track structures may not be capable of retaining the tight tolerances required for HSR service while simultaneously withstanding HAL freight traffic without incurring excessive rates of track degradation. To address the needs of both types of rail traffic, an alternative track structure may be necessary to ensure adequate stability and reliability.

In 2000, the Portland Cement Association (PCA) initiated a research program entitled Cooperative Slab Track Research and Demonstration Program for Shared Freight and High-Speed Passenger Service. The objective of the program was to demonstrate concrete slab performance under HAL load with Class 9 standards. The research program was planned and carried out in the following three phases:

Phase 1: Literature review, development of design methodology, and life-cycle cost study. As a result of the Phase 1 study (Tayabji and Bilow, 2001), the DFST and the IDBT forms were selected for full-scale laboratory and field demonstration tests. Phase 1 was completed by PCA and its subsidiary, Construction Technology Laboratories (CTL).

Phase 2: Laboratory demonstration tests of slab track. Phase 2 demonstrated the ability of DFST and IDBT in a laboratory environment to pass the stress and fatigue tests required for 39-ton axle loads (Ball, 2004). Phase 2 was completed by CTL.

Phase 3: Field slab track demonstration tests from July 2003 to July 2006. Tests were funded primarily by FRA and conducted at TTC in Pueblo, Colorado, by TTCI. Phase 3 was completed by PCA, FRA, and TTCI.

This report summarizes the results and findings of Phase 3.

1.2 Objective

An extensive slab track testing program was designed and started in July 2003 on the HTL at the TTC's FAST. The target tonnage for the 3-year testing program was 150 MGT, but the actual accumulated total tonnage at the end of July 2006 was 170 MGT. During the 3 yr of testing and monitoring, various measurements were conducted to demonstrate the durability of the slab track for 39-ton axle loads while maintaining the track geometry conditions of a Class 9 track. More specifically, the testing program was designed to:

- Quantify slab track performance
- Quantify the actual load environment and the corresponding vibration behavior of the slab track
- Quantify stress and deformation behaviors of individual slab track and subgrade components
- Quantify slab track stiffness characteristics

As part of the slab track demonstration and testing program, the project was also intended to:

- Demonstrate that a slab track can be built to HSR track tolerances (Class 9 track)
- Validate the slab track design procedures developed in Phase 1 and the laboratory tests completed in Phase 2 (this task was completed by PCA and CTL)

1.3 Approach

The testing program was designed to achieve the previously stated objectives and included static and dynamic measurements and both short- and long-term monitoring. Some measurements were conducted using onboard transducers on test vehicles while other measurements were performed using transducers installed in the slab track (wayside transducers). The following is a list of measurements and monitoring conducted throughout the testing program:

- Track geometry and track geometry change over time
- Vertical track modulus and stiffness
- Lateral track gage strength
- Dynamic vehicle/track interaction in terms of wheel/rail forces measured via instrumented wheelsets (IWS)
- Vertical and lateral rail forces measured using wayside load station
- Rail-to-slab vertical and lateral deflections
- Vertical deformation in slab, subbase, and subgrade

- Subgrade pressure
- Vibration attenuation from rail to slab
- Rail bending strain, strains of slab surface, and steel reinforcement bars
- Maintenance records

1.4 Scope

The slab track test section in the HTL is in a 5-degree curve with 4-inch superelevation. The total slab track section is 500 ft long, including 250 ft of the IDBT and 250 ft of the DFST. The transition from each slab track to the ballasted track is in a spiral from the 5-degree curve to the tangent.

Although the 500-foot slab track test section was designed, constructed, and maintained as Class 9 track, the transitions and the rest of the HTL are Class 4 track. The slab track test section represented a track condition considered severe for Class 9 track because Class 9 track would generally not be built in a 5-degree curve and its proximity to Class 4 track was a factor. In addition, a 36-ton axle load is considered HAL in revenue service on North American railroads whereas the nominal axle load of the train operating on the HTL at FAST is 39 tons. Although not the focus of this testing, performance of fasteners was examined as necessary for slab track.

In this report, the results, discussions, and conclusions presented are based on the testing of the slab track for the duration of 3 yr (July 2003–July 2006) and for a total accumulated traffic of 170 MGT. At the time of this writing, the slab will remain in track until a reason to remove it develops, such as new testing space needs, operational safety, or another concern or need develops.

2. Design and Construction of Slab Track Test Section

2.1 HTL and Load Environment

2.1.1 HTL and Section 38

The HTL is located at FAST and is one of the several tracks used at TTC for advanced testing. Figure 1 shows the HTL and other test tracks at TTC.

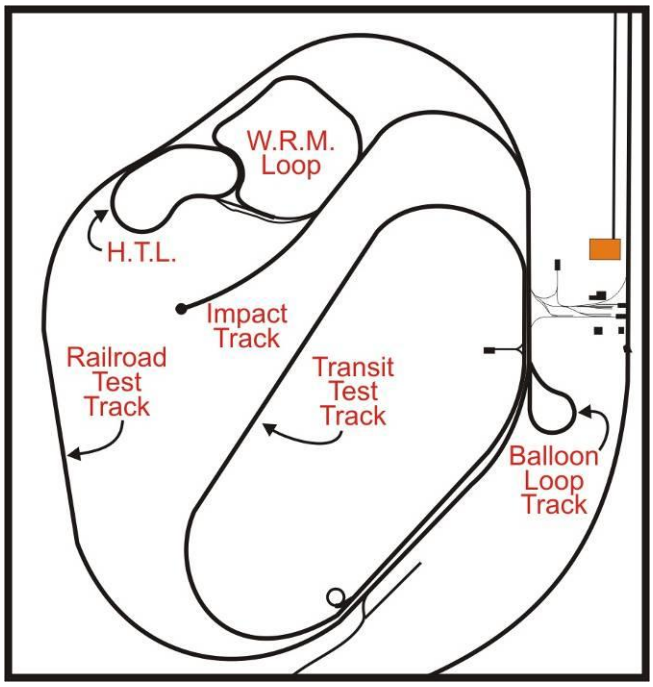

Figure 1. Test Tracks at TTC

The HTL is a test loop 2.7 mi long and is used primarily for track component reliability, wear, and fatigue research under HAL traffic. As Figure 2 shows, the HTL is divided into test sections, which generally correspond to tangents, spirals, curves (three 5-degree curves and one 6-degree curve), and turnouts. Several experiments are currently being conducted in this loop, such as rail performance, weld performance, evaluation of ties and fasteners, frogs, turnouts, ballast, and subgrade.

The slab track test section has a 5-degree curve with 4-inch superelevation and is located in the bypass track in Section 38. Section 38 is approximately 510 ft long. Section 37 and Section 39 are adjacent to Section 38 and are in spirals to the tangents. The two transitions from the slab to the ballasted track are located in these two spirals. Note, Section 31 and Section 7 of the HTL have the same curvature and superelevation as Section 38 and are used for comparisons as ballasted track with Section 38, including the slab track. As ballasted track, Section 31 has mixed concrete and wood ties whereas Section 7 has only wood ties.

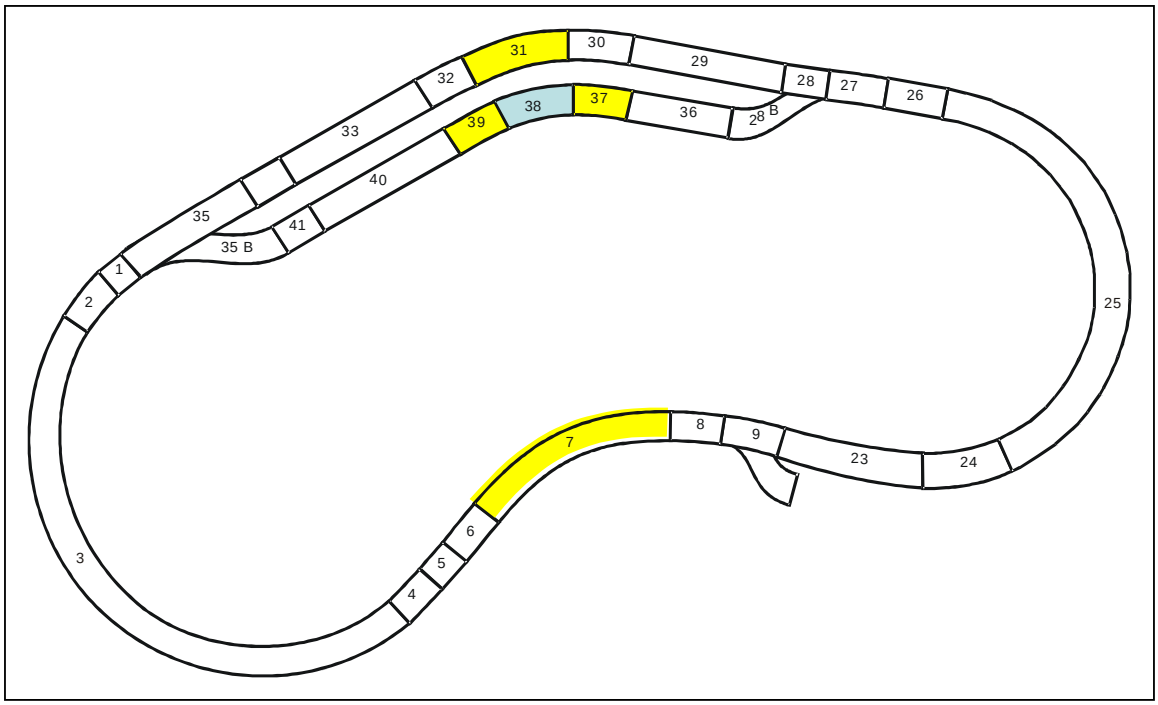

Figure 2. Tonnage Loop (Slab Track in Section 38)

2.1.2 Operation and Load Environment at FAST

Figure 3 shows the test train at FAST running through the slab track test section on the HTL. The train at FAST generally consisted of three or four locomotives and 60–80 loaded freight cars. Each car weighed 315,000 lb. The nominal axle load of the freight cars is 39 tons, whereas the nominal axle load of the locomotives is 32 tons. Axle spacing is 72 in for the freight cars and 108 in for the locomotives. The train runs at a nominal speed of 40 mph and generally operates from late night to early morning of the next day, accumulating approximately 1 MGT each night. The lapse time between the last freight car and the first locomotive is roughly 2.3 min. Depending on the annual operating budget provided by the AAR and FRA, trains at FAST generate 100–150 MGT per year, with roughly a 50/50 split between traffic on the mainline and the bypass during the 3 yr of the slab track testing program (July 2003–July 2006). Additionally, the traffic at FAST is scheduled such that approximately 50 percent is accumulated with the train running CW, while the other 50 percent is accumulated with the train running CCW.

In addition to the HAL trains at FAST, short test trains (consists) are often put together with several HAL freight cars and an instrumentation coach car. These short test trains are intended for various testing purposes and experiments within the FAST program.

Figure 3. FAST HAL Train Running on the HTL

Figure 4 shows the distributions of vertical and lateral wheel loads recorded in the HTL by using IWS installed under a freight car at FAST. Figure 5 shows the results recorded for Section 38. These results were recorded before the slab track was built into this section. Section 5 describes how the IWS technology is used to measure wheel and rail forces. The results shown in Figure 4 and Figure 5 were obtained at 40 mph in both the CW and CCW directions and were part of the load environment data provided to PCA and CTL for analysis and design of the slab track test section in the HTL.

The distributions of wheel loads shown in these two figures provide a range of wheel loads—the maximum and minimum wheel loads that are generated under 39-ton axle loads. For example, in Section 38, vertical wheel loads varied between 15 and 70 kip, while lateral wheel loads varied between -5 and 30 kip. More importantly, these distribution results indicate how often each load level would occur in the HTL or Section 38. For example, in Section 38, when the train operated in the CW direction, the median vertical wheel load on the high rail (outside rail) was 43 kip while the medium vertical wheel load on the low rail (inside rail) was 35 kip. Note, at 40 mph with 4-inch superelevation, Section 38 has a 2-inch underbalanced condition, meaning more vertical load would be carried on the high rail than on the low rail.

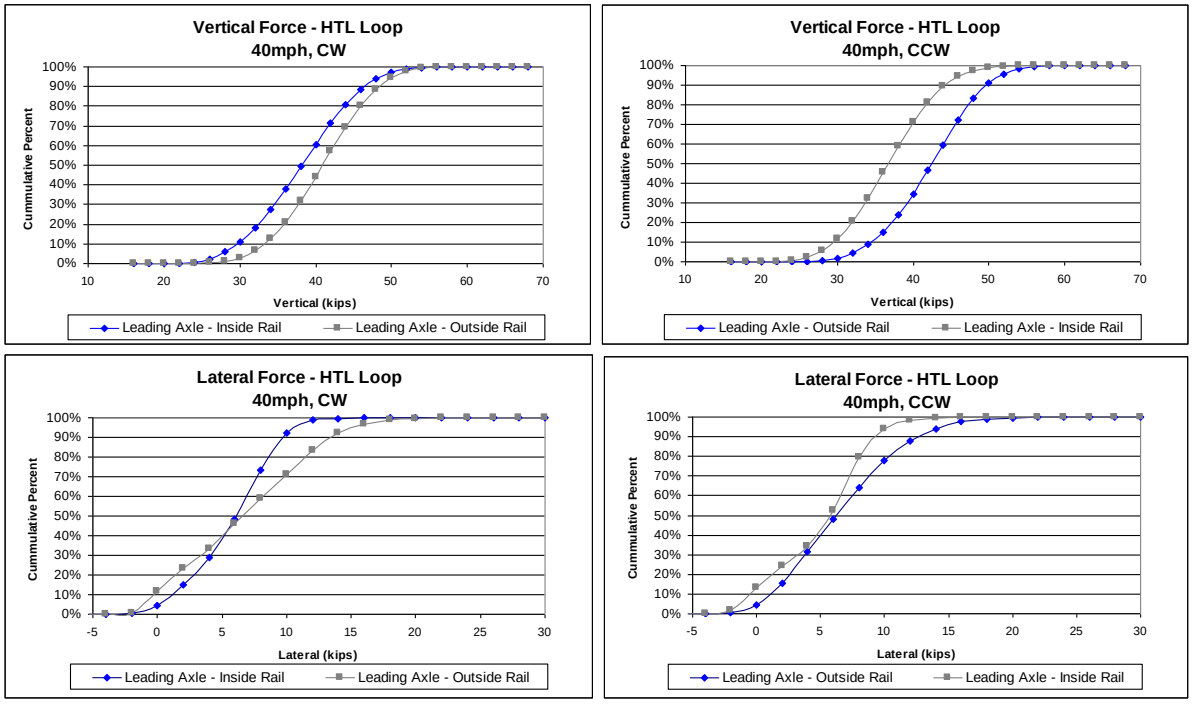

Figure 4. Distribution of Vertical and Lateral Wheel Loads in the HTL

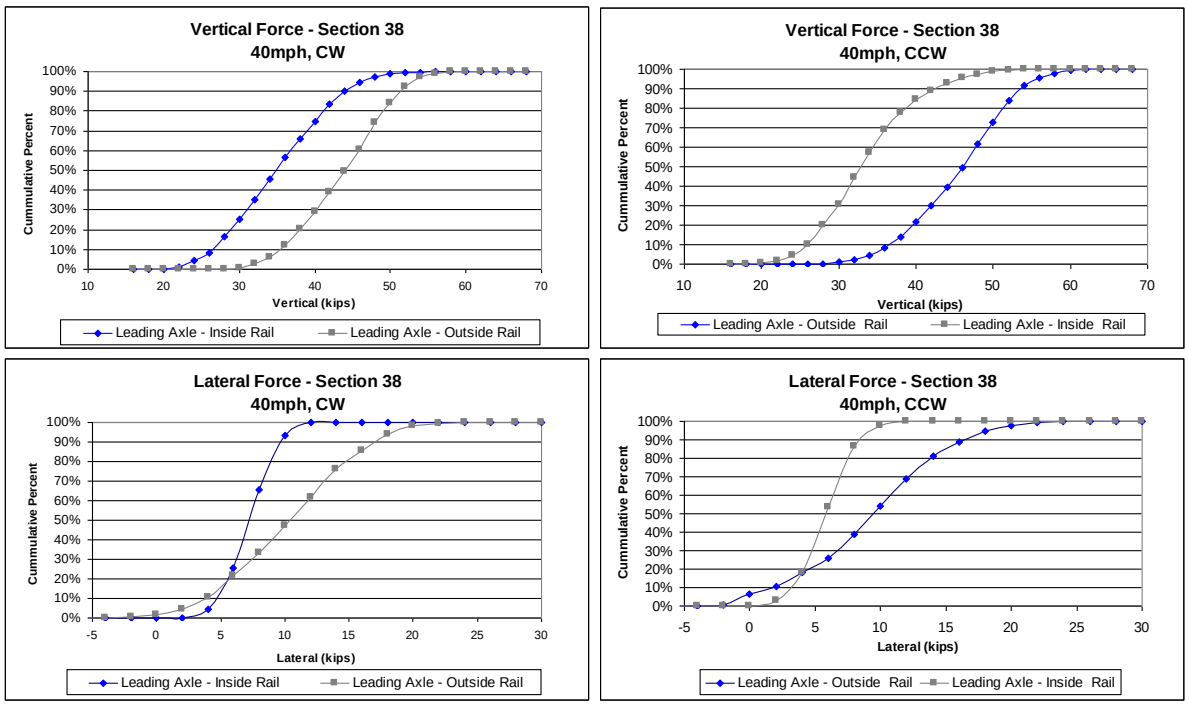

Figure 5. Distribution of Vertical and Lateral Wheel Loads in Section 38

2.2 Design and Construction of Slab Track Test Section

Although the focus of this report is on the performance testing of the slab track, this section gives a description of the design and construction of the slab track in the HTL. Additional information about the design and construction of the slab track can be found in the following references:

- Kucera et al., 2003
- Lotfi and Oesterle, 2005
- Bilow and Li, 2005

2.2.1 Slab Track Design and Construction

PCA and CTL (Lotfi and Oesterle, 2005) completed the design of the slab track test section, including structural analysis, concrete mix design, slab profile, and reinforcing design. TTCI designed the actual layout of the test section based on the existing alignment and grade conditions of Section 38.

Figure 6 shows the overall plan view of the slab track test section in the HTL. As shown, this test section is located in Section 38 (bypass) and includes 250 ft of the IDBT slab track and 250 ft of the DFST slab track. The 250-foot length for each slab was regarded as sufficient to ensure that the wayside instrumentation (Sections 5–9) located near the middle of each slab would not be impacted by the effect of adjacent ballasted tracks. As mentioned earlier, Section 38 is a 5-degree curve and has a 4-inch superelevation. At the end of the IDBT and the DFST, a 25-foot transition zone was installed between the slab track and the existing ballasted track.

Figure 6 also shows the typical cross-sections of the DFST and the IDBT. The rails are fastened directly to the slab on the DFST, which is supported on a 6-inch layer of soil cement[1] subbase and the underlying subgrade. The rails are supported by two independent block ties on the IDBT that are supported by the slab, the soil cement subbase, and the subgrade. The Amtrak Construction Standards for Class 9 Track (with an allowable speed of 200 mph) were used for the construction of the slab track test section. More specifically, the following tolerances were used for the construction of the slab track in the HTL:

- Surface limit (deviation at midordinate of 62-foot chord) 1/8 in
- Deviation in crosslevel 1/8 in
- Alignment limit (deviation at midordinate of 62-foot chord) 1/8 in
- Gage limit +1/16–3/32 in

[1] See Subbase for a definition of *soil cement*.

To meet the tight construction tolerances, a top-down construction method was used for the installation of the slab track test section. The top-down construction procedure requires establishing the accurate position (alignment, gage, surface, and crosslevel) of the rails to the tolerances listed above, then building the rest of the track from the rails down to the fastening and to the casting of the reinforced concrete slab on the prebuilt soil cement subbase and subgrade. In the succeeding sections, descriptions are given regarding how each component of the slab track, including subgrade, subbase, IDBT, and DFST concrete slab were built. Additional information can be found in a paper by Kucera et al. (2003).

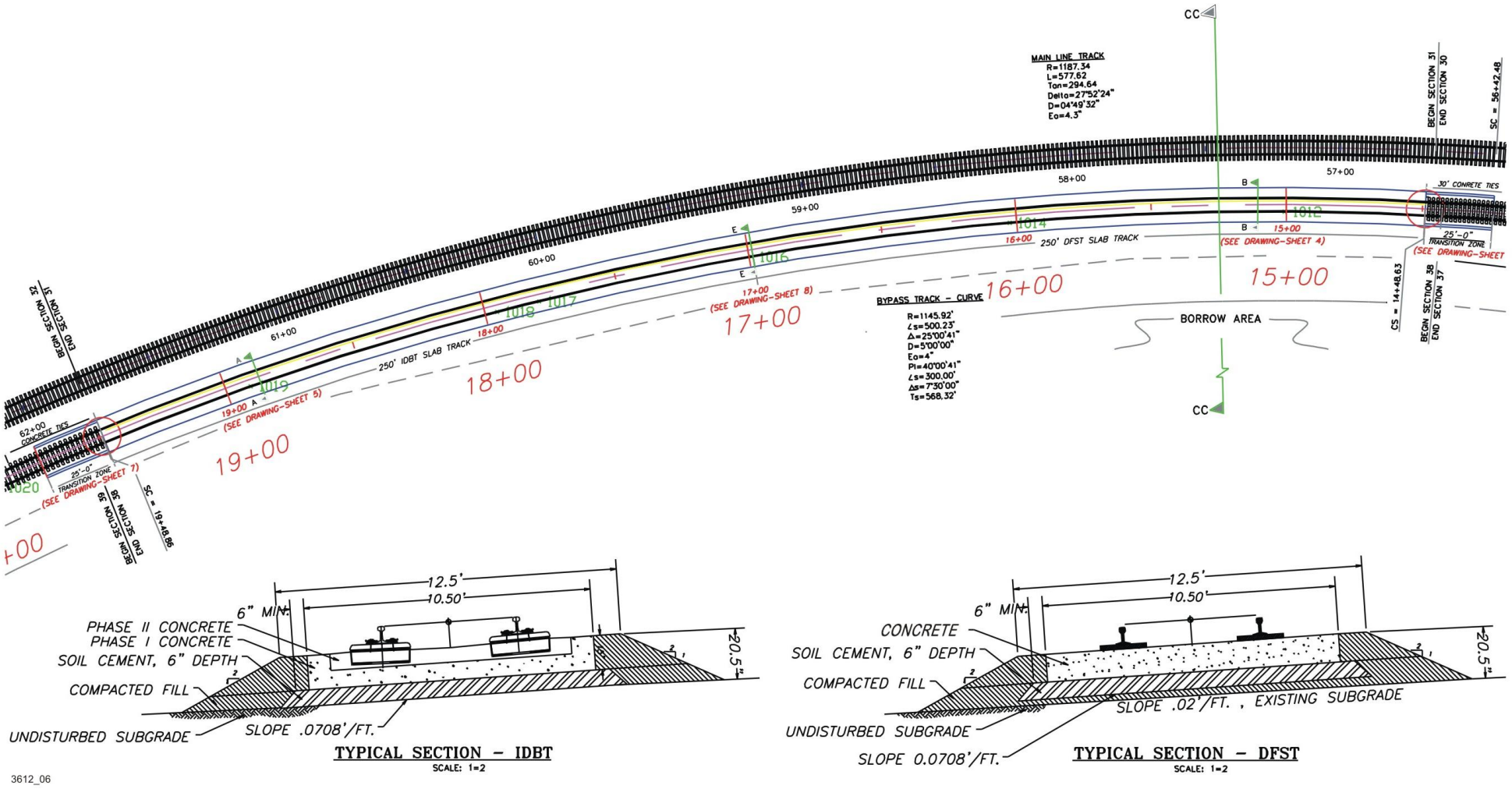

Figure 6. Slab Track Plan and Details

2.2.2 Subgrade

To prepare for the slab track construction, the existing ballasted track was removed. The subgrade was then graded to the proper line and elevation. The subgrade soil consists of silty sand (PI = 5.9, LL = 18.5). Soil moisture content varied between 5 and 12 percent. The surface of the subgrade was recompacted at an optimum moisture content of 10.5 percent. The modulus of the soil was above 10,000 psi with compressive strength above 50 psi. The subgrade soil was considered as strong as track foundation support. Figure 7 shows the final prepared subgrade surface. Note, from the IDBT to the DFST, the subgrade has a slight downhill grade (0.4 percent).

Figure 7. Subgrade Surface for Slab Track Test Section

2.2.3 Subbase

The subbase is a 6-inch soil cement layer. This layer was installed by mixing 5 percent of cement (based on soil weight) with the soil from the borrow area (the same silty sand) and was compacted at an optimum moisture content of 12.5 percent. Compaction was specified to be 98 percent of the maximum (modified Proctor), with the maximum being 118 pounds per cubic foot (pcf). The target compressive strength was 700 psi, with subsequent cores showing actual strength between 780 and 840 psi. Figure 8 shows several pictures of the construction of the test section and the final surface of the soil cement layer.

Figure 8. Soil Cement Subbase Surface for Slab Track Test Section

2.2.4 Direct Fixation Slab Track

Figure 9 illustrates the plan and details of the DFST test section. The concrete slab is 1 ft thick, 10 ft 6 in wide, and built with 5,000 psi strength concrete. The Acoustic Loadmaster DF fasteners, manufactured by Advanced Track Products, Inc., are spaced at 2-foot intervals and are used to anchor the rails to the slab by four anchor bolts. For the DFST, track resilience and damping are provided primarily through the rubber pads installed between the fastener plates and the slab surface. As a reference, the laboratory test at CTL (Ball, 2004) showed 0.22 in of deflection under 39-kilopound vertical load, resulting from pad deformation.

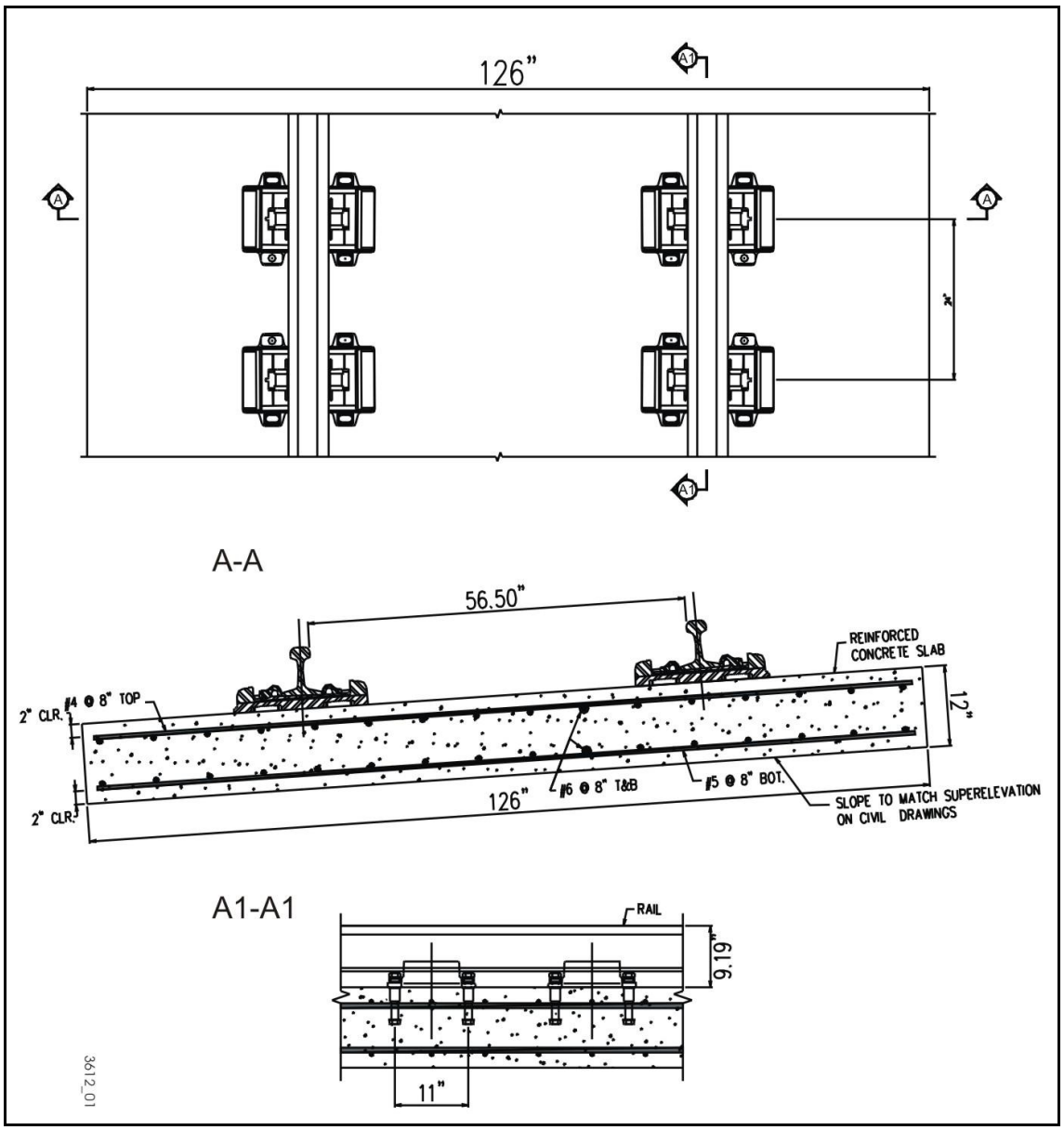

Figure 9. DFST Plan and Details

Figure 10 shows construction of the DFST. As shown, the reinforced concrete was cast in place with the rails and fasteners already established in position, using the top-down construction method. The positions of the rails were set up using a fixture known as the iron horse, used to support the rails and fasteners and adjusted to obtain proper surface, alignment, crosslevel, and gage of the rails. The iron horse fixtures were provided by Amtrak and are shown being spaced at 10-foot intervals along the track in Figure 10.

Note, before the construction of the DFST, the rails were painted white to reduce the effect of sunlight on the rail temperature. This practice, however, was not followed later during the construction of the IDBT.

Figure 10. Construction of DFST Using Top-down Method

2.2.5 Independent Dual Block Track

Figure 11 shows the plan and details of the IDBT test section. The IDBT, also known as low vibration track (LVT), consists of a 7.75-inch-thick reinforced bottom concrete slab (Phase 1 slab) 10 ft 6 in wide and built with 5,000 psi strength concrete, two independent block ties, and a self-compacting, unreinforced concrete slab (Phase 2 slab). The IDBT block ties were supplied by Permanent Way Corporation. The rails were fastened to the block ties using a fastening system provided by Sonneville International Corporation. For the IDBT, track resilience and damping were provided primarily through the rubber boots as well as the pads installed inside rubber boots. For reference, the laboratory test in CTL (Ball, 2004) showed 0.16 in of deflection under a 39-kilopound vertical load due mainly to the rubber boot and pad deformation.

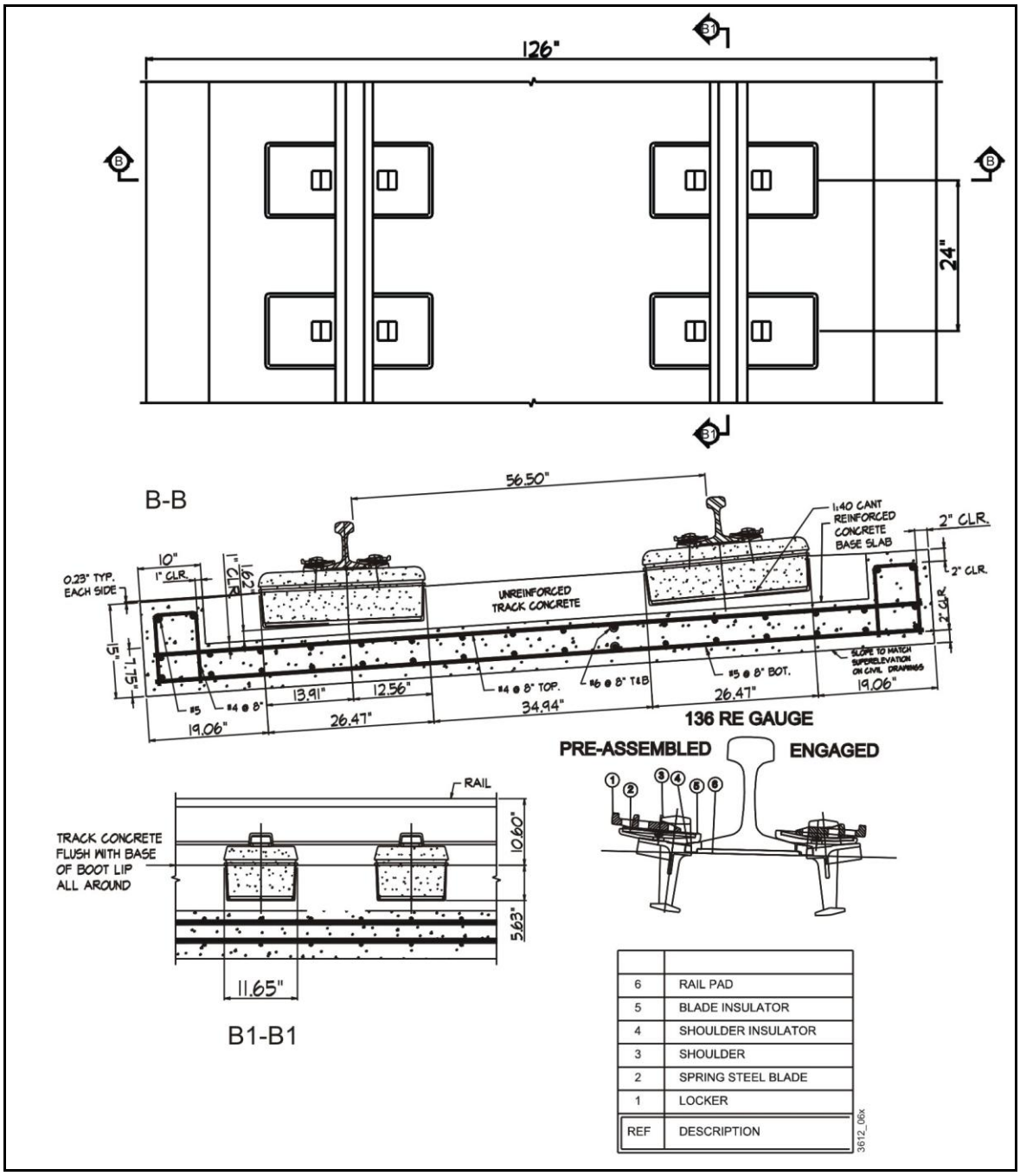

Figure 11. IDBT Plan and Details

To construct the IDBT test section, the reinforced base slab (Phase 1 slab) was cast first. Then the precast block ties fitted with rubber boots and pads were set in place above the bottom slab together with the fastenings and the rails using the iron horse fixtures. The self-compacting concrete (Phase 2 slab) was poured around the block ties. Figure 12 shows the construction of the IDBT.

Figure 12. Construction of the IDBT Using Top-down Method

2.2.6 Transitions

The IDBT and DFST slab track sections were connected directly and their interface was detailed to provide continuous steel reinforcement. Figure 13 shows the interface plan and details between the IDBT and the DFST.

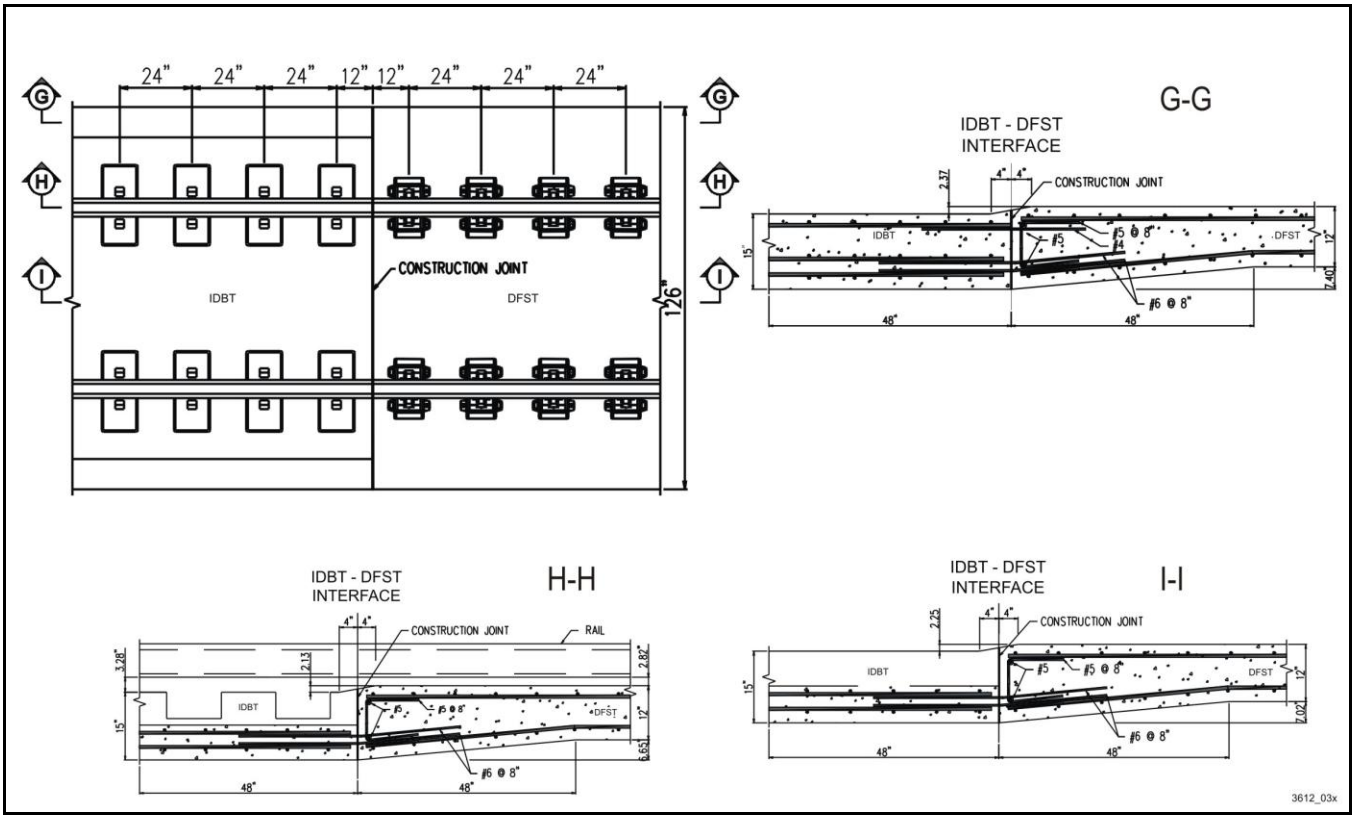

Figure 13. IDBT and DFST Interface Plan and Details

To accommodate the difference in track modulus between the slab track and the adjacent ballasted track, a 25-foot-long transition zone was designed and built. The transition was designed to have a 1-foot-thick reinforced concrete slab with upturned curbs to retain the ballast, a 12-inch ballast layer, and concrete ties. Figure 14 shows the plan and details of the DFST transition design (note, the IDBT has the same transition design as the DFST).

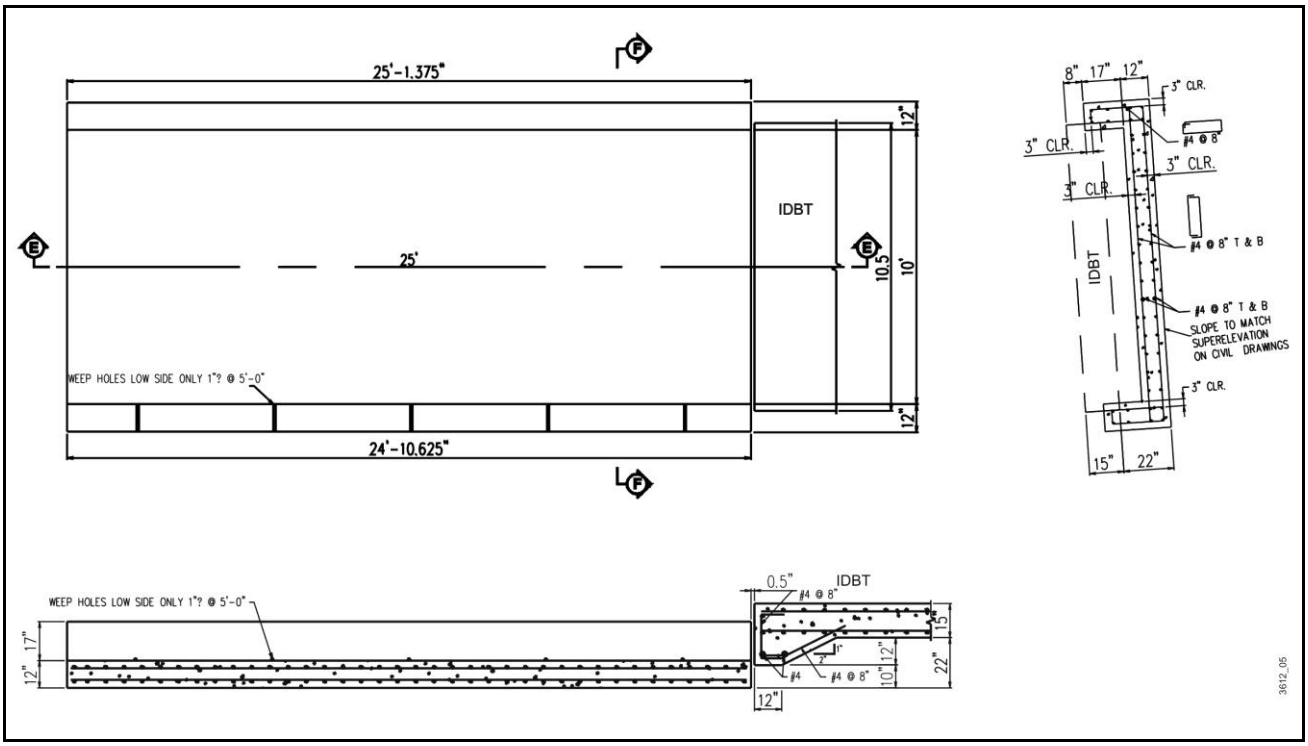

Figure 14. DFST Transition Design

Figure 15 shows the 25-foot base slab built in the transition to the IDBT test section and the final view of the transition track to the DFST test section. Note, from the end of each slab (IDBT or DFST), there are 18 concrete ties (over a distance of 36 ft) with Pandrol clips before all ties become wood ties in either Section 37 or Section 38.

Figure 15. Base Slab in Transition to the IDBT and DFST Transition

2.2.7 Rail

The rails installed on the slab track test section were new 136 RE rails. They were installed as continuous welded rails. This was accomplished by welding (thermite welds) 80-foot rails. Altogether, there were 14 field welds in the slab track test Section 38.

2.2.8 Completion of Slab Track Construction

The construction of the 500-foot slab track test section in the HTL was completed on July 22, 2003. The slab track was built within Amtrak's Class 9 track construction tolerances, with one exception: alignment toward the end of the DFST slab exceeded the allowable limit of 0.5 in for Class 9 track. Further discussion of this is continued in Alignment.

Because the slab track was built, it has been maintained in compliance with FRA's Class 9 track safety standards. Note, the adjacent ballasted track and transitions were built and are maintained in compliance with FRA's Class 4 track safety standards. Table 1 lists the completion of the major milestones for the slab track construction. Figure 16 shows the final views of the two slab tracks following their construction in Section 38.

Table 1. Milestones of Slab Track Construction

Task	Date in 2003 Completed
Existing track removal	April 14
Subgrade preparation	April 15–24
Soil cement subbase	April 24
IDBT Phase 1 concrete	May 14
IDBT and DFST transition slab	May 16–23
DFST slab	June 13
IDBT Phase 2 concrete	June 30
Final rail welding	July 22

Figure 16. Views of IDBT (top) and DFST (bottom) following Construction

2.3 Design and Construction

2.3.1 Design

Adequate design and proper construction procedures are critical to the success of any DFST project. Direct fixation track is structurally more complex than traditional ballasted track, therefore, making the direct fixation system more sensitive to variations in subgrade and substructure. Neither ballasted track nor direct fixation track can bridge voids or subgrade support variations because of natural geological variations. Whereas ballasted track allows railroad engineers to repair structurally inadequate track sections during maintenance, direct fixation systems must be designed and constructed to accommodate local variations in track support conditions. This will ensure adequate long-term performance and attain the main benefit of direct fixation track: reducing future maintenance costs.

Reduced life-cycle costs for direct fixation track structures necessarily rely on knowledge of local geology and subgrade properties to ensure proper design for adequate long-term performance. The site investigation defines the subgrade properties and variability. These variations must be accounted for during design of the structural cross section, including concrete thickness and reinforcing steel details. The same information is required to achieve a structurally adequate ballasted track design using the AAR design procedure. This expense should, therefore, not increase the cost of a direct fixation project over ballasted track. The one exception is where state of practice design procedures is not utilized and the age-old process is used to construct track regardless of site conditions using standard ballast and subballast thicknesses. In this case, the small design savings are far offset by the large maintenance costs required to repair structurally inadequate track sections.

Uniform track support conditions are often difficult to achieve. Engineers use various construction and soil stabilization methods to improve the shallow subgrade soil properties and reduce the variability often associated with the subgrade surface as completed for the construction of the test section. The specific details for any subgrade improvement method will be site-specific but should be utilized for both direct fixation and ballasted track.

2.3.2 Construction Challenges

Construction of DFST for high-speed applications is a challenge due to the required tight tolerances on the order of 1/8 in. Construction processes to achieve such tight tolerances are complicated by environmental changes such as temperature, precipitation, humidity, and blown debris. Several studies have shown improved methods of constructing slab for transportation applications such as slipform paving. Because of the short test section that was built, this specialized construction procedure was not used.

Expansion and contraction of the rail due to temperature changes is an impediment to the construction of direct fixation track for high-speed applications. Mitigation of rail thermal heat gain using a light-colored paint was attempted but was not adequately successful to be repeated during the construction process. Using the top-down construction process (previously described) made achieving Class 9 construction standards possible but still difficult. Bracing the iron horses is required to maintain rail position. Class 9 construction standards were generally achieved. One exception was at the end of the slab where the curvature of the track that

extended beyond the end of the slab was modified shortly after construction to achieve Class 9 standards. Adjustment of direct fixation track following construction can generally be made within small tolerances as allowed by the fasteners, but the degree of adjustment required during construction may not be available in direct fixation fasteners.

3. Track Geometry Performance of Slab Track

3.1 Objective

From the inception of slab track performance testing and monitoring, track geometry condition has been one of the main performance parameters measured. The objective of track geometry measurements is to quantify and demonstrate whether the slab track test section can withstand 39-ton axle load traffic while maintaining the track geometry conditions of a Class 9 track.

3.2 Tonnage Accumulation on Slab Track

The trains at FAST started to operate on the slab track on July 30, 2003. Figure 17 shows the tonnage accumulation history for the slab track test section. Over a period of 3 yr, a total of 170 MGT was accumulated, exceeding the 150 MGT target originally set for the program.

Because slab track performance monitoring includes how track geometry might degrade with traffic, tonnage accumulation history is shown in Figure 17 before track geometry performance results are discussed.

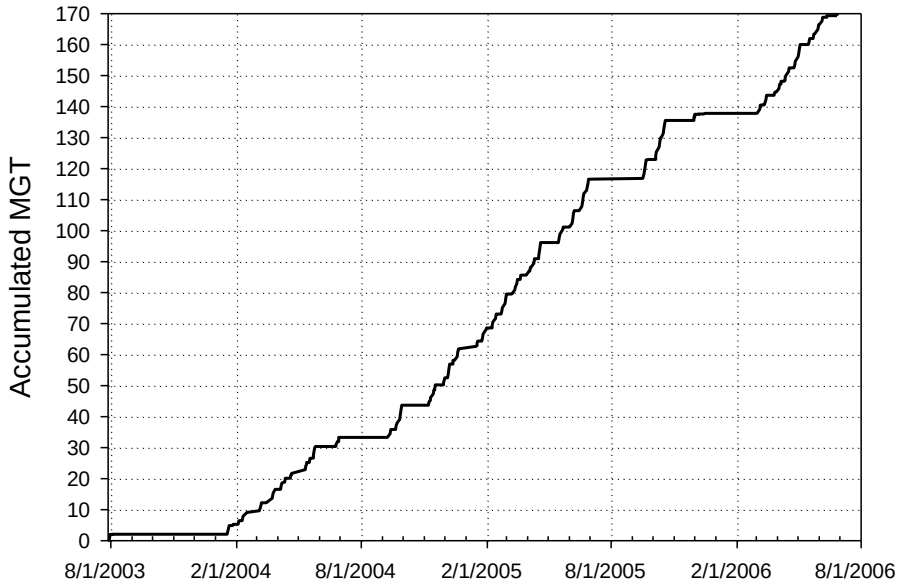

Figure 17. Tonnage Accumulation on Slab Track

3.3 Track Geometry Measurement Methods

Several measurement methods were used to monitor how the geometry of the slab track would change due to the HAL traffic. The following sections describe the measurement methods used.

3.3.1 Top-of-Rail Elevation Survey

Surface elevations of both rails were measured by using a digital level at every third fastener/tie location throughout the slab track test section and its transitions. Fastener and tie locations are numbered CCW at FAST on each HTL section. The slab track section is defined by the fastener/tie location numbers shown in Table 2.

Table 2. Slab Track Test Section Defined by Fastener/Tie Location Number

Begin-Section 38	Begin-DFST	DFST-IDBT Interface	End-IDBT	End-Section 38
1	5	129/130	254	258

Top-of-rail (TOR) elevation surveys were performed at 0, 0.5, 2, 5, 9, 22, 62, and 169 MGT. Surveys were conducted more frequently during the early phase following the construction of the slab track than during the later phase of the testing program. As will be presented later in this section, the slab track test section (either DFST or IDBT) experienced less than a 0.3-inch elevation change over an accumulated traffic of 169 MGT.

3.3.2 Slab Movement Survey

For each slab track, two reference points were fixed to the slab surface. The reference points were used to monitor how much the DFST and IDBT slabs would move from the beginning to the end of the testing program. The movements of the slabs were measured in terms of elevation change as well as lateral position change. The lateral position change was defined by the radial distance change of the reference points with respect to their permanent benchmarks installed in the field.

3.3.3 Track Geometry Measurement System

TTCI's track geometry measurement system (TGMS) was used to measure track geometry conditions of the slab track. This system is an inertia/laser-based noncontact measurement system purchased from Imagemap, Inc. The system has been used extensively on the test tracks at TTC as well as on revenue service tracks for various research and testing projects. The system is portable, which means it can be installed onto the trucks of various vehicles. At the early phase of the slab track project, this system was attached to an empty freight vehicle (tank car). Later, the system was moved and installed on TTCI's track loading vehicle (TLV) (see Figure 18).

Figure 18. TTCI's Track Geometry Measurement System Attached to an Empty Tank Car (left) and TTCI's Track Loading Vehicle (right)

The TGMS measured track geometry conditions during track geometry testing as defined by the parameters, including the following (note, the abbreviation given for each parameter in parentheses):

- Curvature (TGCU)
- Superelevation (TGSE)
- Surface of left and right rails (TGSL, TGSR)
- Alignment of left and right rails (TGAL, TGAR)
- Crosslevel (TGXL)
- Gage (TGGI)

For the slab track testing, FRA's Track Safety Standards were used to determine if the slab track test section (Class 9) and the adjacent transitions (Class 4) were in compliance with the standards.

3.3.4 Other Measurements

In addition to TOR, the slab movement determined by survey, and track geometry was obtained using hand-string midchord offset (MCO) measurement to determine track alignment.

3.4 Initial Track Geometry of Slab Track

3.4.1 Surface

Figure 19 shows the initial TOR elevation survey results for both rails in the test section. As illustrated, a 4-inch superelevation exists between the outside (high) and inside (low) rails. As mentioned in Subgrade, a slight downhill grade (0.4 percent) exists from the IDBT to the DFST. Figure 19 illustrates that the slab track test section (both the IDBT and the DFST) had a very smooth surface condition. In contrast, the surface condition in the transitions showed more variation. Initial TOR elevation results were used to calculate the settlement of the slab track test section by subtracting later TOR elevation survey results from the reference values.

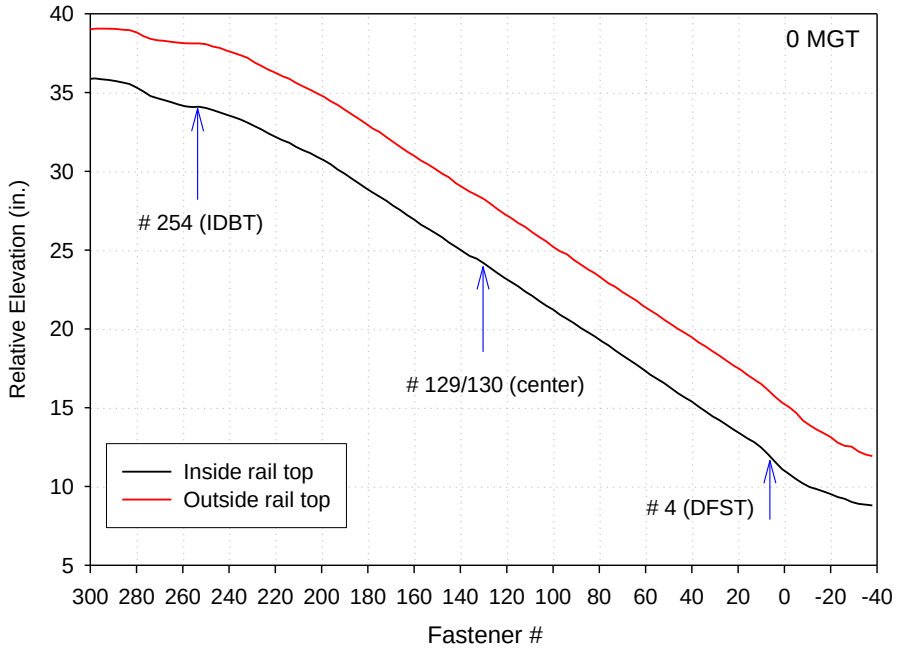

Figure 19. Initial Rail Surface Elevation Results

Figure 20 shows the track surface conditions (surface of left and right rails as well as crosslevel) obtained with the TGMS. The data shown were obtained on December 1, 2003, although track geometry measurements were also taken on July 30, 2003, immediately following the construction of the IDBT. The data collected on July 30, 2003, were not shown because the newly applied white paint on the rails of the IDBT interfered with the laser signal of the TGMS, which caused noise in the recorded data. Nonetheless, between the measurements on July 30 and December 1, only a small amount of traffic (2 MGT) accumulated, as shown in Figure 17.

Figure 20 shows that the slab track test section had a very smooth surface and little crosslevel deviation, consistent with the results shown in Figure 19. The surface of the transitions, however, is not as smooth but is still well within the allowable limits shown in Table 3.

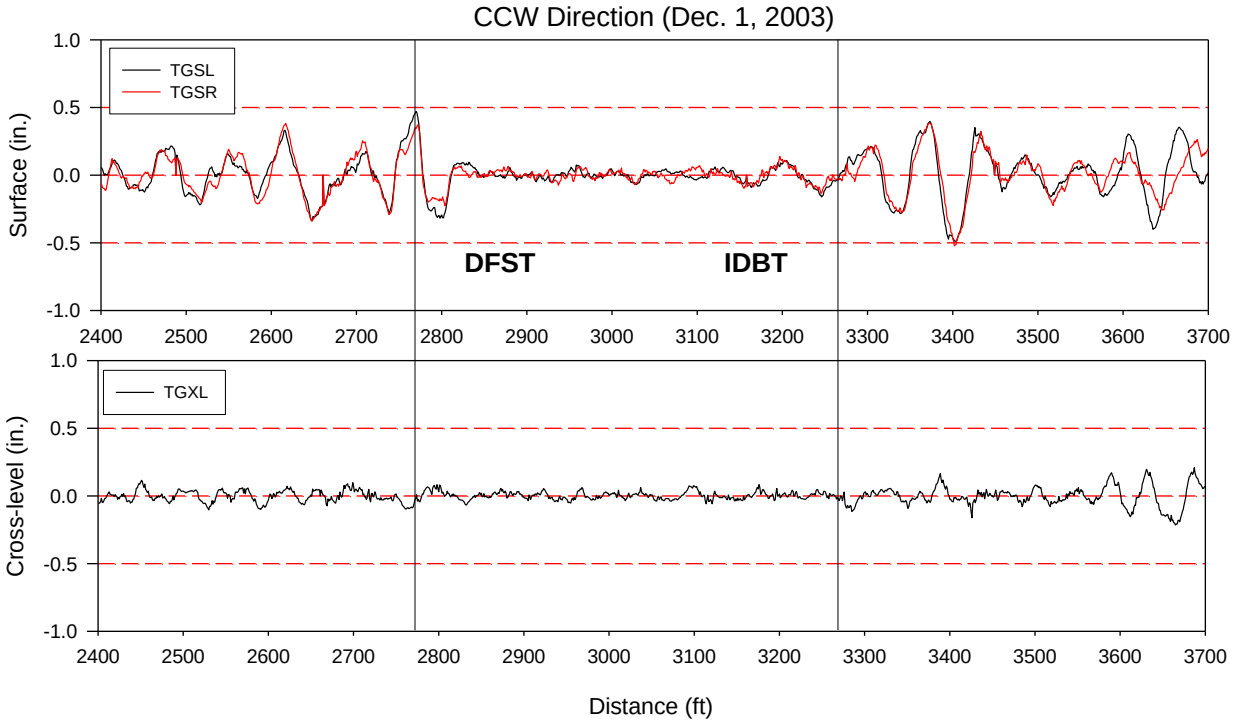

Figure 20. Initial Track Surface via TGMS

Table 3. Allowable Track Geometry Limits Used in Slab Track Testing

Parameter	**Class 4**	**Class 9**
Gage	-0.5 in/+1.0 in	-0.5 in/+0.75 in
Gage—rate of change (31 ft)		0.5 in
Alignment (62 ft MCO)	±1.5 in	±0.5 in
Surface (62 ft MCO)	±2.0 in	±0.75 in
Crosslevel	±1.25 in	
Crosslevel variation (62 ft)	±1.75 in	±1.5 in

At or near the end of each slab (IDBT or DFST), track geometry deviation in terms of MCO often appeared at a larger magnitude than in the middle part of the slab track. This was due to the proximity of the Class 4 track and because a rougher spot in a transition within 62 ft would make the MCO data appear larger, solely because of the way that the data were calculated.

3.4.2 Gage

Figure 21 shows the initial gage results for the slab track test section and the adjacent ballasted track. As illustrated, the initial track gage met the allowable limits shown in Table 3. There were no exceptions in wide or narrow gage or in excessive rate of change within 31 ft.

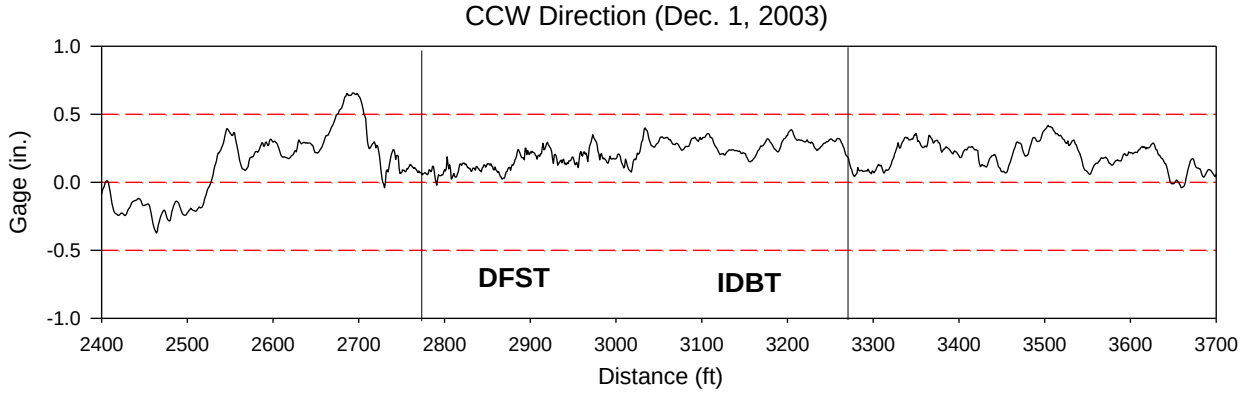

Figure 21. Initial Track Gage via TGMS

3.4.3 Alignment

Figure 22 shows the initial alignment results for the slab track and the adjacent ballasted track along with the curvature measurement results. Near the end of the DFST, alignment deviation exceeded the allowable limit of 0.5 in for Class 9 track (Table 3). This misalignment was caused by a change of track from Class 9 to Class 4 and a change of track curvature from the DFST slab track (5 degrees) to the ballasted track in test Section 37 (spiral). This misalignment was later corrected and will be discussed in Alignment.

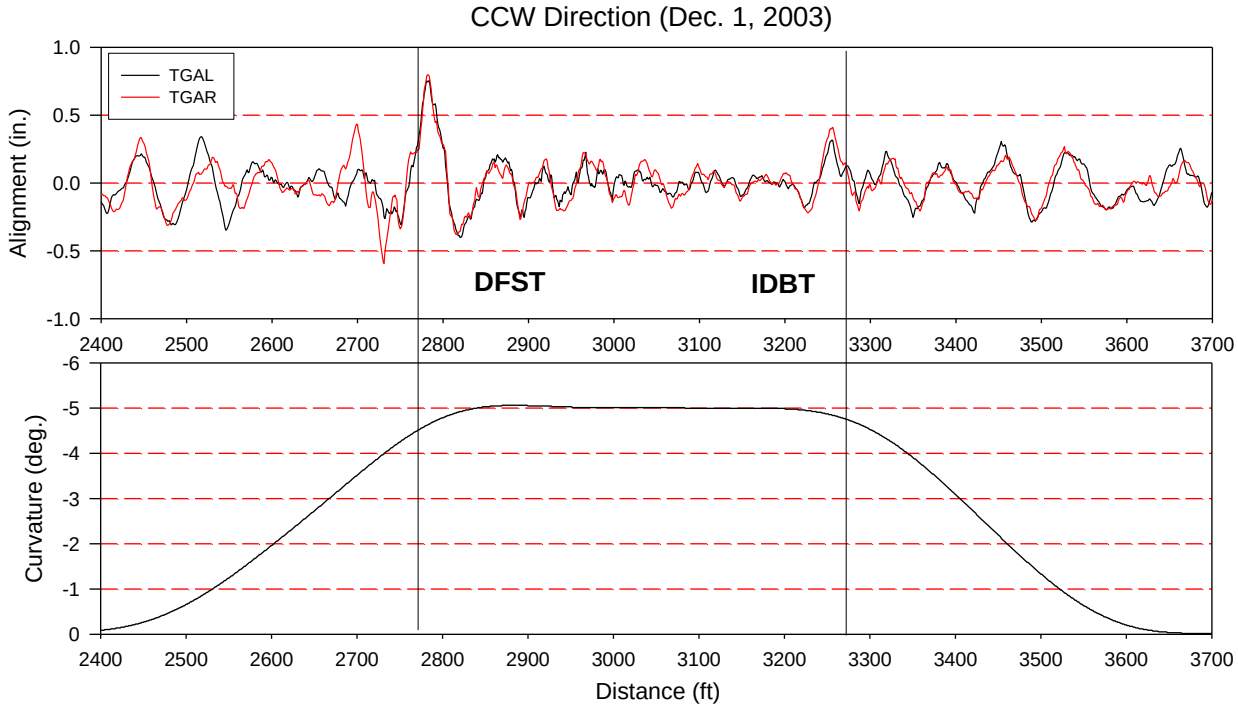

Figure 22. Initial Track Alignment via TGMS

3.5 Track Geometry Maintenance and Change over Time

3.5.1 Alignment

Figure 22 shows that because of the misalignment measured near the end of the DFST, the track in Section 37 (spiral) and a part of the DFST track were realigned on April 21, 2004, using TTCI's production tamper. To facilitate the alignment adjustment toward the end of the DFST, the bolts of 10 fasteners for both high and low rails were loosened. The slots of the DFST plates are such that they can allow some lateral movement of rails (roughly 0.5 in either way). The production tamper was then used to line the track from the ballasted track in test Section 37 to the DFST slab track by using the best fit as determined by the tamper.

Figure 23 shows the 62-foot-hand-string MCO results obtained just before the alignment work. As illustrated, the maximum MCO near the end of the DFST was approximately 5.88 in. Because the hand-string MCO data included the curvature component, a subtraction of 5 in (MCO because of a 5-degree curve) in the DFST gives a maximum misalignment of 0.88 in. This is similar to the results shown in Figure 22 using the TGMS.

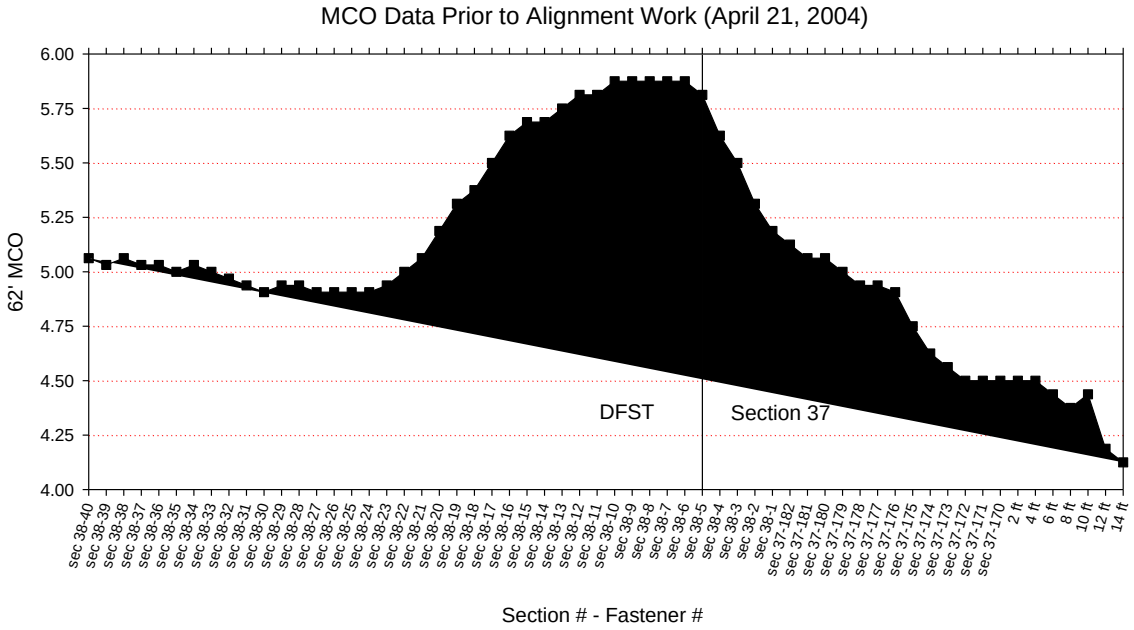

Figure 23. Hand-String MCO Data Showing Misalignment toward the End of the DFST

The hand-string MCO measurement was repeated after the alignment work. Figure 24 shows the measured results. The alignment work corrected the misalignment shown in Figure 22 and Figure 23. Immediately after the alignment work, the maximum alignment deviation was less than 0.2 in.

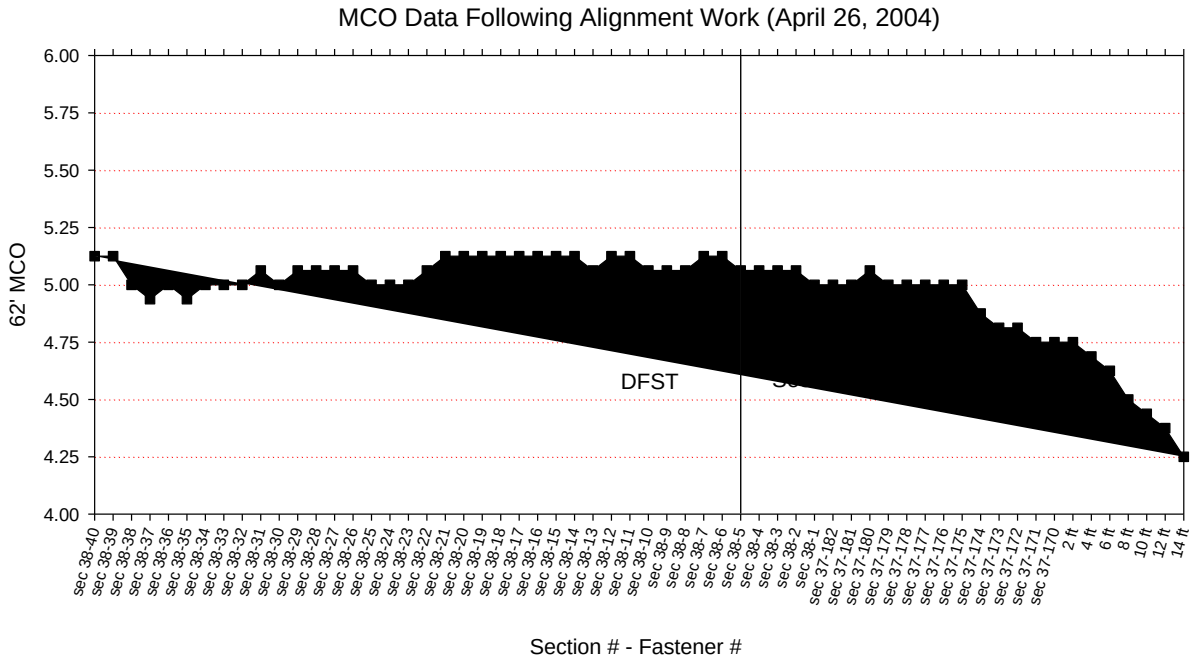

Figure 24. Hand-String MCO Data Showing Correction of Misalignment

After this adjustment on April 21, 2004, no further alignment work was done on the slab track. Nevertheless, alignment conditions toward the ends of the slab track (DFST and IDBT) degraded somewhat over time, due to more severe track conditions in the transition areas, such as the change of the Class 9 track to the Class 4 track and the change from a 5-degree curve to the spirals.

Figure 25 shows the comparison of track alignments recorded on December 1, 2003, and May 18, 2006 (at 162 MGT), just before the end of the testing program. For the slab track itself (DFST or IDBT), alignment changed very little. Alignment change or degradation, as mentioned above, occurred primarily at the transitions. The misalignment correction conducted on April 21, 2004, caused the reduction of alignment deviation near the end of the DFST.

Because of the tough alignment transition and the way that MCO is calculated, higher magnitudes of alignment deviations can be seen at the ends of the DFST and IDBT, regardless of accumulated MGT. Nevertheless, both slab track types (DFST or IDBT) were able to maintain Class 9 alignment conditions throughout the testing program.

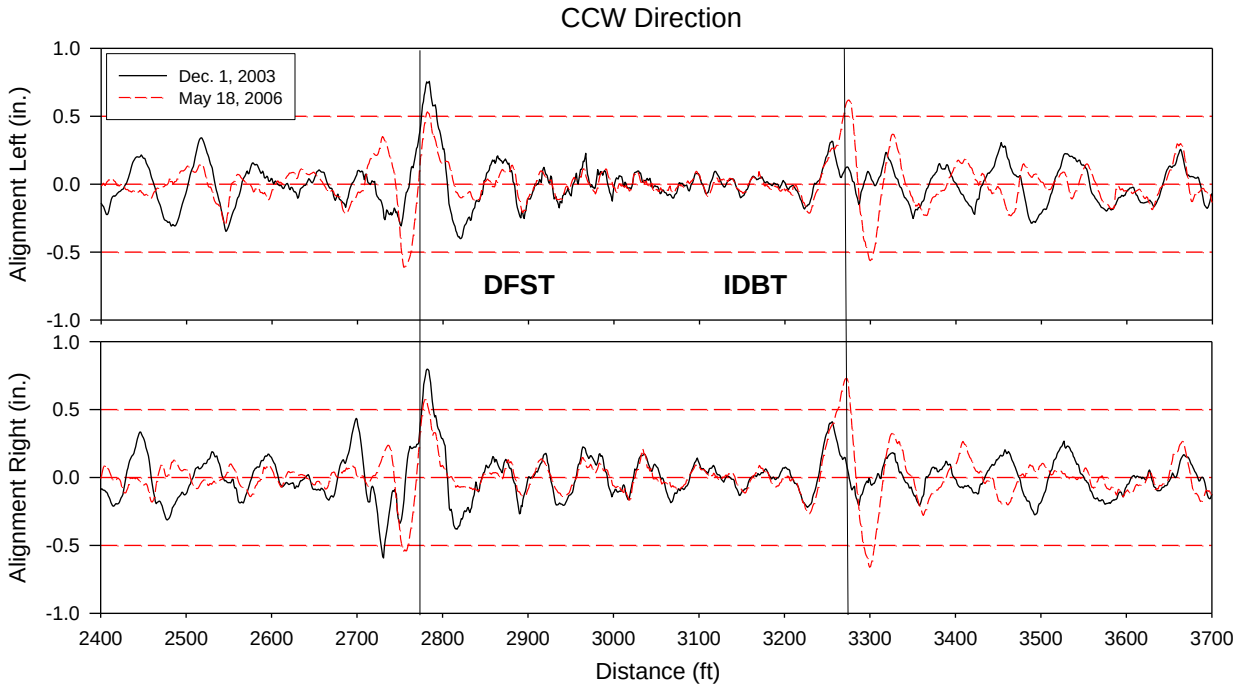

Figure 25. Change of Track Alignments over Time

Figure 26 shows the survey results obtained at 0 and 169 MGT, with the difference (delta) indicating lateral movements of the IDBT and DFST concrete slabs. As described earlier, four reference marks were set up on the surface of the concrete slabs, as shown in Figure 26. Lateral movement of each reference point was quantified by the distance change between a reference point and its permanent benchmark installed in the field. Very small lateral movements (less than 0.3 in) of the concrete slabs were recorded from the beginning to the end of the testing program.

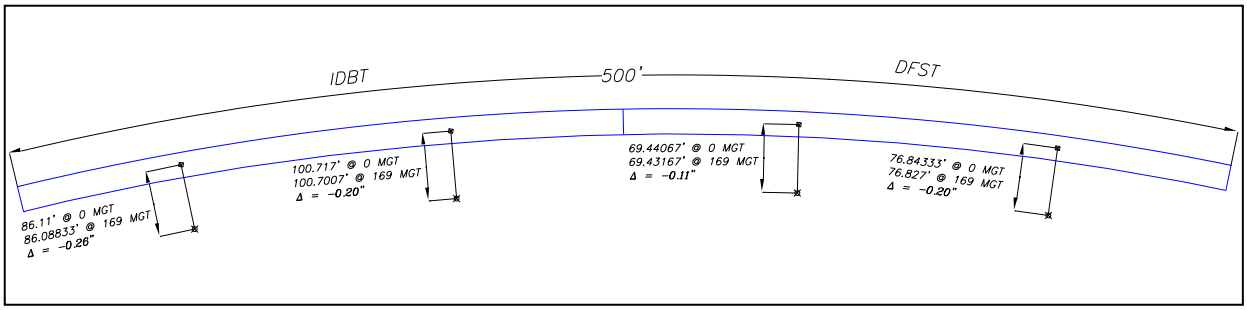

Figure 26. Lateral (Radial) Movement of the IDBT and DFST Slabs

3.5.2 Gage

Figure 27 shows the comparison of gage test results from the beginning to the end of the test program. Only a small amount of gage degradation was on the slab tracks with most occurring at the ends. The allowable limits shown in Table 3 (wide gage, narrow gage, and rate of change) were not exceeded throughout the testing program. The test section never required gage correction during the test period.

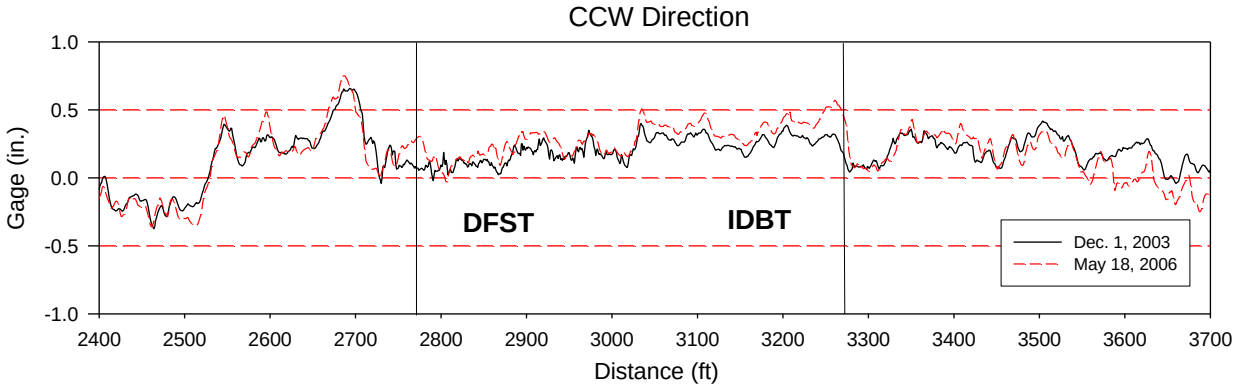

Figure 27. Change of Track Gage over Time

3.5.3 Surface of Slab Track and Transitions

Figure 28 shows the comparison of surface test results from the beginning to the end of the testing program. As shown, the surface of the slab tracks (DFST and IDBT) is superior to that of the adjacent ballasted track. Larger deviations at the ends of the slabs were caused by the rougher track in transitions.

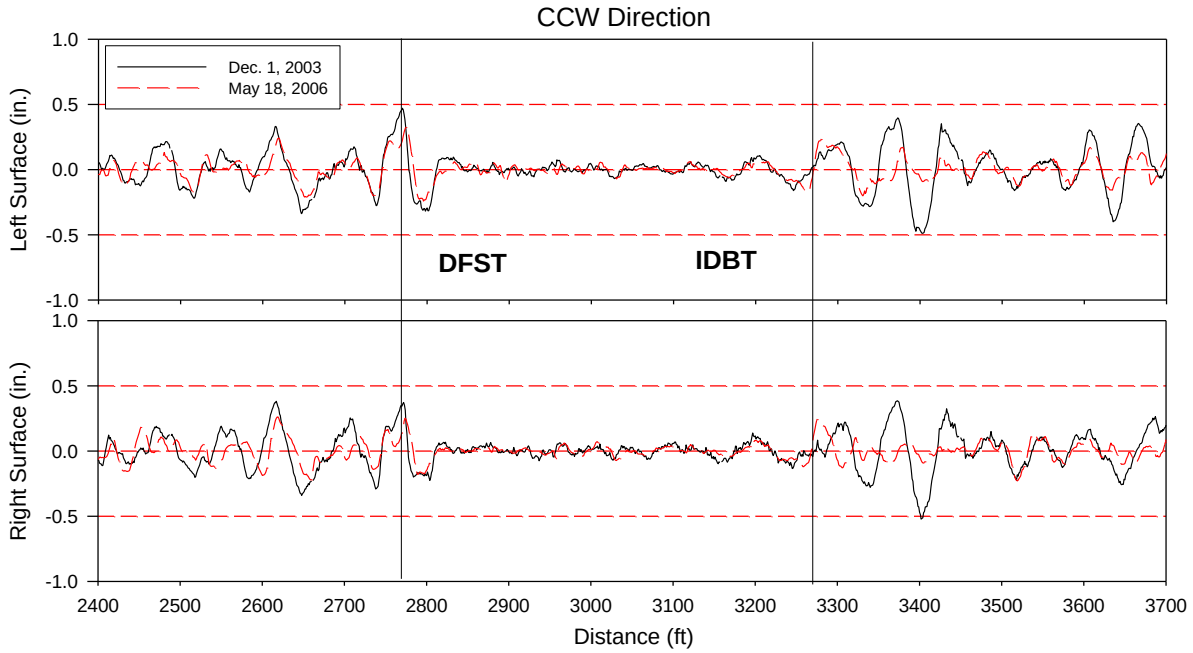

Figure 28. Change of Track Surface over Time

3.5.4 Cumulative Settlement of Slab Track and Transitions

During the testing program, the ballasted transitions to the slab tracks (IDBT and DFST) were given spot tamping and surfacing several times to smooth out the differential settlements accumulated between the slab track and the adjacent ballasted track.

To illustrate the differential settlement between the slab track and its transitions, Figure 29 shows the cumulative settlements measured from the TOR and their transitions. The settlement is calculated as the difference in TOR elevation taken between various MGT levels shown in each graph and the initial elevation data shown in Figure 19.

Before considering cumulative settlement results associated with the slab track (IDBT and DFST) and its adjacent transitions, one needs to realize that the absolute magnitudes of settlement at any MGT level and at any locations were small, as shown in Figure 29. The maximum settlement or rise of the slab track was less than 0.3 in, and the maximum settlement or rise of the ballasted transition track was only around 0.6 in. With respect to the allowable limits of track geometry surface parameters shown in Table 3, the magnitudes of the settlement shown in Figure 29 are of lesser significance as far as the safety allowance is concerned.

Within the above context, the following section describes spot tamping and surfacing work done in the transitions and discusses several issues related to the surface conditions of the slab track and transitions.

The slab track transitions experienced much larger settlement than the slab track. During the 3 yr of the testing program, several spot tamping operations were performed to smooth out the differential settlement in the transition areas. In the transition of the DFST slab track, spot tamping work was performed twice with ballast added and the track actually lifted, a procedure called design-lift tamping. In the transition of the IDBT, this design-lift tamping procedure was never used; conventional spot tamping was performed several times.

The DFST settled roughly 0.1 in during the testing program. Almost all of the DFST settlement occurred within the first 0.5 MGT of traffic. This result could be anticipated as the track shakes down during construction. The relative uniformity of the initial settlement and lack of appreciable settlement after 0.5 MGT is indicative of quality foundation construction. The IDBT actually rose 0.1–0.3 in, which was caused by fine sand that was gradually blown into the cavities between the IDBT tie blocks and cavities of the IDBT Phase 2 slab. Further discussion of this issue is provided in the next section.

In the last graph of Figure 29 (settlement at 169 MGT), the elevation changes of the four reference points installed on the slab surface are also shown. As illustrated, the vertical movement of the IDBT and DFST slabs was very small. It can be concluded that little settlement existed from the subbase and subgrade layers because the total settlement seen from the TOR or the slab surface was minor.

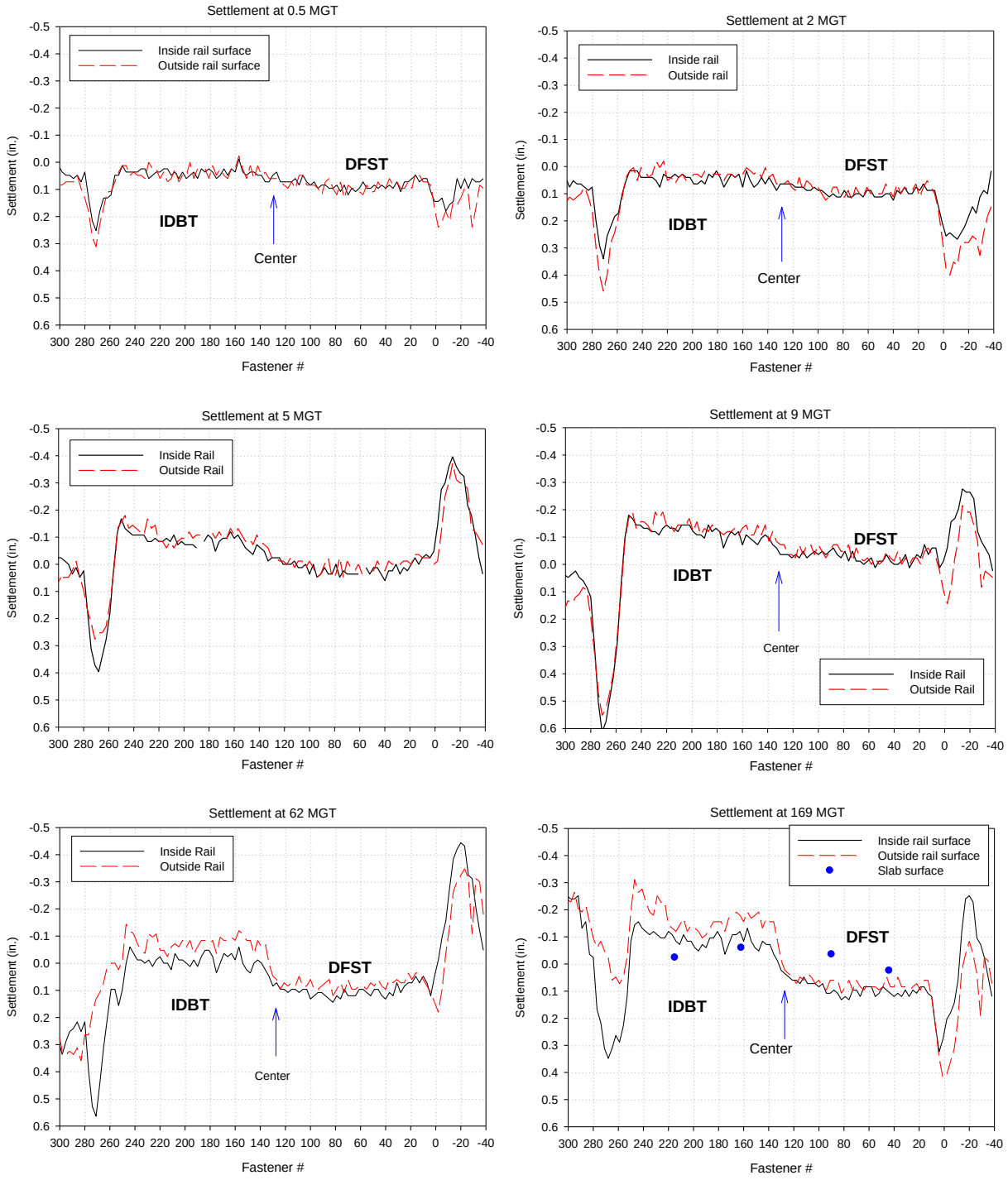

Figure 29. Cumulative TOR Settlement of Slab Track and Transitions

3.6 Other Observations about the Slab Track Test Section

The observations below are directly or indirectly related to track geometry performance of the slab track:

1. As mentioned in Rail, there were 14 field thermite welds in the slab track test section. None failed during the testing program for a total of 170 MGT as compared with the average life of 80 MGT for welds installed in similar 5-degree curves in the HTL.

2. There were no surface defects observed for the rails in the slab track test section. Rail wear due to 170 MGT of HAL traffic was insignificant. No corrugation development was observed.

3. On the basis of the feedback from train locomotive engineers at FAST, ride quality over the slab track test section was superior to that of the rest of the HTL.

After a few million gross tons into the testing program, fine windblown sand and buildup of a gray material was observed around tie blocks on the IDBT slab surface. Figure 30 shows the fine sand deposit and gray material around the ties.

Figure 30. Fine Sand Deposit and Buildup of Gray Material around IDBT Tie Blocks

This buildup of gray material resulted from fine windblown sand gradually getting into the gaps of the IDBT components. Rainwater had direct access to the gaps as well. Under train operation, dirty water was observed flushing out of the boots following a rainfall. As a result, a gray material built up around block ties over time.

Although it was a gradual process, the fine sand deposited in the IDBT was considered to be the cause of the cumulative rise of TOR elevation of the IDBT, as Figure 29 indicates. The sand also caused an increase in track modulus (Figure 34) and a small change in dynamic rail deflection (refer to Figure 58) of the IDBT slab track during the 3 yr of testing. This issue will be discussed in Section 4 and Section 6.

4. Slab Track Stiffness Characterization

4.1 Introduction

One advantage of concrete slab track is that vertical and lateral track stiffness can be optimized by specifying elastomeric pad stiffness to match anticipated vehicle traffic. For this project, assuming a rather stiff subgrade, a finite element program was used to optimize slab element and pad stiffness for heavy freight loading (Lotfi and Oesterle, 2005). Characterization of slab track stiffness was accomplished through the measurements of vertical track modulus and lateral gage strength. Vertical track modulus or stiffness is an important property for a slab track. Track response behavior under dynamic wheel loads and its long-term performance is directly dependent on this property.

The slab track test section in the HTL is built on a soil cement subbase and a firm subgrade as previously described in Section 2. As such, its resilience is derived from the rubber pads installed between rails and the slab (DFST) or from the rubber boots and pads between block ties and the slab (IDBT). One of the critical elements of the design process is to design a pad resilient enough vertically to spread the vehicle load over numerous fasteners, minimizing the load on individual components, yet stiff enough to control lateral movement of the rail and gage spreading. The design for this application resulted in a rather soft pad with relatively low vertical stiffness as seen in Figure 31. An area of concern was the amount of pad compression under full wheel load. Repetitive axle passes could result in elastomer heating and degradation of its load bearing/spreading characteristics.

Measurement of lateral gage strength or stiffness can give a direct indication of lateral track response performance, particularly for the DFST, where resilient pads are used directly at the rail-slab interface. Although an elastic fastening system is always used in a slab track design, track gage spreading or lateral rail movement under dynamic wheel loading may be of concern with resilient pads.

4.2 Vertical Track Modulus Testing

4.2.1 Test Methods

For a railroad track, track modulus is used as a measure of vertical stiffness of the rail foundation and is defined as the supporting force per unit length of rail per unit vertical deflection under a vertical load as determined by Equations 1 and 2 (Selig and Waters, 1994):

$$u = k^{4/3}/(64EI)^{1/3} \quad (1)$$

$$k = P/Y \quad (2)$$

where u = track modulus (in the unit lb/in/in)

P = vertical wheel test load

Y = deflection

E = Young's modulus of rail

I = moment of inertia of rail cross section

In Equations 1 and 2, the ratio of load over deflection (k) is known as track stiffness. Because of often nonlinear behavior of the load-deflection relationship, track modulus or the stiffness is often determined between two testing loads in terms of Equations 3 and 4 (Selig and Li, 1994):

$$u = ((P_2\text{-}P_1)/(y_2\text{-}y_1))^{4/3}/(64EI)^{1/3} \quad (3)$$

$$k = (P_2\text{-}P_1)/(y_2\text{-}y_1) \quad (4)$$

where P_2 = heavy test load (often 40 kip)

P_1 = seating test load (often 10 kip)

y_2 = deflection under heavy test load

y_1 = deflection under seating load

For the slab track test section in the HTL, vertical track modulus and stiffness were measured using two different methods: (1) static track modulus testing, and (2) in-motion track stiffness testing using TTCI's TLV.

In a static track modulus test, static vertical wheel loads are applied on the rails, and the corresponding rail deflections (difference in elevation change for targets on the rails) are measured. Equations 3 and 4 are then used to calculate track modulus.

For in-motion track stiffness testing, a continuous track deflection profile is measured under a moving test load using TTCI's TLV (Li et al., 2004). For a given constant vertical test load (e.g., 40 kip), lower track deflection indicates higher track stiffness. A continuous track deflection profile also gives an indication of how uniform or variable track stiffness is along a track.

4.2.2 Test Results and Discussion

Figure 31 shows the test results of static track modulus for the entire slab track test section obtained at 2 MGT. During this test, track modulus measurements were taken at every sixth tie/fastener location along the slab track. Track modulus was determined from the deflection measured between two test load levels (10 and 40 kip) as described above.

As Figure 31 illustrates, track modulus was quite uniform for each of the IDBT and DFST slab tracks. For the IDBT, track modulus was about 3,000 lb/in/in, while for the DFST, track modulus was about 2,100 lb/in/in. These results were surprisingly lower than originally expected, especially for the DFST. It was expected that track modulus of the slab track test section would be much higher than 3,000–4,000 lb/in/in, which is the range for the ballasted track in the HTL. The original design intended to match the conventional track stiffness. An

inaccurate estimate of subgrade/foundation modulus (Lotfi and Oesterle, 2005) resulted in the low as constructed track moduli.

The test results shown in Figure 31 were independently verified by other measurements conducted at the same time, such as vertical track deflection test results under dynamic wheel loads, and TLV in-motion track stiffness test results, presented in the following section.

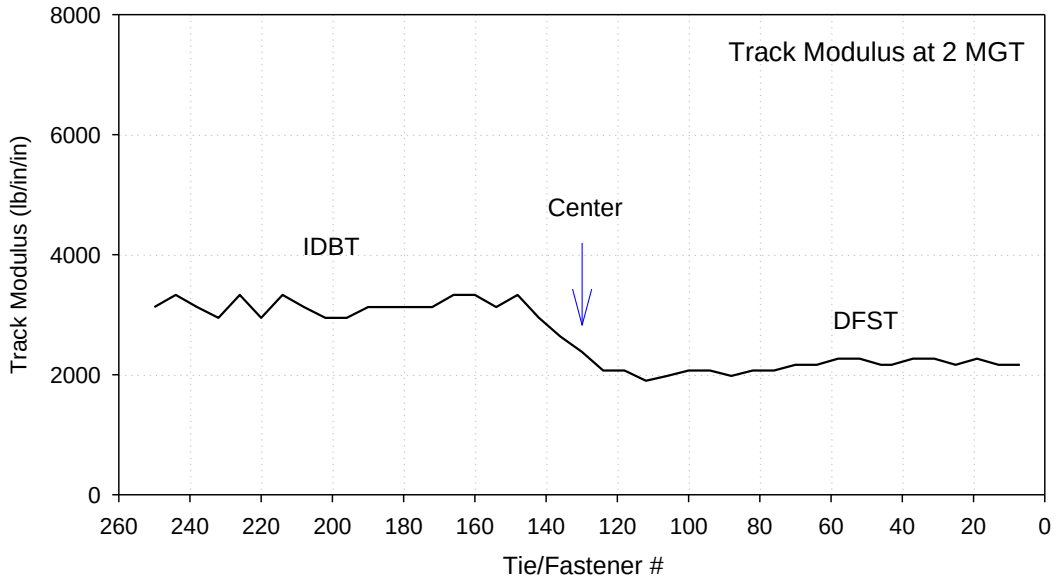

Figure 31. Track Modulus Test Result of Slab Track (IDBT and DFST)

Figure 32 shows vertical track stiffness test results of in-motion testing, obtained by the TLV on December 8, 2003, at 2 MGT of traffic level. Figure 32 shows a continuous vertical track deflection profile along the slab track (Section 38) and the adjacent ballasted track in Section 37 and Section 39, obtained under a constant wheel load of 40 kip. As illustrated, the DFST showed an average deflection of 0.2 in while the IDBT showed an average deflection of 0.15 in. The results shown in Figure 32 are consistent with the results shown in Figure 31—the DFST exhibited higher deflection or lower track modulus than the IDBT. Note, in this in-motion test, the consist was traveling in the CCW direction. As such, the results of the DFST appeared before the test results of the IDBT. Also, the deflection results as shown come from offset-based measurements and are not the exact deflections generated under the test load (Li et al., 2004).

Figure 32 also shows that deflections generated in the DFST were higher than those in the adjacent ballasted track, indicating that the DFST was more resilient than the adjacent ballasted track. The IDBT presented track deflections (or track stiffness) similar to the adjacent ballasted track. Nevertheless, both slab tracks (DFST or IDBT) showed more uniform track stiffness than the adjacent ballasted track.

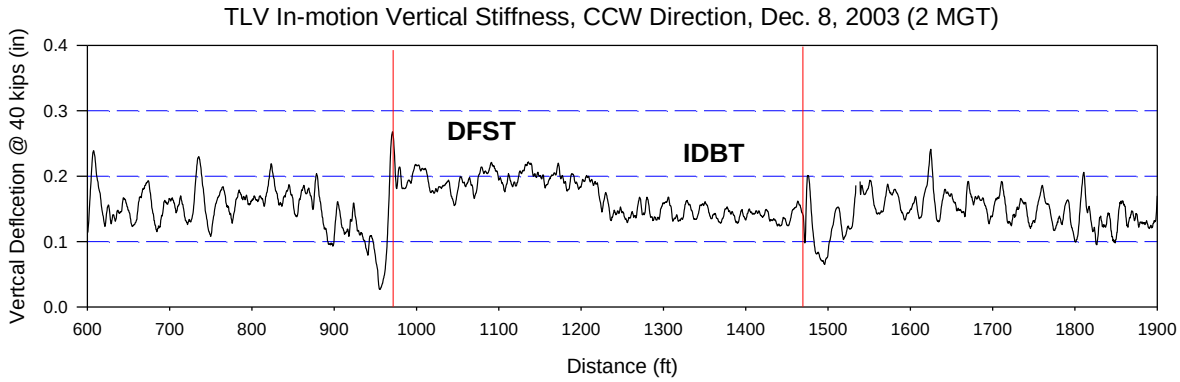

Figure 32. In-motion TLV Track Stiffness Test Results

Figure 32 shows that immediately adjacent to the DFST or IDBT (the 25-foot transition area), track deflections were significantly lower than those of the slab tracks or the ballasted track nearby. As described in Section 2, the 25-foot transition was built with a base slab underlying the ballast layer and included concrete tie; therefore, it should be much stiffer than the adjacent ballasted track. This is indicated by the test results shown in Figure 32.

The issue was that the design and installation of the 25-foot transitions did not achieve their objective in providing a gradual stiffness transition from the ballasted track to the stiffer slab track. Because the slab track was either more resilient than or equally resilient to the ballasted track, the installation of these two transitions became unnecessary at least in terms of track stiffness.

Figure 33 shows the actual track modulus test results for the two 25-foot transition areas. As illustrated, these transition areas had average track moduli between 4,600 and 5,000 lb/in/in, significantly higher than the modulus of either slab track and also higher than the track modulus for the ballasted track on the HTL (3,000–4,000 lb/in/in).

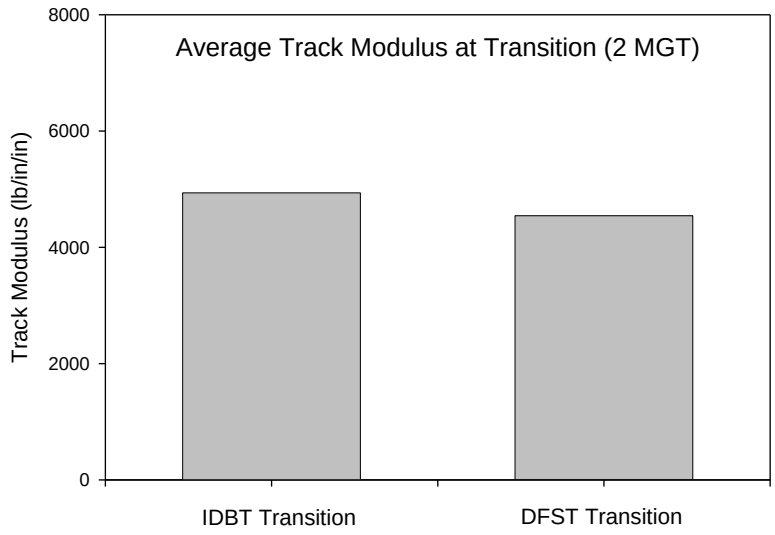

Figure 33. Track Modulus Test Result of Transition Track (IDBT and DFST)

Toward the end of the testing program at 169 MGT, static track modulus was measured again for the entire slab track test section. Because the test results from the first test indicated very uniform track stiffness along each slab track (IDBT or DFST), track modulus measurements were taken only at every 12th tie/fastener location during the second test.

Figure 34 shows the test results obtained at 169 MGT. For comparison purposes, the test results obtained at 2 MGT are also included in Figure 34. The track modulus for the IDBT increased noticeably. As compared with 3,000 lb/in/in measured at 2 MGT, track modulus of the IDBT measured at 169 MGT varied between 5,900 and 10,000 lb/in/in; this became an issue of concern because a track with a modulus higher than 10,000 lb/in/in may not be capable of accommodating large, dynamic vehicle-track interactions. Why did this increase occur? It was first considered that the measurements might be in error, but the analysis of the other test results and observations proved the validity of the track modulus test results of the IDBT at 169 MGT.

The track modulus test results measured for the DFST at 169 MGT showed an increase from that measured at the beginning of the program (2 MGT). As compared with the early average of 2,100 lb/in/in, track modulus measured at 169 MGT was 3,000 lb/in/in, which is nearly a 50 percent increase in stiffness. A concern was that the elastomer stiffened and became more brittle, but no tests were performed to determine the stiffness.

The test results shown in Figure 34 were also corroborated by the track vertical deflection results presented in Section 6. Under dynamic wheel loads, the magnitude of vertical deflections between the rail base and the concrete slab resulting from the rubber boots and pads decreased over time from the early test to the test conducted toward the end of the testing program.

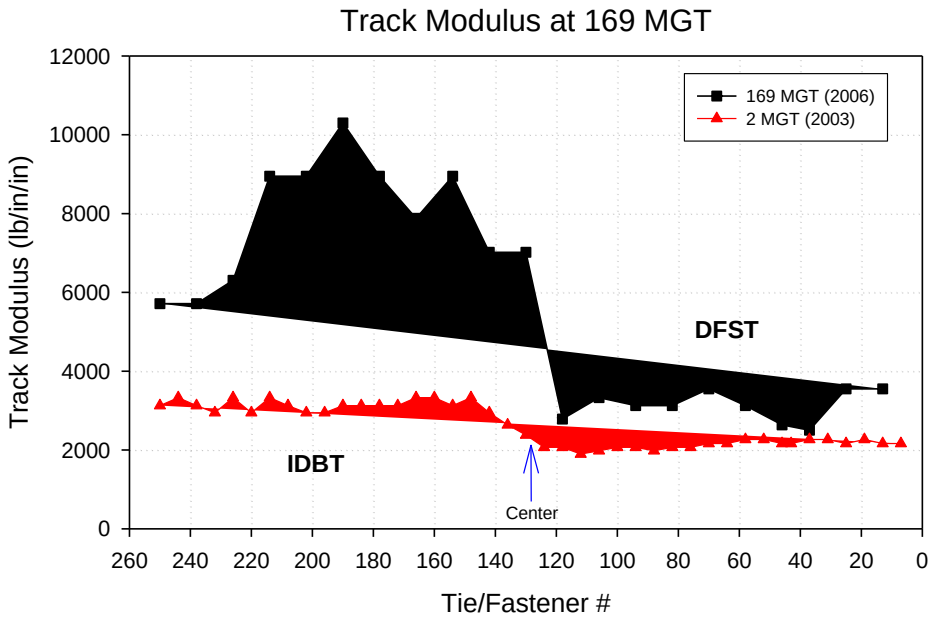

Figure 34. Track Modulus Test Results of Slab Track (IDBT and DFST) at 169 MGT

As discussed in Section 3, a small but cumulative rise of the rail elevations was caused by fine windblown sand depositing in the space between the IDBT components. This process also would cause an increase in track modulus by limiting the deflection of the block ties within the rubber boots. The fine sand would also be flushed out with rainwater under train operation, resulting in the gray material near the dual blocks noted during visual inspections.

4.3 Gage Strength Testing

Lateral track gage strength testing was conducted several times throughout the testing program as part of track stiffness characterization testing for the slab track. Track gage strength is essentially the rail restraint capacity of ties and fasteners in maintaining proper track gage under wheel loads.

During a TLV gage strength test, constant 18-kilopound lateral and 33-kilopound vertical wheel loads are applied to each rail of the track (gage-spreading load). The collected data provide information of unloaded gage, loaded gage, and delta gage (delta gage = loaded gage – unloaded gage). Unloaded track gage gives an indication of unloaded track geometry conditions, while loaded and delta gage characterize lateral gage strength or stiffness at the rail-tie interface provided by the fastening. In terms of delta gage, higher magnitudes would indicate lower gage strength or lower gage stiffness.

Figure 35 shows track gage strength test results obtained at 2 MGT, including unloaded gage, loaded gage, and delta gage. The maximum loaded track gage for the slab track was approximately 57 in. The unloaded gage test results were similar to those measured using TTCI's TGMS (see Section 3.3.3). The delta gage results indicated more uniform lateral gage strength or stiffness for the IDBT and DFST than for the adjacent ballasted track. Between the DFST and IDBT, the former showed larger delta gage and indicated lower lateral track stiffness

at the rail-fastener interface for the DFST. This was consistent with vertical track stiffness test results—for instance, the DFST also had lower vertical track stiffness than the IDBT. In addition, resilient rubber pads used in the DFST are installed at the rail-slab interface, which directly affects lateral gage strength or stiffness. On the other hand, resilient rubber boots/pads in the IDBT are installed at the tie block-slab interface, therefore, having less effect on the lateral gage strength or stiffness.

The DFST also showed larger gage spreading (lower gage stiffness) than the adjacent ballasted track. Again, this was consistent with the comparison of vertical track stiffness between the DFST and the adjacent ballasted track section. Therefore, in the case of the DFST, where vertical track stiffness is determined primarily by the elastic rubber pads, lateral gage strength is also determined by the stiffness characteristics of those pads.

The IDBT showed delta gage similar to the adjacent slab track, although it was more uniform. In the case of the IDBT, rubber boots and pads were again installed between tie blocks and the concrete slab, which made gage strength less affected. Gage strength of the IDBT was mainly affected by the rail fastening system installed between rails and tie blocks (see Figure 11).

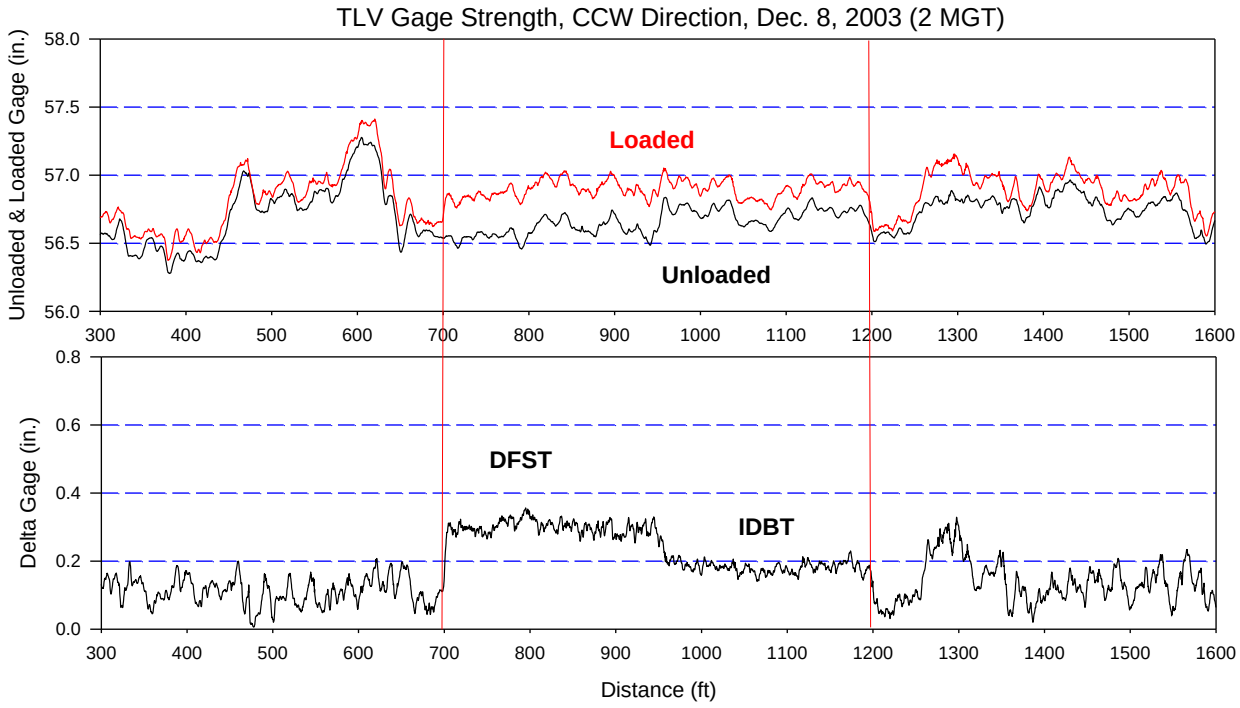

Figure 35. Track Gage Strength Test Results at 2 MGT

Two additional gage strength tests were conducted later in the testing program: one at 106 MGT and another at 169 MGT. Figure 36 shows the test results obtained at 169 MGT. Both DFST and IDBT showed more uniform lateral gage strength or stiffness than the adjacent ballasted track.

For the DFST, there was a significant increase of delta gage or decrease of lateral gage strength or stiffness. As compared with the test results obtained at 2 MGT, there was little increase in unloaded track gage, but there was a significant increase in loaded track gage. Compared with the early 0.3 in of delta gage generated under the TLV test load (33 kip vertical and 18 kip lateral), delta gage increased to an average of 0.5 in (between 0.4 and 0.6 in) at 169 MGT. Note, this increase was also observed to be 0.4 in during measurement at 106 MGT. This gradual decrease in gage strength seems to support the concern that the rubber pads used in the DFST might be too soft under 39-ton axle load operation. Under a gage spreading lateral wheel load, a rail supported on a soft pad would generally move more laterally than a rail supported on a stiff pad. However, the gage widening ratio (GWR) is within the allowed limit based on FRA's Track Safety Standards for Class 9 track.

There was little increase in delta gage due to 169 MGT of traffic for the IDBT. Some change was noted in unloaded track gage. From 2 to 160 MGT, unloaded track gage increased from 56.8 to 57.1 in. This slight increase was consistent with the gage change measured with the TGMS (Figure 27). Note that for the IDBT, the gage strength or stiffness is determined primarily by the elastic fastening system, which showed little degradation over time. The rubber boots and pads installed between tie blocks and the concrete slab would have little effect on the gage strength.

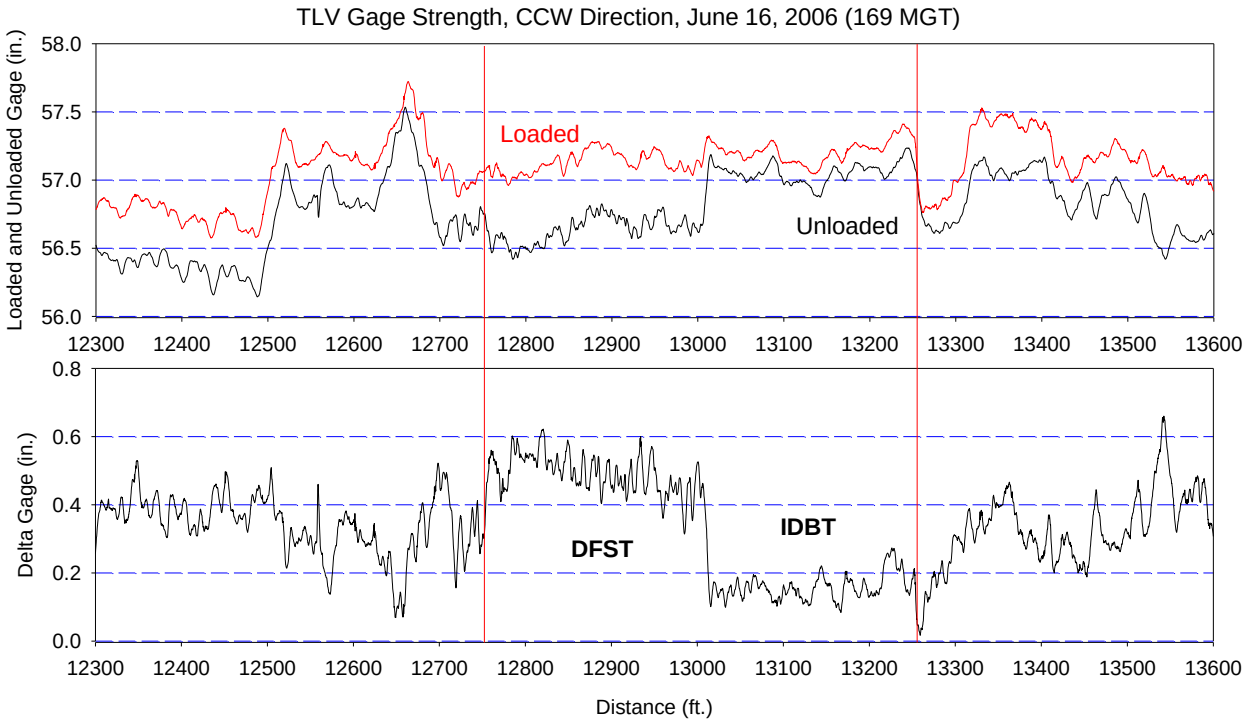

Figure 36. Track Gage Strength Test Results at 169 MGT

5. Dynamic Wheel Load Measurements on Slab Track

5.1 Objective

One of the major measurements under the slab track testing program was that of dynamic wheel loads on the slab tracks as generated under train operations at FAST. Dynamic wheel loads were measured several times throughout the testing program to quantify slab track performance in terms of vehicle-track interaction and the load environment of the slab track test section.

Because of the superior track geometry of the slab tracks, dynamic vehicle track interaction levels were expected to be lower than those generated in the ballasted track sections in the HTL. It was necessary to quantify the slab track load environment to interpret slab track responses such as stress and deformation of slab track components.

5.2 Test Methods

Dynamic wheel loads were measured using two different methods. One method involved the use of TTCI's IWS, and the other involved the use of strain gage circuits installed on the rails (wayside load stations). The following section provides a brief description of each method.

5.2.1 Instrumented Wheelsets

TTCI's IWS technology was used every year as part of the testing program at FAST to measure wheel/rail forces for the entire HTL. An IWS can measure vertical and lateral wheel loads at wheel-rail contact points along the track while the test train runs at a given operating speed.

During the IWS testing, data were collected at a sampling rate of 500 hertz (Hz) with an antialiasing low-pass filter at 100 Hz. For IWS testing on the HTL, data also included the signal of automated location detector (ALD) markers placed at various track locations to define and identify various test sections.

An IWS test often uses a short test train. For example, Figure 37 shows a short test train (consist) used in July–August 2003, immediately after the construction of the slab track test section. This short train was made up of a locomotive, an instrumentation coach, an empty tank car, and two HAL freight cars. The leading truck of the first freight car was equipped with a pair of IWS. The data acquisition system was housed in the instrumentation coach.

Figure 37. Short Test Consist including IWS (2003)

A major advantage of using an IWS is that it provides load measurements for the entire HTL, thereby providing test data for vehicle response comparison from section to section. In this section, IWS test results from several HTL sections, Section 7 and Section 31 (refer to Figure 2), are used for comparison between the slab track and the ballasted track sections of the same curvature and superelevation.

5.2.2 Wayside Load Stations

In addition to using IWS technology, strain gages were installed on the rails to measure wheel loads generated on the slab tracks. For each slab track (IDBT and DFST), strain gages were installed on the high and low rails at the center of each slab and were calibrated to measure both vertical and lateral wheel loads. During each measurement, data were collected with each passing train. The sampling rate was 2,048 Hz with a 256-hertz low-pass filter.

Figure 38 shows the wayside load station installed at the center of the IDBT. As mentioned, the load stations were installed on both high and low rails; thus, four load stations were used for the slab track test section. During the testing program, wheel-rail forces were measured at three different MGT levels:

- 0.6 MGT—July 30 and August 1, 2003
- 65 MGT—January 24 and 25, 2005
- 169 MGT—June 5 and 6, 2006

During each test, data were recorded under normal train operation at 40 mph. In addition, data were collected under the short test consist during the first test, conducted in July and August 2003.

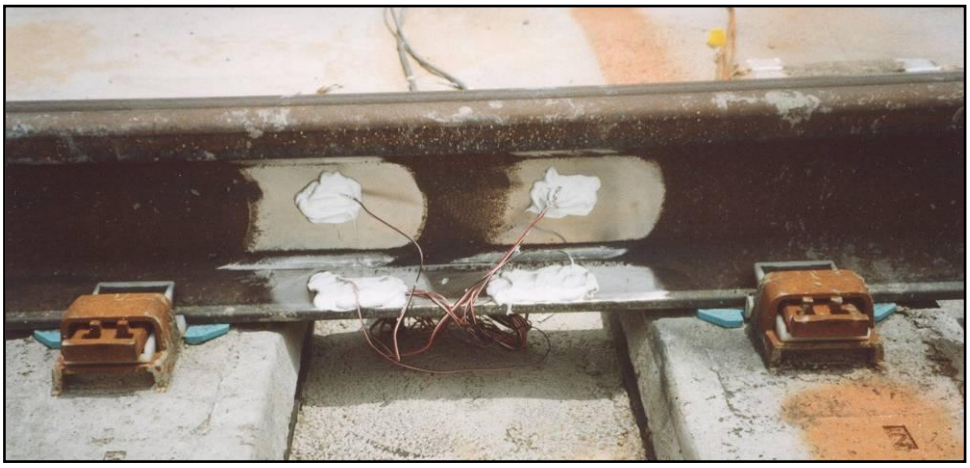

Figure 38. Wayside Load Station

As with IWS data, wayside load station data were used to quantify slab track performance. Additionally, the data were used as the basis to interpret slab track responses such as stress and deformation, which were measured using the wayside transducers at the same locations. It was necessary to quantify the slab track load environment to understand slab track response.

5.3 IWS Test Results

As mentioned, IWS testing was conducted annually from 2003 to 2005. No IWS testing was performed in 2006 under the FAST testing program before this report was prepared in August 2006. The actual IWS tests were conducted on the dates listed below; together with the measurements from the wayside load stations, they provided extensive results to achieve the objectives listed earlier.

- July 30, 2003 (0.6 MGT)
- July 16, 2004 (33 MGT)
- August 4, 2005 (117 MGT)

5.3.1 Vertical Wheel Load

Figure 39 shows the vertical wheel loads measured using IWS in July 2003 when the short test train ran over the slab track and the adjacent ballasted track. The results included the runs in both the CCW and CW directions on the HTL. In the CCW direction, the left wheel (VA 35) was on the low rail whereas the right wheel (VB 35) was on the high rail. In the CW direction, the left wheel was on the high rail and the right wheel was on the low rail.

As Figure 39 indicates, dynamic wheel loads varied throughout the slab track and the adjacent ballasted track due to car-body rocking action at 40 mph. Nevertheless, it is obvious that the slab track test section (either IDBT or DFST) showed lower magnitudes of dynamic forces than the adjacent ballasted track. In addition, the IWS data signals in the slab track test section were not

as noisy as those in the adjacent ballasted track, indicating dynamic wheel loads with lower impact components (lower frequency responses).

Because the slab track test section is in a 5-degree curve with 4-inch superelevation, the average vertical wheel load was always higher on the high rail than on the low rail due to unbalanced speed at 40 mph.

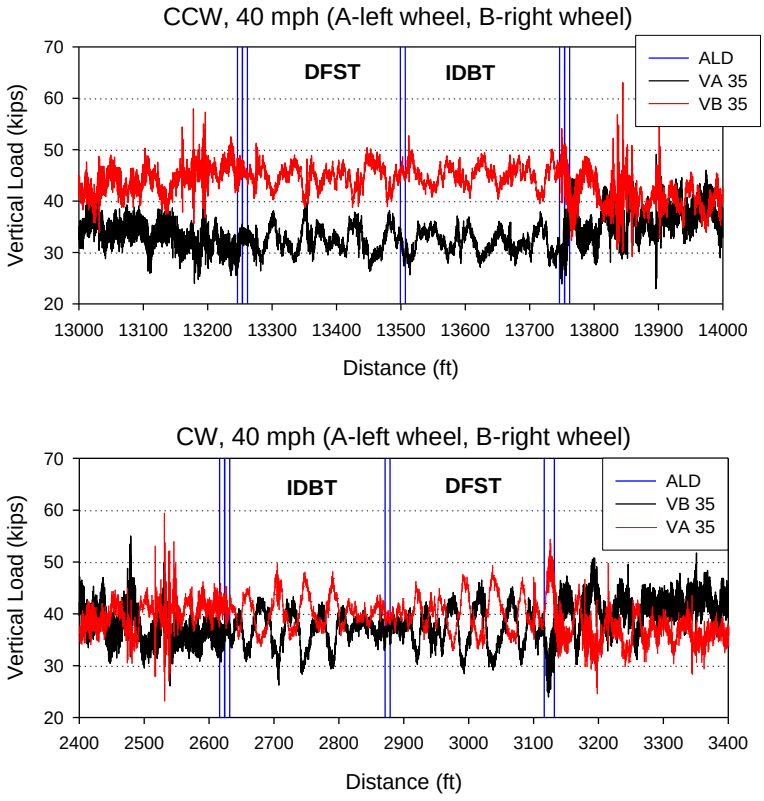

Figure 39. Vertical Wheel Loads via IWS (2003)

Figure 40 shows the comparison of vertical wheel loads on the high rail in terms of statistical values (maximum, minimum, average, and standard deviation) between Section 38 (slab track) and Section 31 (ballasted track). As previously shown in Figure 2, Section 31 is the mainline track and is adjacent to Section 38. During the IWS testing conducted in July and August 2003, the test runs were on both the mainline track and the bypass track, thus providing data for direct comparison between Section 38 and Section 31, which have the same curvature and superelevation.

As Figure 40 shows, in either the CCW or the CW direction, the dynamic wheel loads (in terms of maximum, minimum, and standard deviation) were always higher on the ballasted track than on the slab track. Note that larger values of standard deviation, maximum, and the difference between maximum and minimum all correspond to larger dynamic wheel-track interactions.

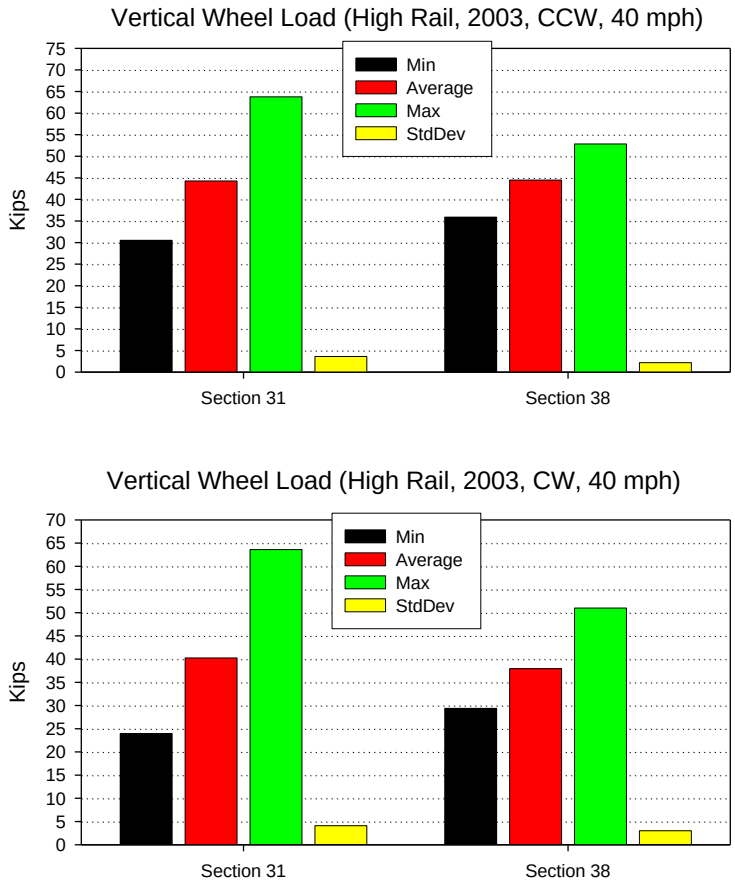

Figure 40. Section 38 (Slab Track) vs. Section 31 (Ballasted Track) Vertical Load in 2003

Similar test results were obtained in 2004 and 2005. For example, Figure 41 shows the comparison of vertical wheel loads between Section 38 (slab track) and Section 31 (ballasted track) from the tests conducted in 2004. Again, regardless of the direction of the test train operation on HTL, the dynamic wheel loads (in terms of maximum, minimum, and standard deviation) were always higher on the ballasted track than on the slab track.

In 2005, the IWS test was conducted on the HTL for a test train running only on the bypass. No IWS data were recorded for Section 31 on the mainline track. Figure 2 in Section 2 of this report shows ballasted track in test Section 7 as having the same curvature and superelevation as that in Section 38. Therefore, a direct comparison was made between Section 38 and Section 7 (Figure 42). Because an additional ALD marker was placed at the IDBT and DFST interface, the statistical values were obtained separately between the two slab tracks.

Again, for either slab track (IDBT or DFST), the vehicle-track interaction was lower on the slab track test section than on the ballasted track. For either train running direction, the ballasted track generated larger dynamic wheel loads than the slab track. No significant differences were observed between IDBT and DFST in terms of dynamic vertical wheel loads.

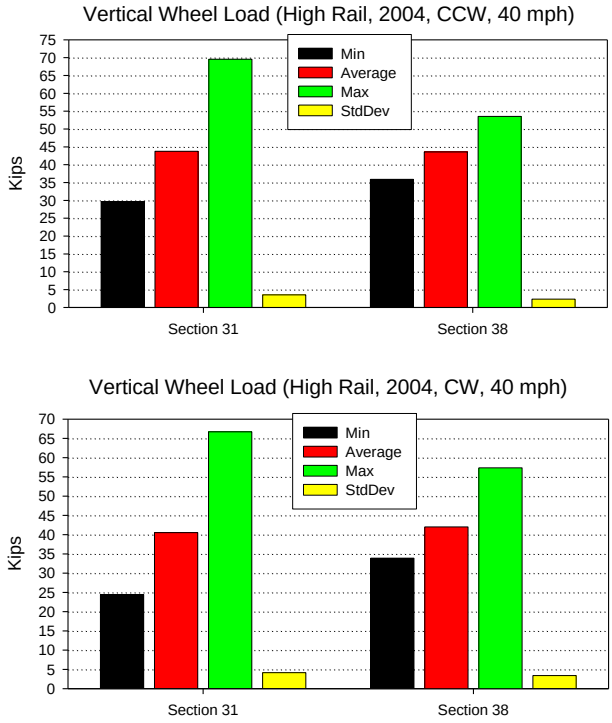

Figure 41. Section 38 (Slab Track) Compared with Section 31 (Ballasted Track) Vertical Load in 2004

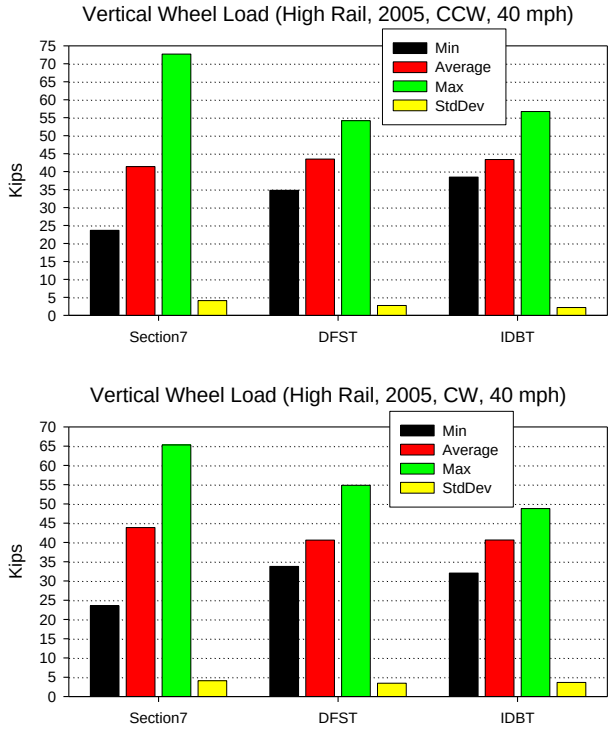

Figure 42. Section 38 (Slab Track) Compared with Section 7 (Ballasted Track) Vertical Load in 2005

5.3.2 Lateral Wheel Load

Figure 43 shows the lateral wheel loads measured in 2003 using IWS when the test train ran over the slab track at 40 mph. The results on both the high and low rails are shown for the CCW and CW running directions of the test train. As expected, the high rail experienced higher lateral wheel loads than the low rail. The maximum lateral force was recorded in the CW direction and was about 20 kip. Adjacent to the slab track are spirals (Section 37 and Section 39) to the tangent track; therefore, lateral wheel loads decreased due to reduced curvature.

On the high rail, lateral wheel load varied from the minimum to the maximum, indicating significant dynamic lateral vehicle track interaction beyond just a constant steady vehicle curving action. In the case of only steady curving action, lateral wheel load appears to be more consistent through the body of a curve.

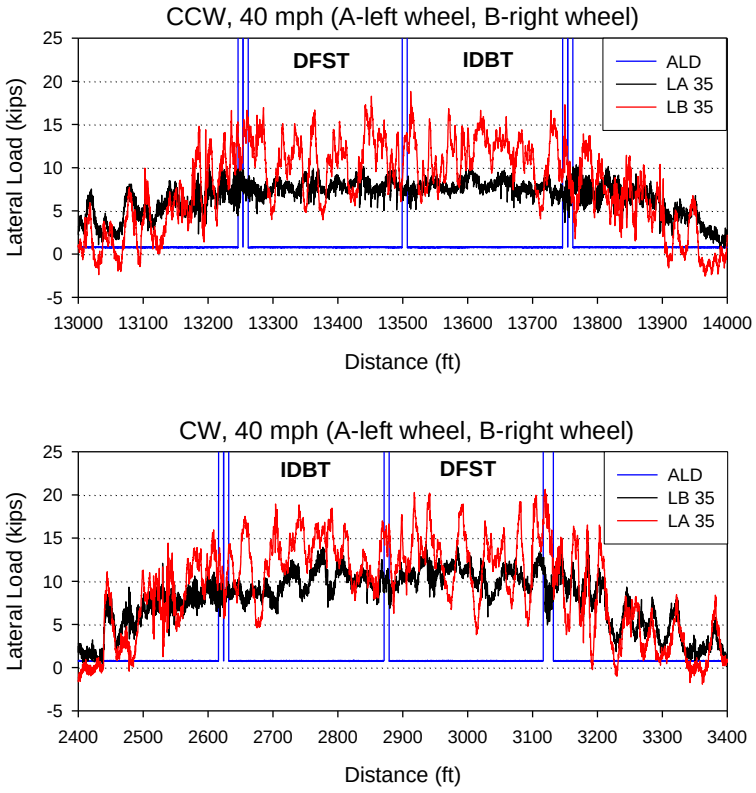

Figure 43. Lateral Wheel Loads via IWS (2003)

Figure 44 shows the comparison of lateral forces in terms of statistical values (minimum, average, maximum, and standard deviation) between Section 38 (slab track) and Section 31 (ballasted track). Although not as significant, especially in the CW running direction of the test train, the slab track test section still generated lower dynamic lateral wheel loads than the ballasted track with the same curvature and superelevation.

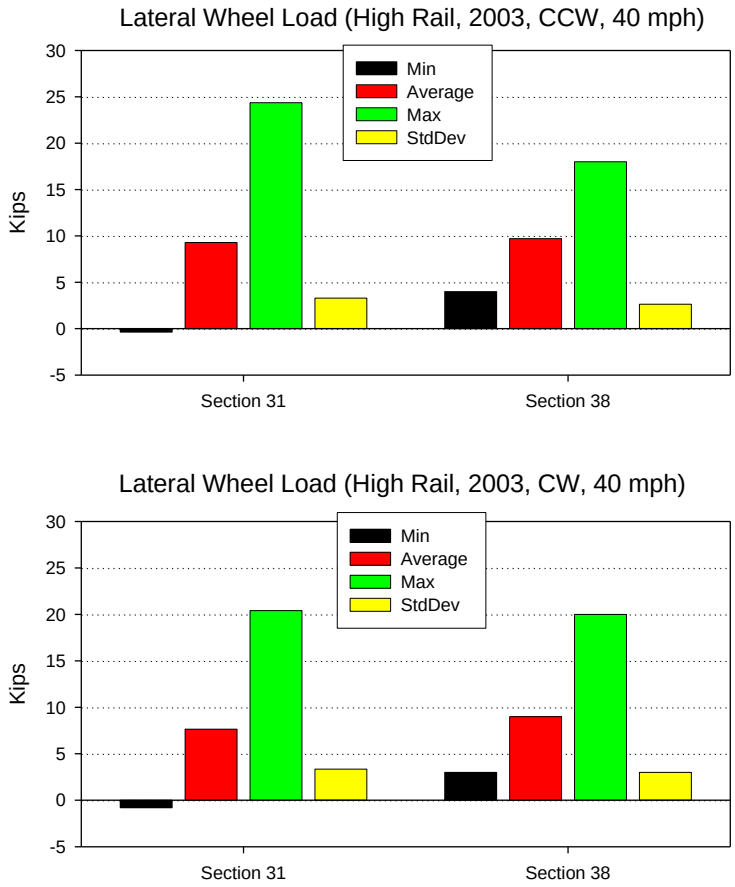

Figure 44. Section 38 (Slab Track) vs. Section 31 (Ballasted Track) Lateral Load in 2003

In the IWS tests conducted in 2004 and 2005, lateral forces measured on the high rail showed some significant lateral vehicle-track interaction at the transition areas, particularly when the test consist was exiting the slab track test section.

Figure 45 shows the test results obtained in 2005 for the test train traveling at 40 mph in both directions. As illustrated, lateral forces in the slab track did not change much from the data collected in 2003; however, at the ends of the slab track, there was significant variation of lateral wheel load (mainly on the high rail). The maximum lateral wheel load was about 27 kip. The variation was even more obvious when the test consist was exiting the slab track, regardless of the running direction on the slab track.

Similar trends of lateral wheel load variation in the transitions were observed in the IWS test data obtained in 2004, although they were not as large as in the data collected in 2005. A careful examination of the test results obtained in 2003 (shown in Figure 43) also indicated larger lateral forces in the transition areas, especially at the exit transition.

Therefore, the misalignment and its growth in the transition areas (report Section 4) had a significant effect on lateral vehicle-track interaction and should be a track geometric parameter that requires extra attention.

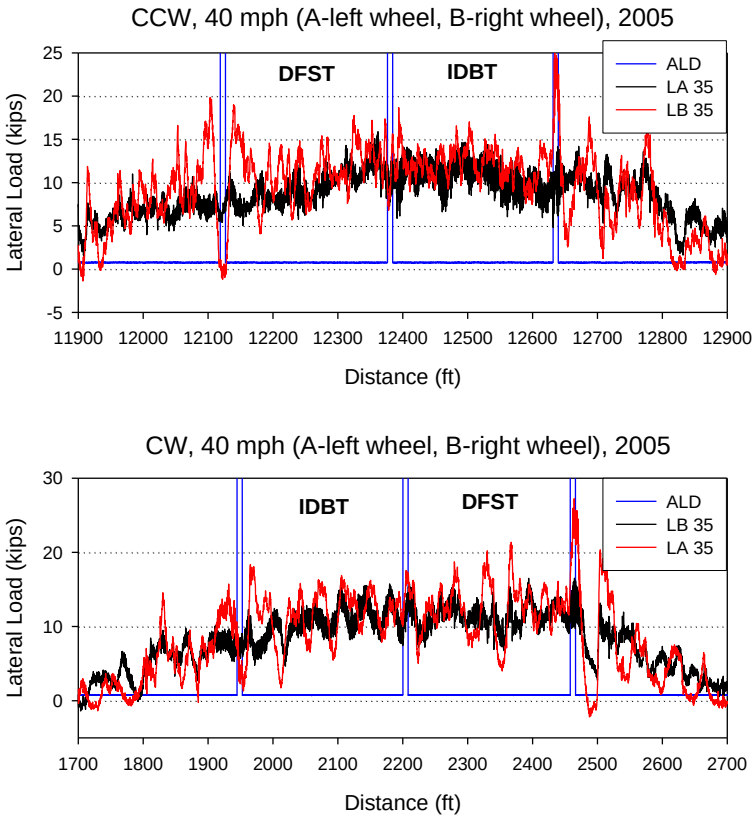

Figure 45. Lateral Wheel Loads via IWS (2005)

5.4 Wayside Load Station Test Results

As described earlier, four wayside load stations were installed for the IDBT and DFST to measure vertical and lateral wheel loads on both the high and low rails located at the center of each slab. Unlike IWS load measurements along a track under the same wheels, the wayside load stations measure load variations at the same track locations due to passes of various axles.

5.4.1 Vertical Wheel Load

Figure 46 shows the vertical wheel loads measured under the short test consist (see Figure 37) in August 2003. The results were collected when the test consist was traveling at 40 mph in the CCW direction. As mentioned earlier, the train was made up of a locomotive, an instrumentation coach, an empty tank car, and two HAL freight cars. The vertical wheel loads recorded on both rails showed obvious variation of axle loads from vehicle to vehicle in this short test consist.

As expected, the vertical wheel load recorded on the high rail was higher than on the low rail due to unbalanced operating speed. The maximum dynamic vertical wheel load was 55 kip and was recorded at the IDBT load station. The maximum vertical wheel load recorded at the DFST load station was 47 kip.

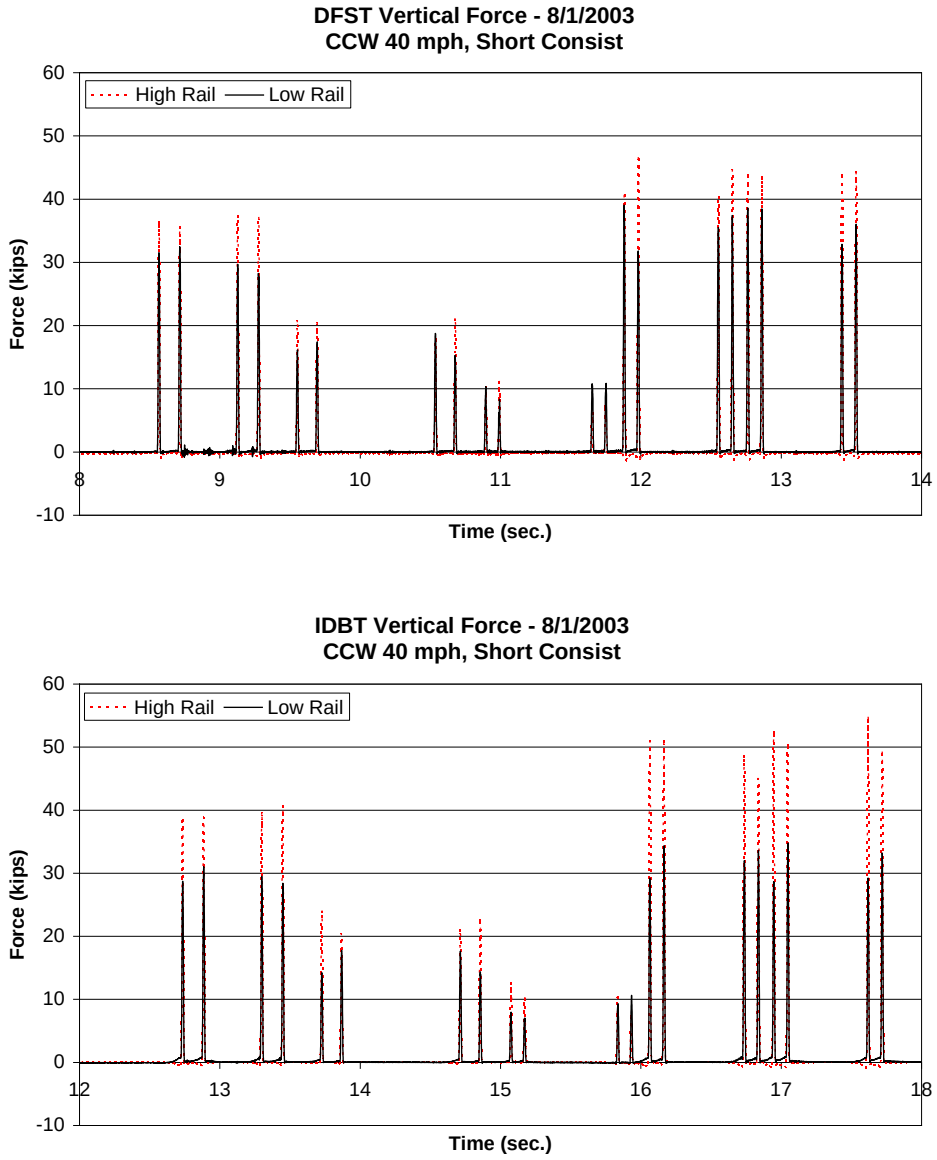

Figure 46. Vertical Wheel Loads via Wayside Load Station (2003): Train Traveling in CCW Direction

Figure 47 shows the vertical wheel loads measured when the short test consist was traveling at 40 mph in the CW direction. Again, the vertical wheel load recorded on the high rail was higher than on the low rail. The maximum dynamic vertical wheel load was 50 kip and was recorded at the DFST load station. The maximum vertical wheel load recorded at the IDBT load station was 47 kip.

Note, the vertical wheel loads shown in Figure 46 and Figure 47 will be used to interpret dynamic track responses such as vertical deformation recorded under the same short test consist presented in later sections.

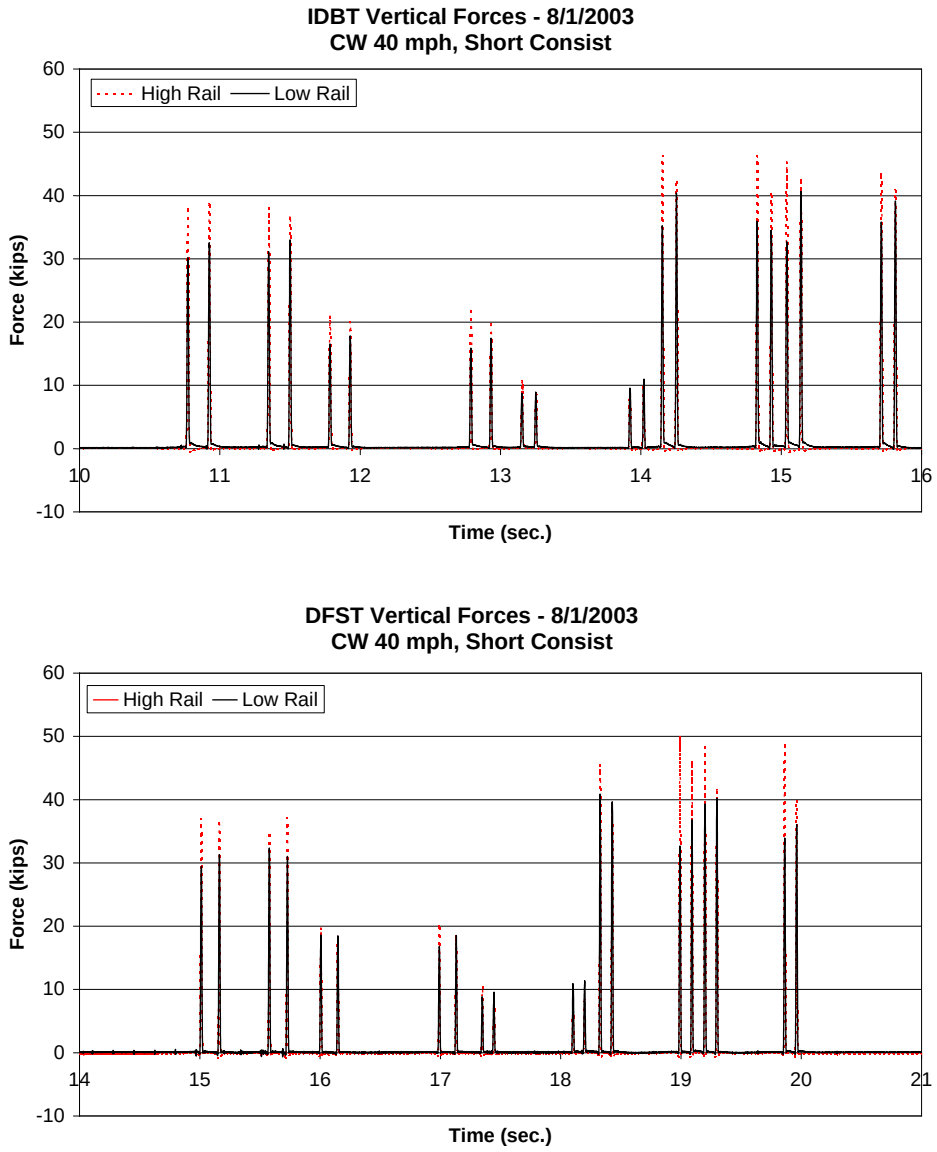

Figure 47. Vertical Wheel Loads via Wayside Load Station (2003): Train Traveling in the CW Direction

The actual measurements under train operation at FAST were taken three times in July through August 2003 and once in January 2005 and June 2006. To deal with greater amounts of data generated under each train, the data were processed to get the statistical values (maximum, minimum, average, and standard deviation) from all peak values obtained under all train passes from each of the three tests.

Figure 48 shows the statistical results for all three tests conducted in three different years. All data were recorded when the trains at FAST were running in the CCW directions. As shown from 2003 to 2006, no obvious increase existed of vehicle-track interaction for the vertical loads recorded on both the high and low rails in terms of these statistical values for either the DFST or the IDBT.

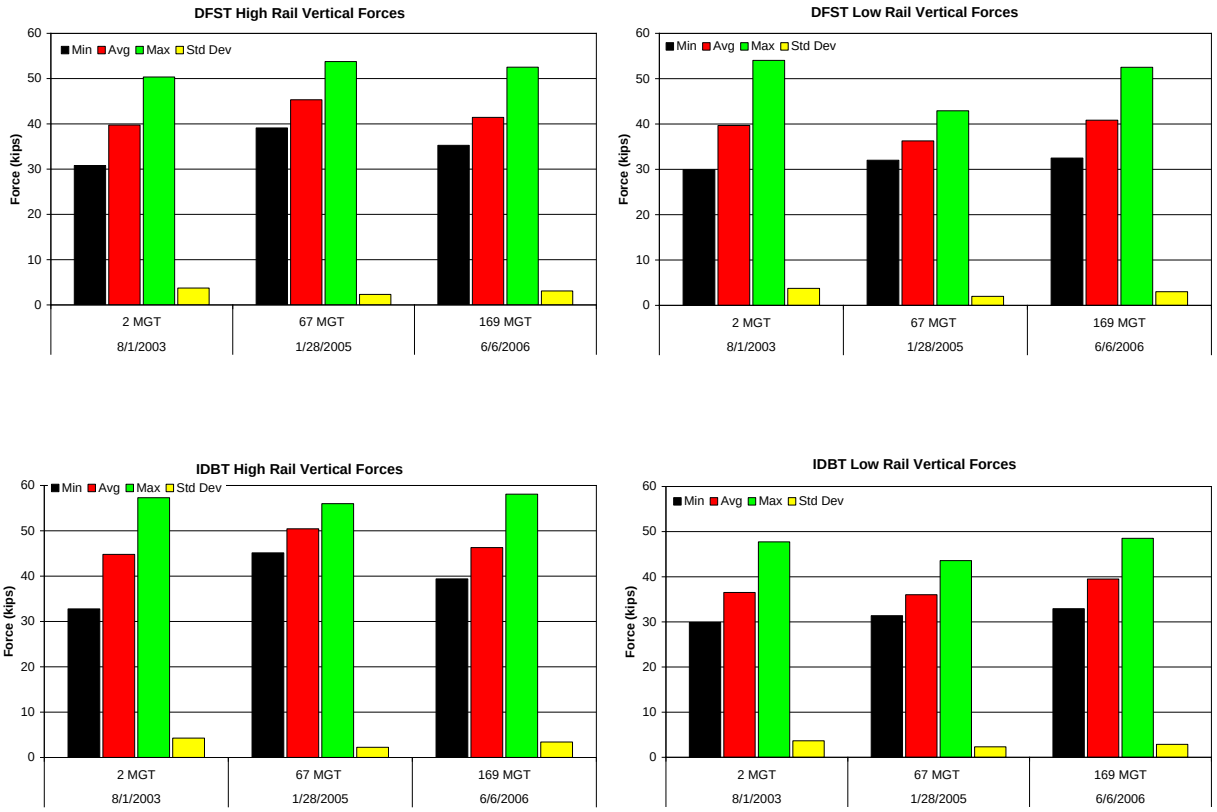

Figure 48. Vertical Wheel Loads Recorded under FAST Trains from 2003 to 2006

5.4.2 Lateral Wheel Load

Figure 49 shows the lateral wheel loads measured under the short test consist on August 1, 2003. The results were obtained when the test consist was traveling at 40 mph in the CCW direction. The lateral wheel loads recorded on both rails showed variations due to change of axle loads from vehicle to vehicle. Generally, higher axle loads would generate higher lateral wheel loads. The leading axle of each truck also generated higher lateral wheel load than the trailing axle. Under this run, the maximum lateral wheel load was close to 16 kip, recorded on the high rail in the IDBT.

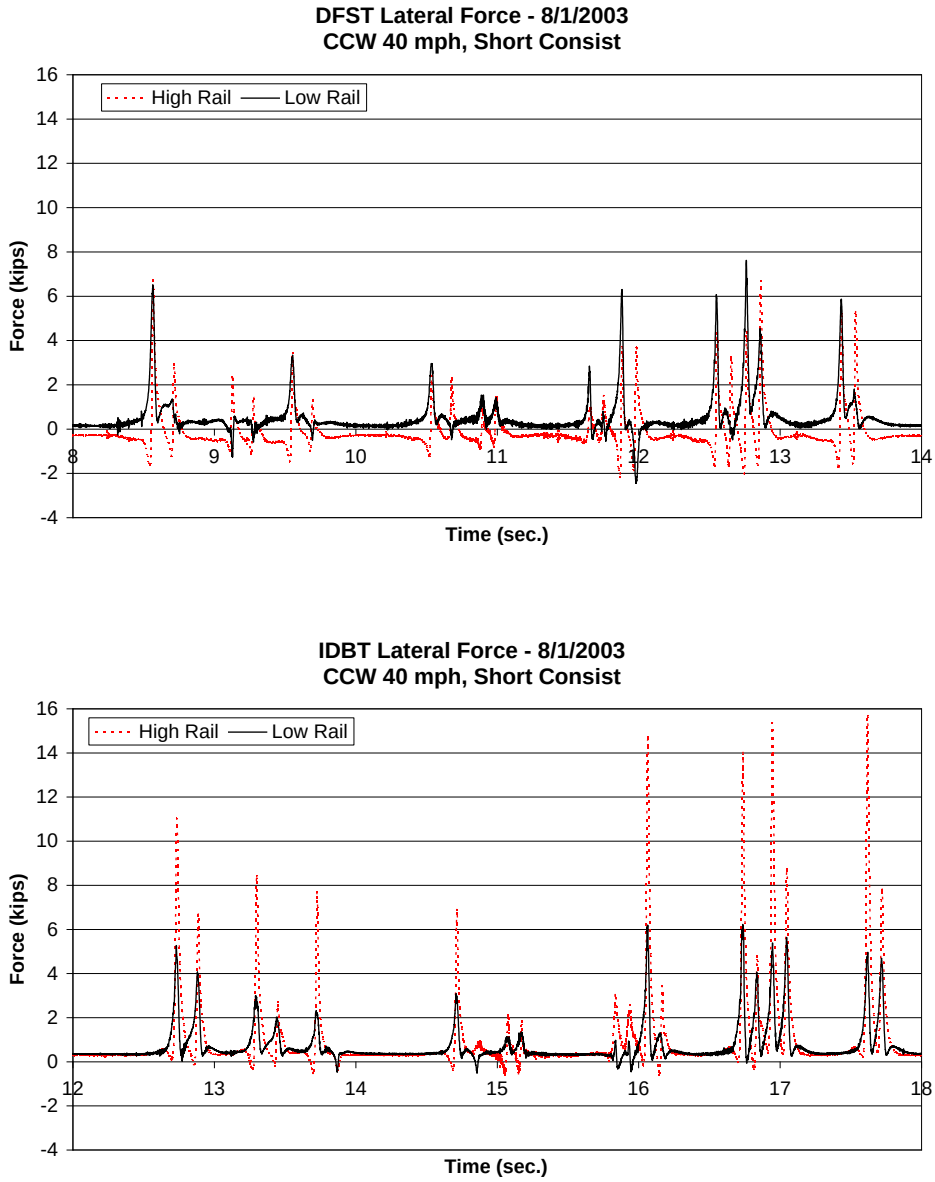

Figure 49. Lateral Wheel Loads via Wayside Load Station (2003): Train Traveling in the CCW Direction

Figure 50 shows the lateral wheel load recorded when the test train was traveling at 40 mph in the CW direction. The maximum lateral wheel load was 13 kip, recorded on the high rail from the DFST and IDBT load stations.

From the IWS test results (Figure 43 and Figure 45), lateral wheel loads generated on the high rail were generally higher than on the low rail. This was true in terms of wayside load station data shown in Figure 49 and Figure 50. However, a wayside load station measures lateral wheel loads only at a given track location; therefore, the difference in lateral wheel loads between the high and low rails may not be as large as that shown over the length of a given track segment.

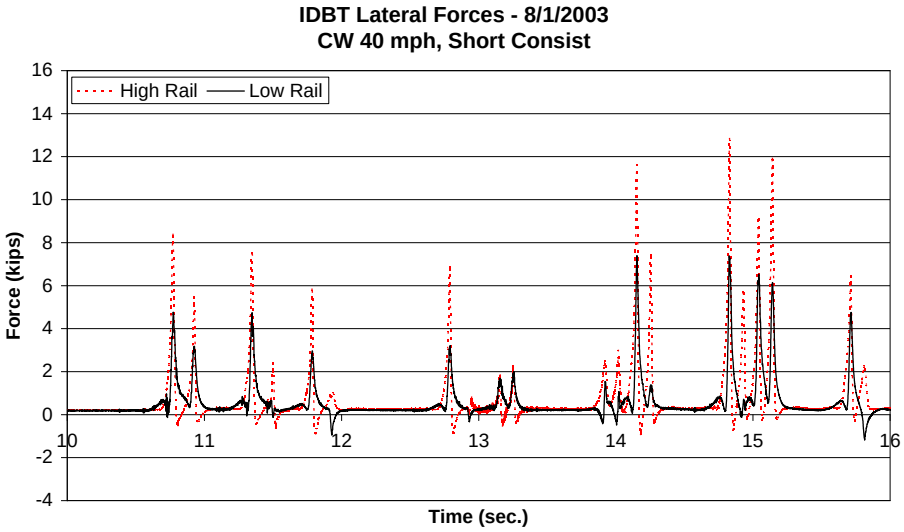

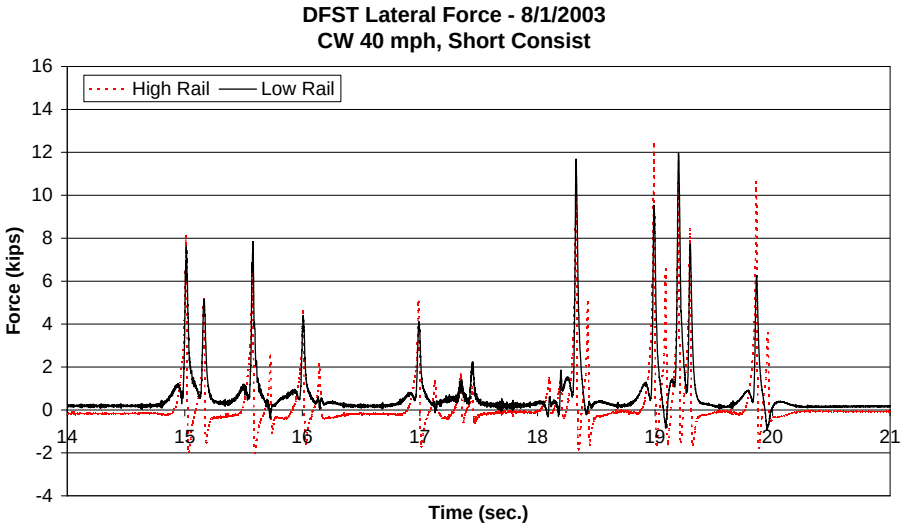

Figure 50. Lateral Wheel Loads via Wayside Load Station (2003): Train Traveling in CW Direction

Figure 49 and Figure 50 show the lateral wheel loads generated under the short test train. As mentioned, lateral wheel loads were also recorded every year under normal FAST train operation. For each FAST train pass, hundreds of axles passed by each load station. The data recorded were processed to obtain the statistical values (maximum, minimum, average, and standard deviation) from all peak values acquired under all train passes from each of the three tests.

Figure 51 shows the statistical results for all three tests conducted in 2003, 2005, and 2006. As shown, there was an increase of lateral wheel loads on both the high and low rails from the test conducted in 2003 to the one conducted in 2005. From 2005 to 2006, the trend was not quite obvious. As mentioned, lateral wheel loads on the low rail were generally lower than those on the high rail.

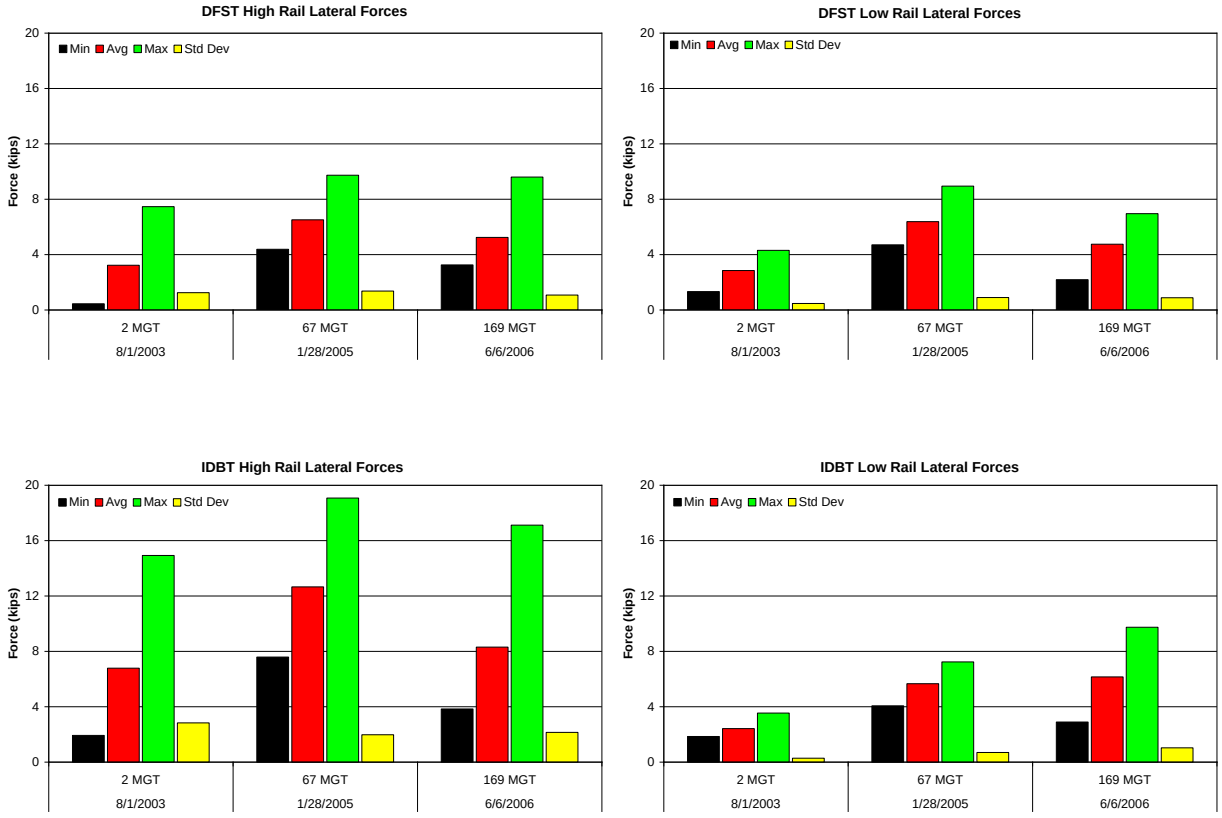

Figure 51. Lateral Wheel Loads Recorded under FAST Trains from 2003 to 2006

Finally, although test results are not presented in terms of single wheel, net axle, and truck side L/V ratios, no exceptions were in terms of vehicle-track interaction safety limits based on FRA's Track Safety Standards for Class 9 track.

6. Deflection of Slab Track Components under HAL

This section presents test results of dynamic deflection responses of slab track components under HAL train operation. The slab track test section was instrumented to measure the following dynamic track responses:

- Vertical and lateral rail-to-slab deflections
- Vertical deformation of concrete slab, soil cement subbase, and subgrade

Dynamic deformation was expected to occur primarily between the rails and the concrete slab, with less deformation expected from the subbase and subgrade layers because of the resilience of the slab track test section that was provided mainly from the rubber pads (DFST) or the rubber boots/pads (IDBT) and the firm subbase layer and subgrade.

6.1 Instrumentation for Deformation Measurement

6.1.1 Linear Variable Differential Transformer for Rail-to-Slab Deflection

Field instrumentation was set up for measuring vertical and lateral rail deflections relative to the concrete slab. In the case of the DFST, rail-to-slab deflection essentially reflects the deformation due to direct-fixation rail fastenings and pads installed between the rail base and the concrete slab. In the case of the IDBT, rail-to-slab deflection reflects the deformation due to the rail fastening between the rail base and the block ties. More importantly, it reflects the deformation due to rubber boots and pads installed between the tie blocks and the concrete slab (Phase II slab for IDBT).

Linear variable differential transformers (LVDTs) were used to measure vertical and lateral rail-to-slab deflections under train operation. Like all other wayside transducers, rail-to-slab deflection transducers (LVDTs) were used for both the high and low rails near the center of each slab (IDBT or DFST); however, because of the space required for each transducer, the wayside transducers were not all positioned in the same manner at the same locations. Figure 52 shows the actual layout of most wayside transducers for the IDBT (also for the DFST).

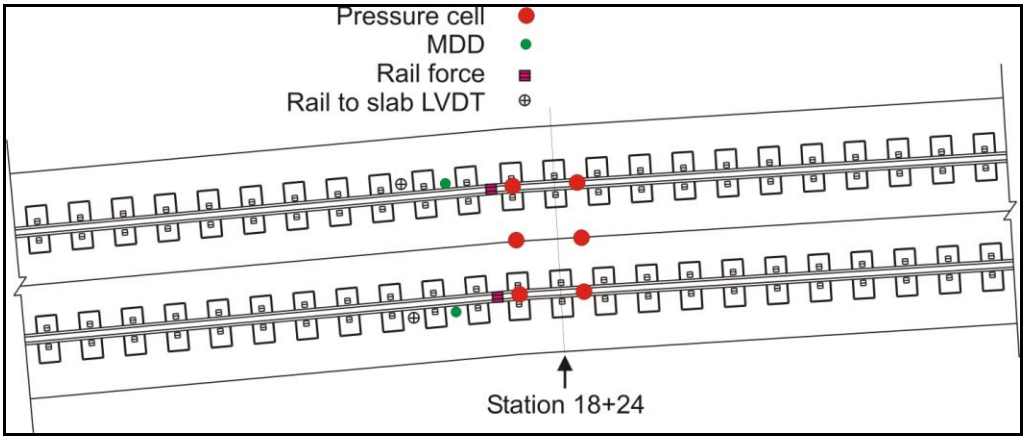

Figure 52. Layout of Wayside Transducers for IDBT (also for DFST)

Figure 53 shows the LVDT transducers installed on both the IDBT and the DFST to measure vertical and lateral rail-to-slab deflections under dynamic wheel loads. As shown, the reference plates were set up on the slab surface so that the deflection could be measured between the rail base and these references using LVDT transducers.

Similar to the wayside load stations, all wayside transducers including rail-to-slab deflection transducers used a sampling rate of 2,048 Hz with an antialiasing low-pass filter of 256 Hz.

Figure 53. LVDT for Vertical and Lateral Rail-to-Slab Deflection (IDBT and DFST)

6.1.2 Multidepth Deflectometers for Deformation in Slab, Subbase, and Subgrade

Multidepth deflectometers (MDD) were installed at four locations by CTLGroup technicians.[2] These locations were near the high and low rails of the IDBT and DFST (see Figure 52 for locations relative to other wayside transducers). For each location, a hole was drilled 10 ft deep through the concrete slab, subbase, and subgrade following the slab track construction. An MDD fixture with four deformation transducers was installed in each hole to measure vertical deformation at four different depths.

Figure 54 shows the layout of four MDD transducers in each hole. These transducers were intended to measure vertical deformation under dynamic wheel loads at four different depths in the concrete slab layer, the subbase layer, and the subgrade. ML in this figure stands for measurement location. The depths of ML1 and ML3 were 5.8 and 2.8 ft, respectively. Figure 55 shows before-and-after installation views of the MDD fixtures.

[2] CTL Group provided the MDD fixtures for the test. Information on the MDD measurement technique can be found at www.CTLgroup.com.

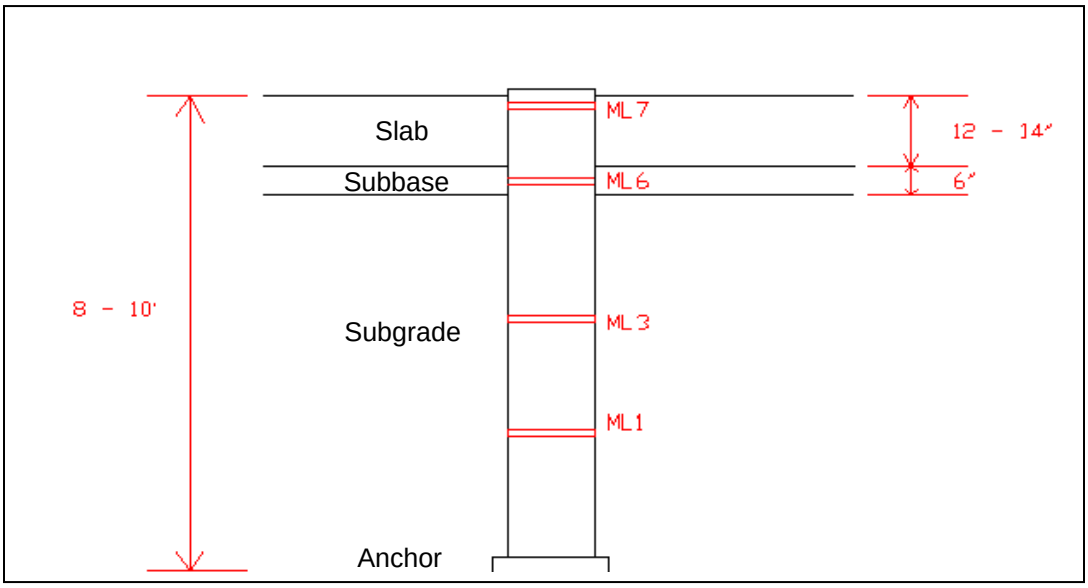

Figure 54. MDD for Vertical Deformation at Four Different Depths

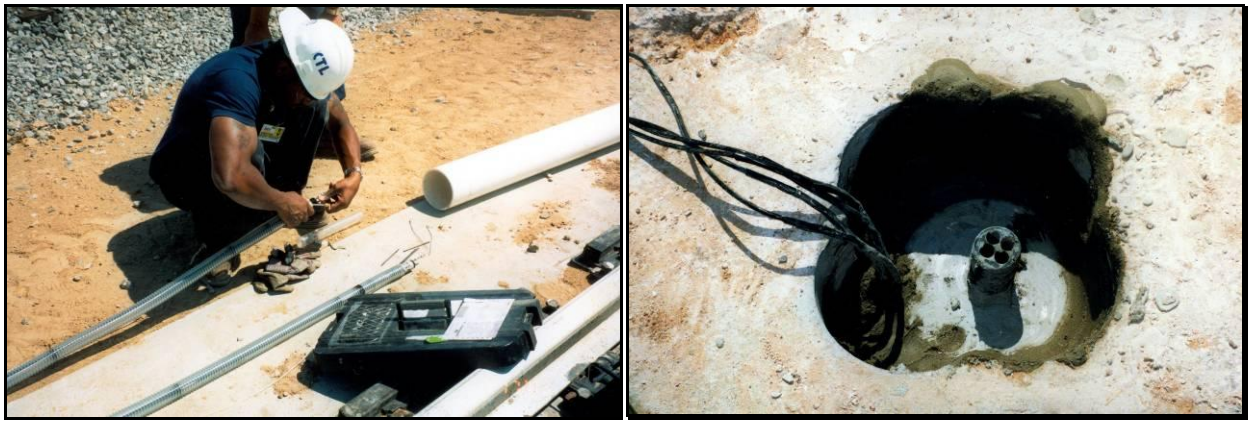

Figure 55. MDD before and after Installation in Slab Track

6.2 Test Results

6.2.1 Vertical Rail-to-Slab Deflection

Figure 56 shows the test results of vertical rail-to-slab deflections for both DFST and IDBT as recorded under the short test train traveling at 40 mph in the CCW direction. As illustrated, larger vertical deflection was generated in the DFST (0.22 in on the high rail) than in the IDBT (0.15 in on the high rail), consistent with the track modulus and stiffness test results shown in Figure 31 and Figure 32 (also similar to the laboratory test results listed in Section 2.2.4 and Section 2.2.5). The more resilient DFST generated larger rail-to-slab deflection than the IDBT.

Both track stiffness and actual load environment need to be taken into account when interpreting deflection results. As a result of larger vertical wheel loads on the high rail than on the low rail, the deflection generated from the high rail was generally greater.

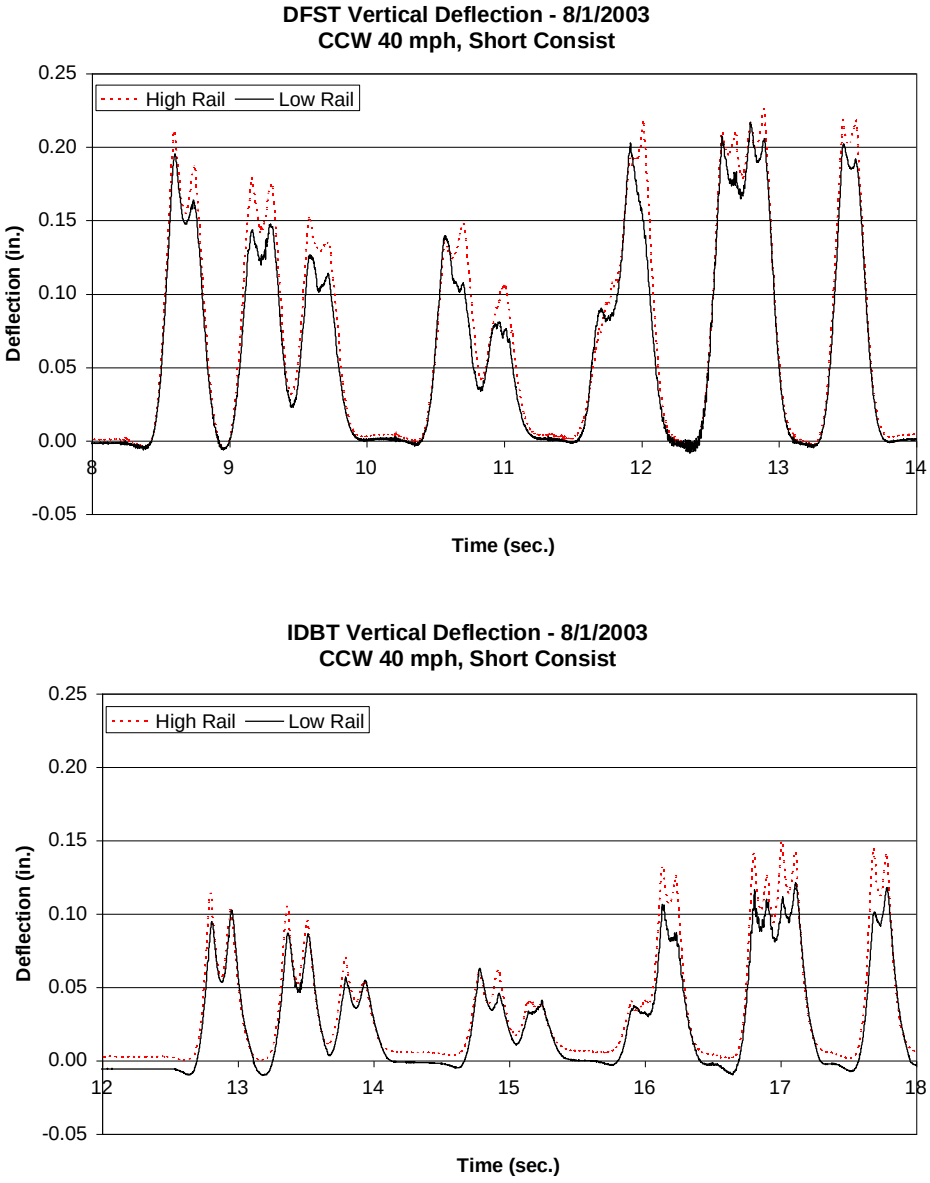

Figure 56. Vertical Rail-to-Slab Deflection under Short Test Consist Traveling in the CCW Direction

The overlapping effects of two adjacent axles under each truck. For the vertical wheel loads shown in Figure 46 and Figure 47, axles under the same truck were essentially independent of each other in terms of dynamic wheel loads generated under each wheel. For the dynamic rail-to-slab deflection, most deflection did not return when the dynamic loading of the following wheel under the same truck occurred.

Figure 57 shows the vertical rail-to-slab deflection test results for both IDBT and DFST under the short test train when it was traveling in the CW direction. The trends of test results were similar to those recorded in the test run of the CCW direction (Figure 56); however, vertical rail deflections in DFST were larger (0.25 in) than those shown in Figure 56 (0.22 in). This was due to the higher generated vertical dynamic wheel loads when the short test train was traveling in the CW direction as shown in Figure 46 and Figure 47.

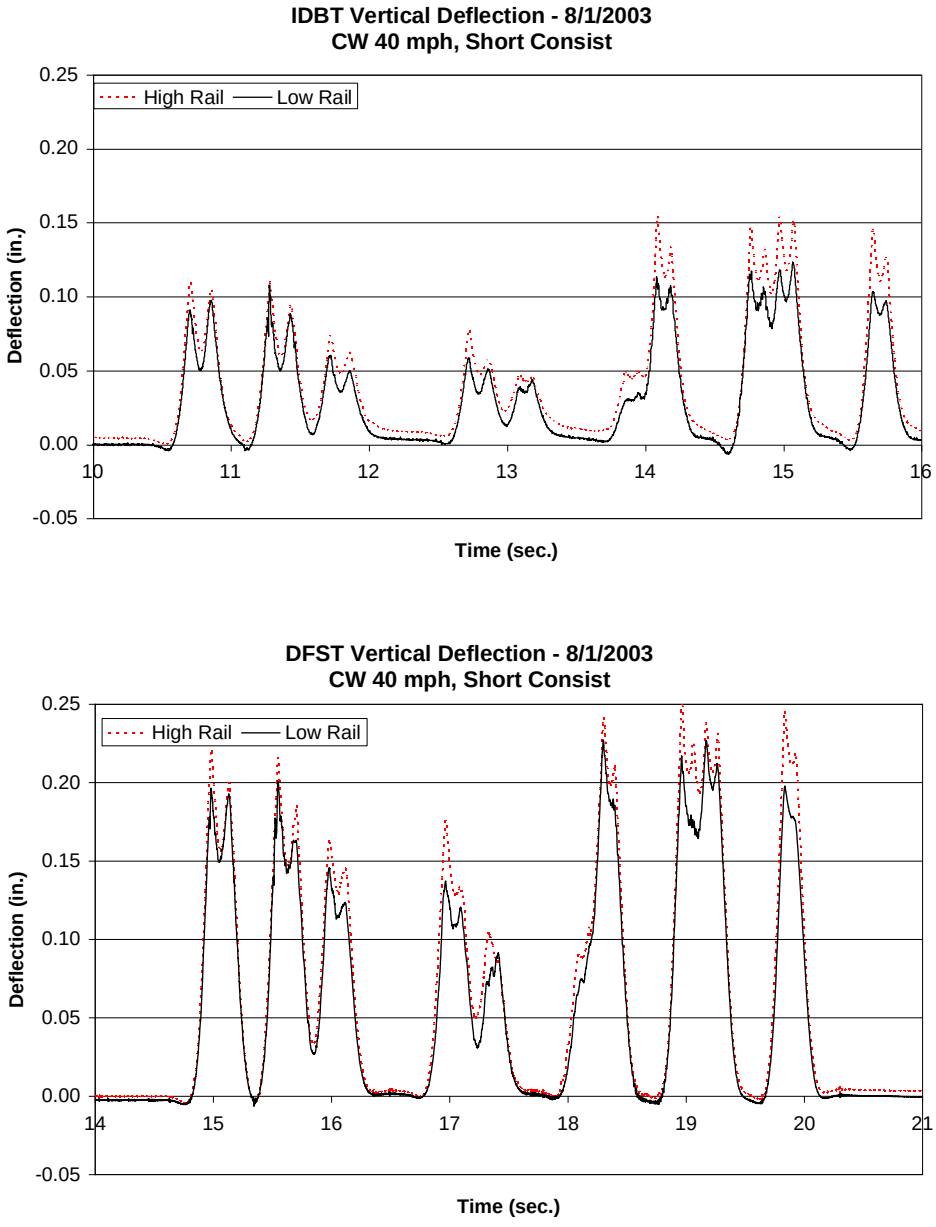

Figure 57. Vertical Rail-to-Slab Deflection under Short Test Consist Traveling in CW Direction

In addition to the measurements taken under the short test train in 2003, rail-to-slab deflections were measured under HAL train operations at FAST in the CCW direction. The dates listed below indicate when rail-to-slab deflections were measured. These dates were basically the same as those for all other measurements obtained via the wayside load stations.

- July 30 and August 1, 2003 (0.6 MGT)
- January 24 and 25, 2005 (65 MGT)
- June 5 and 6, 2006 (169 MGT)

Figure 58 shows the statistical results (minimum, average, maximum, and standard deviation) obtained from each of the three tests conducted from 2003 to 2006. The statistical values were based on the peak values corresponding to all passing wheels from each test conducted.

Again, the DFST exhibited larger vertical rail deflections than the IDBT. Only a minor increase of rail deflection for the high rail from 2003 to 2006 for the DFST was observed and even less for the low rail. The smaller deflection recorded on the low rail in January 2005 was due to lower dynamic vertical wheel loads (see Figure 48). Not only should track stiffness be taken into account but dynamic wheel loads should also be considered to interpret deflection results.

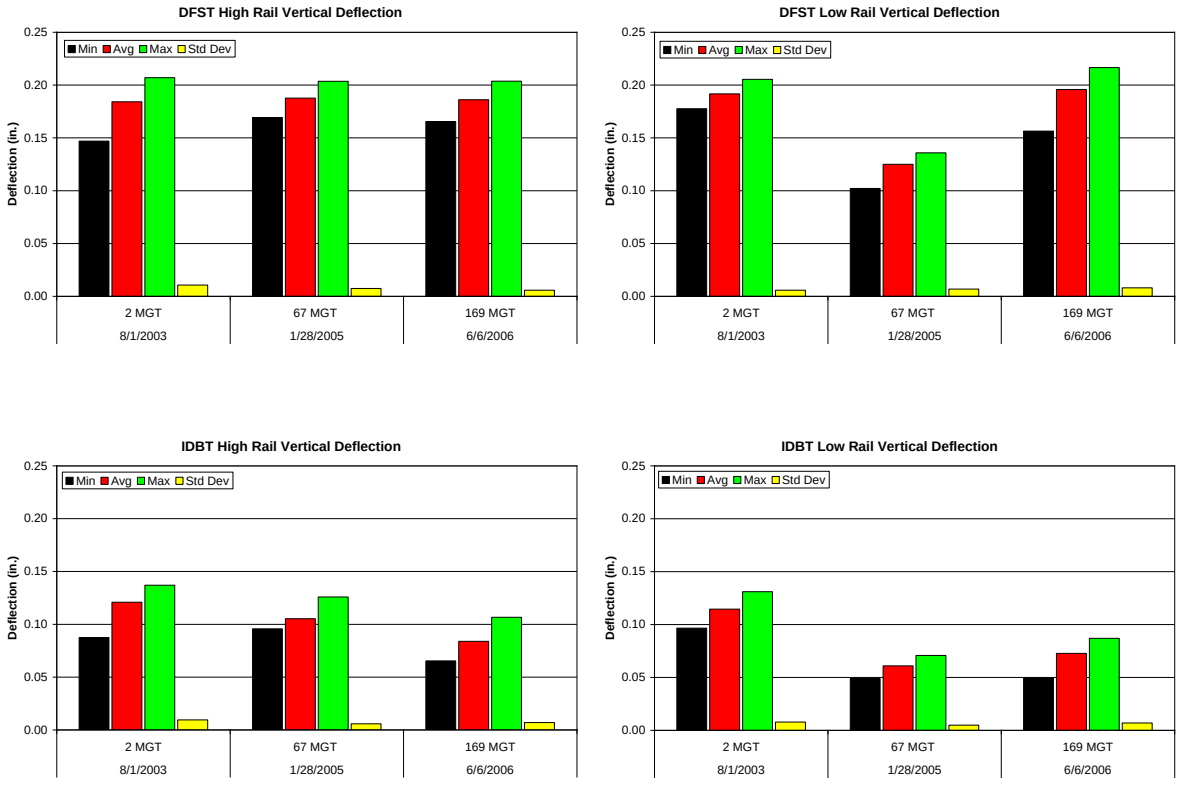

Figure 58. Vertical Rail-to-Slab Deflection under FAST Train (2003–2006)

For the IDBT, both the high and low rails showed a gradual decrease of vertical rail-to-slab deflections, especially if taking into account the vertical wheel loads recorded at the same time (see Figure 48). This trend was consistent with the gradual increase in track modulus or track stiffness for the IDBT (refer to Section 4).

6.2.2 Lateral Rail-to-Slab Deflection

Figure 59 shows the test results of lateral rail-to-slab deflections for both the DFST and the IDBT obtained under the short test train traveling at 40 mph in the CCW direction. The maximum lateral rail-to-slab deflection was close to 0.06 in for both the IDBT and the DFST. In general, the lateral deflections were larger on the high rails than on the low rails due to higher lateral rail forces generated. Again, to interpret lateral rail deflection results shown in Figure 59, the lateral wheel loads shown in Figure 49 need to be considered. For example, in the CCW run shown in this example, lateral wheel loads generated on the DFST were actually lower than those on the IDBT.

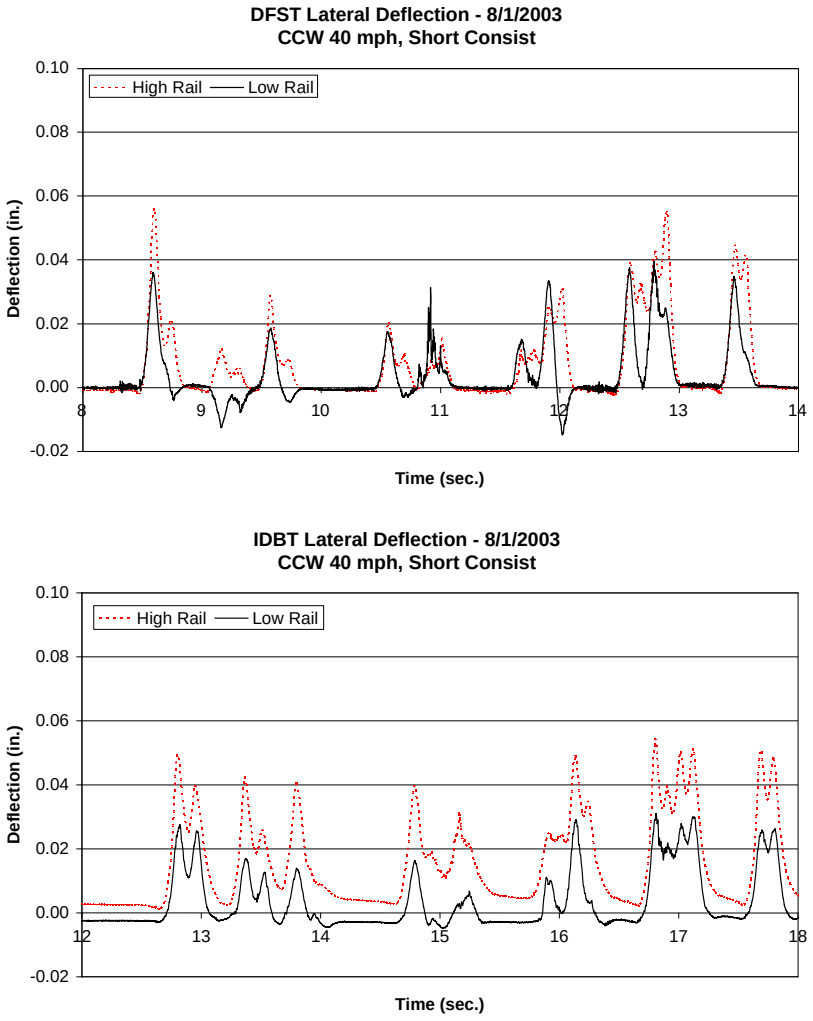

Figure 59. Lateral Rail-to-Slab Deflection under Short Test Consist Traveling in CCW Direction

Figure 60 shows the test results recorded when the short test train was traveling in the CW direction. The maximum lateral rail-to-slab deflection was 0.1 in for the DFST and close to 0.08 in for the IDBT. Again, the lateral rail deflections generated on the high rail were larger than those on the low rail, reflecting higher lateral wheel loads on the high rail.

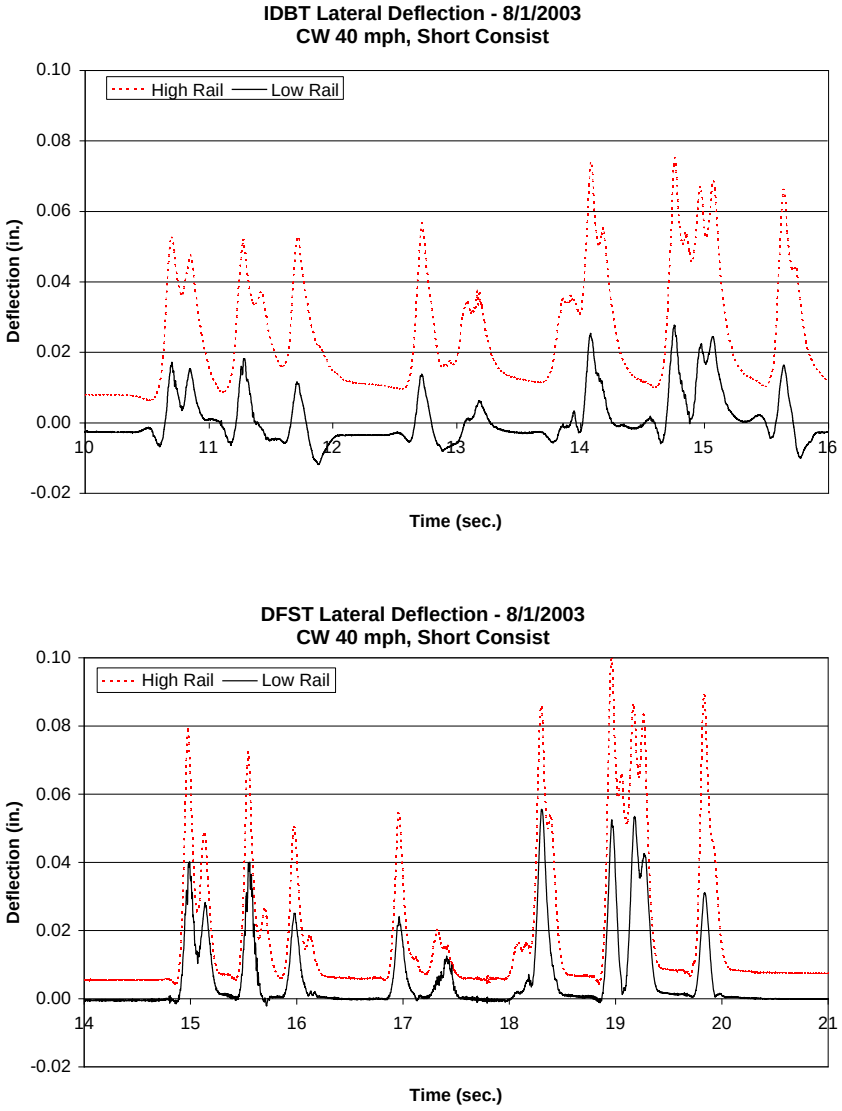

Figure 60. Lateral Rail-to-Slab Deflection under Short Test Consist Traveling in CW Direction

Figure 61 shows the statistical values of lateral rail-to-slab deflections obtained from the three tests conducted in 2003, 2005, and 2006. The statistical values were obtained from peak values corresponding to all passing wheels for the HAL trains at FAST, recorded in each of the three tests conducted.

The DFST again generated larger lateral rail-to-slab deflections than the IDBT. The high rail always exhibited larger deflection than the low rail for both tracks due to higher lateral wheel loads.

From 2003 to 2006, the general trends of lateral rail-to-slab deflection were increasing and appeared consistent with the trend of decreasing gage strength for the DFST (Section 4).

During that same period, the general trends of lateral rail-to-slab deflections were decreasing, particularly for the deflections measured on the high rail for the IDBT. As shown in Figure 58, these trends were consistent with those of vertical rail-to-slab track deflections.

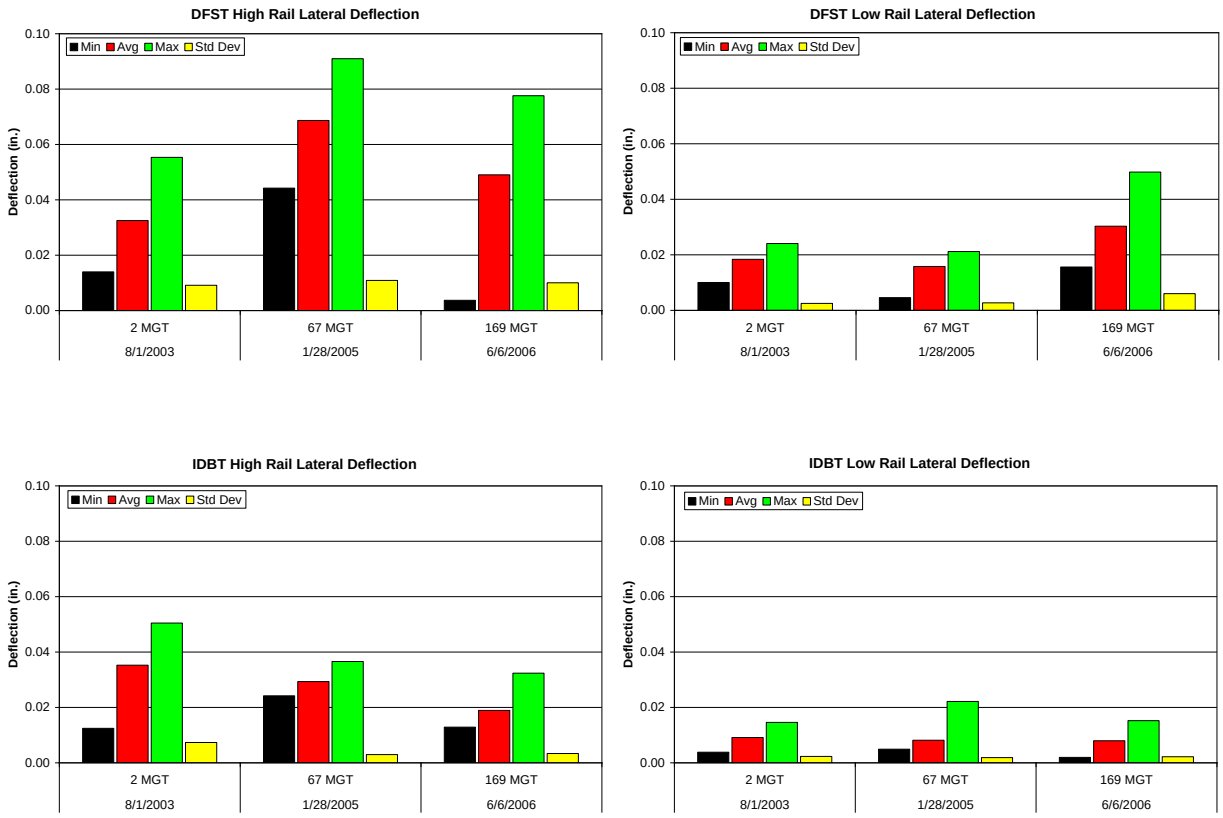

Figure 61. Lateral Rail-to-Slab Deflection under FAST Train (2003–2006)

6.2.3 Vertical Deformation in Slab, Subbase, and Subgrade Layers

Although four locations were instrumented with MDD and each location had four transducers to measure deformation at four different depths, only a few MDD transducers performed properly (outputting data signals). Fortunately, those were enough to verify what was already known. Only small deformation occurred from the layers underneath the concrete slab.

Figure 62 shows the MDD data that were collected under the short test train traveling at 40 mph in the CCW direction. For the DFST, the MDD data included the subgrade deformation (ML3 in Figure 54, or approximately 2.8 ft from the subgrade surface) under both rails. For the IDBT, the MDD data included the subbase deformation under the low rail (inside rail) and the subgrade deformation at two depths (ML3 and ML1 in Figure 54, or 2.8 and 5.6 ft from the subgrade surface) under the high rail (outside rail).

As shown, under HAL wheel loads, the maximum deformation in the subbase and subgrade (2.8 ft) was less than 0.06 in while the subgrade deformation at a depth of 5.8 ft was only 0.01 in.

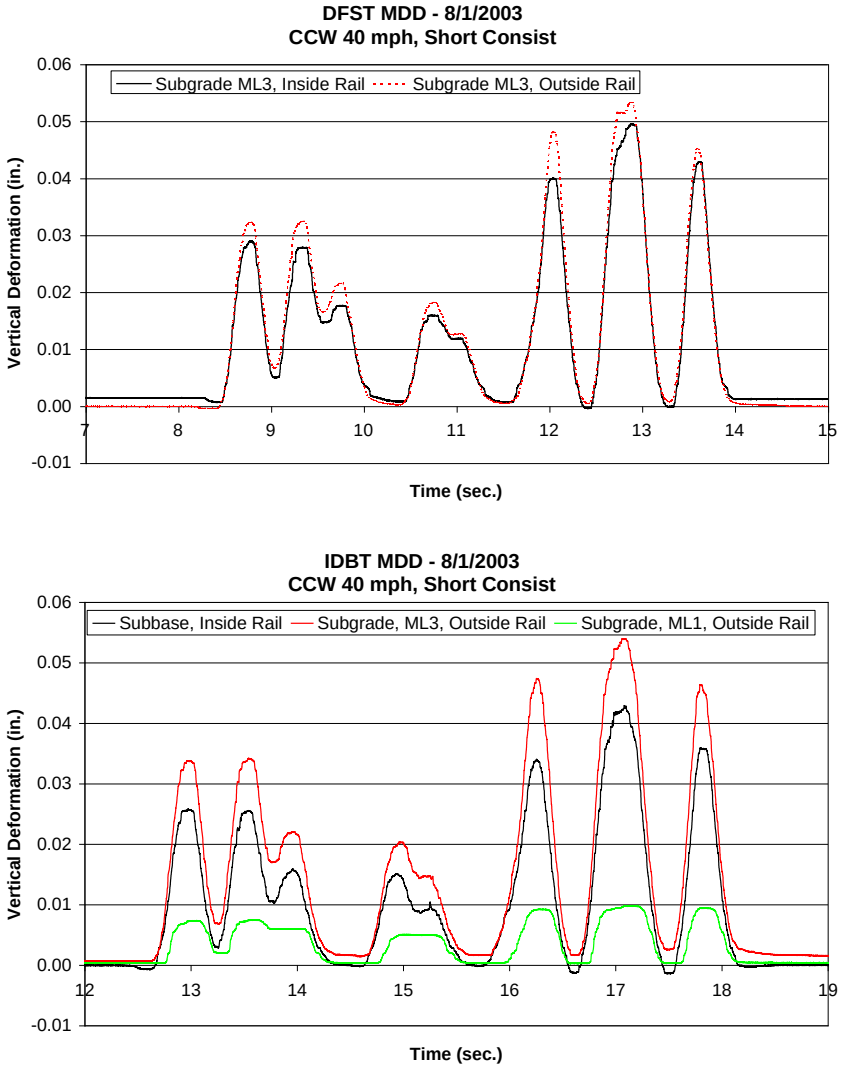

Figure 62. MDD Test Results under Short Test Train Traveling in CCW Direction

Figure 63 shows the MDD test results that were recorded when the short consist was traveling at 40 mph in the CW direction. Again, vertical deformation of less than 0.06 in was in the subbase and subgrade at 2.8 ft and less than 0.01 in at the subgrade depth of 5.6 ft.

As discussed earlier, two adjacent wheels under each truck overlapped each other in terms of rail-to-slab deflection response. In terms of subbase and subgrade deformation—as Figure 62 and Figure 63 show—four adjacent wheels under two closely adjacent trucks can be considered as one load cycle, especially if all four axles have similar weights.

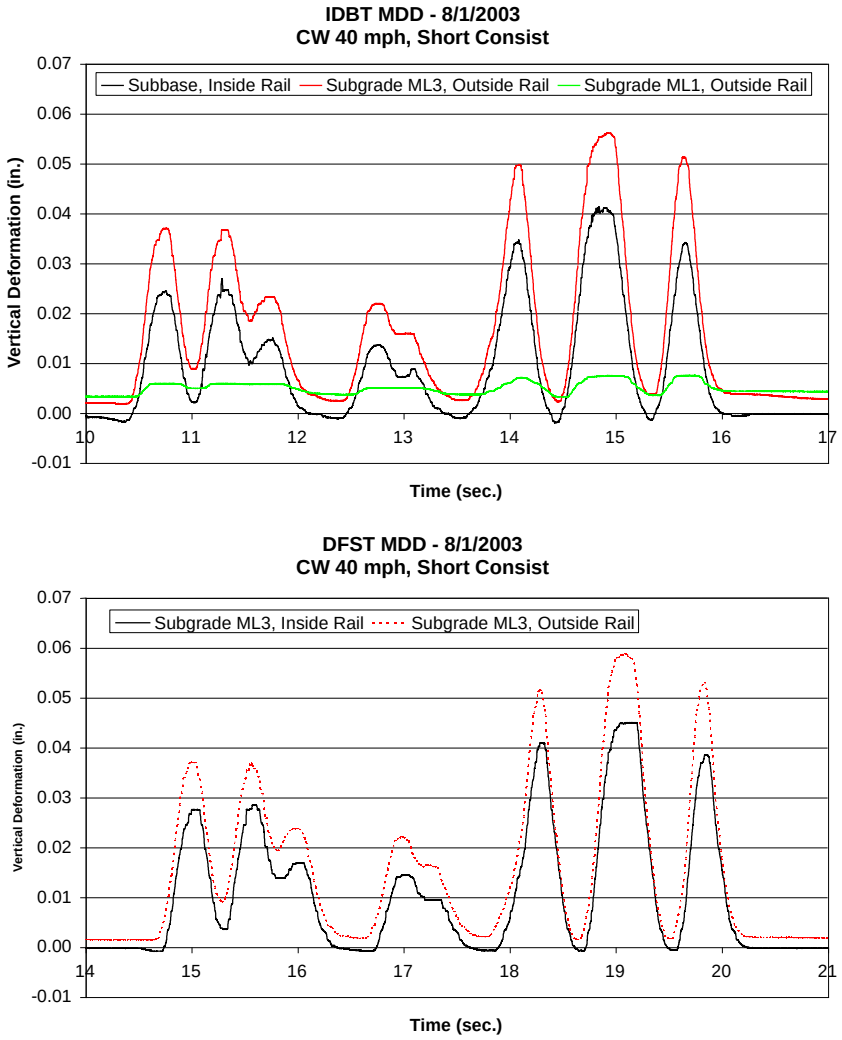

Figure 63. MDD Test Results under Short Test Train Traveling in CW Direction

MDD data were also recorded as part of the wayside measurements conducted in 2003, 2005, and 2006. Little change was observed as far as subbase and subgrade deformation recorded from those MDD transducers that worked. For example, Figure 64 shows the MDD test results obtained in the subgrade at two different depths (2.8 and 5.6 ft) under the train operation at FAST in June 2006. As illustrated, less than 0.06 in was recorded at the subgrade depth of 2.8 ft and less than 0.015 in, at 5.6 ft.

Figure 62 through Figure 64 show that, because of the insignificant deformation, no statistical analysis was performed for the test data collected under trains at FAST from 2003 to 2006.

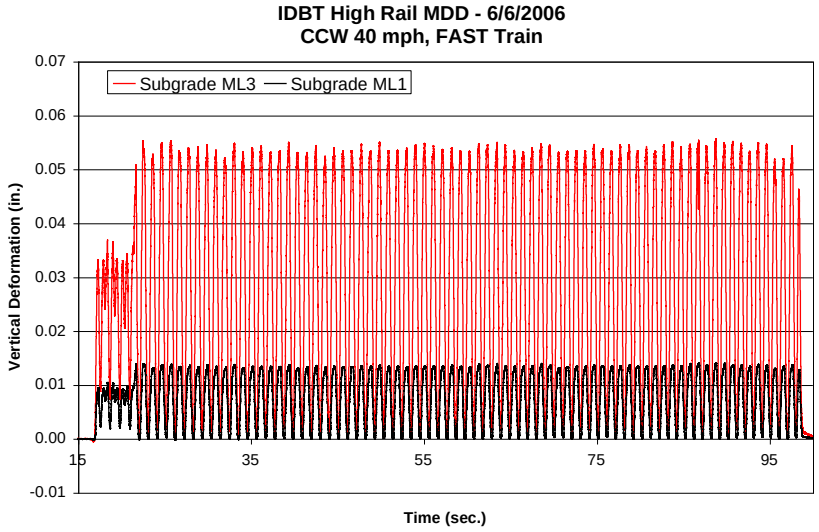

Figure 64. Subgrade Deformation under FAST Train Traveling in CCW Direction

7. Subgrade Pressure under Slab Track

Subgrade pressure was measured under the slab track testing program to quantify the load distribution under the concrete slab and the soil cement subbase layer during HAL train operation. Pressure transmitted to the subgrade was expected to be well below the subgrade soil strength because of the rigid concrete slab and the stiff subbase layer.

7.1 Subgrade Pressure Cell and Installation

Pressure cells made by Geokon (model 3500) were used for subgrade pressure measurements. For each type of slab track (IDBT or DFST), six pressure cells were installed at the central area of each slab. Figure 65 shows the general arrangements of six pressure cells on the subgrade surface. As illustrated, three cells were arranged across the track under a tie. The three other cells were arranged across the track in the crib (between fasteners). Figure 52 shows the relative positions of these six pressure cells with respect to other wayside transducers.

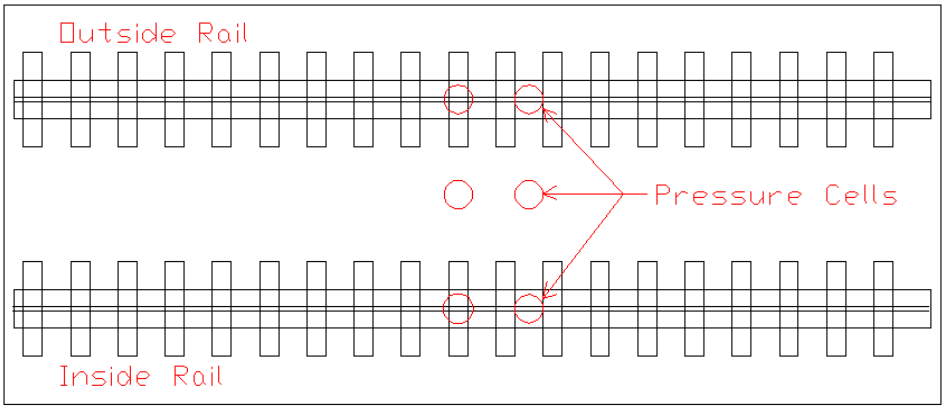

Figure 65. Arrangement of Subgrade Pressure Cells

To install a pressure cell on the subgrade surface, a hole was dug through the finished subbase soil cement layer following its final compaction. Silica sand was applied to the hole to provide a uniform bearing for the pressure cell. After the pressure cell was placed and positioned on the subgrade surface, more silica sand was applied to cover it. Finally, the track crew added newly mixed soil cement to the holes in a single layer, and a hand compactor was used to compact the soil cement above the pressure cell. Figure 66 illustrates the procedure of installing the subgrade pressure cells.

Subgrade pressure data under HAL train operation were collected using the same data acquisition system as for other wayside transducers, the same data sampling rate of 2,048 Hz, and the same antialiasing low-pass filter of 256 Hz.

Although subgrade pressure data were collected three times (in July through August 2003, January 2005, and October 2005), the data collected in 2005 was determined later that it could not be considered reliable because of significant drifting of pressure readings in some pressure cells.

Figure 66. Installation of Subgrade Pressure Cells

7.2 Test Results

Figure 67 shows the subgrade pressure test results under the short test consist traveling at 40 mph. The data were obtained in both CCW and CW directions in August 2003. For the DFST and IDBT, three pressure transducers were installed under the tie and three others, under the crib.

As shown, the maximum subgrade pressure under HAL vehicles was 12 psi, recorded under the outside (high) rail in the IDBT. For the DFST, the maximum subgrade pressure was 11 psi, recorded under the inside (low) rail. Under this short consist, heavier axle loads generated larger subgrade pressures. Regardless, the maximum subgrade pressures generated under HAL traffic were well below the compressive strengths of the subgrade soil, which were above 50 psi.

The relatively low subgrade pressure with respect to soil strength explains the small amount of subgrade deformation. As with the deformation responses of the subgrade, four adjacent wheels under two closely adjacent trucks can be considered as one load cycle as far as subgrade pressure is concerned.

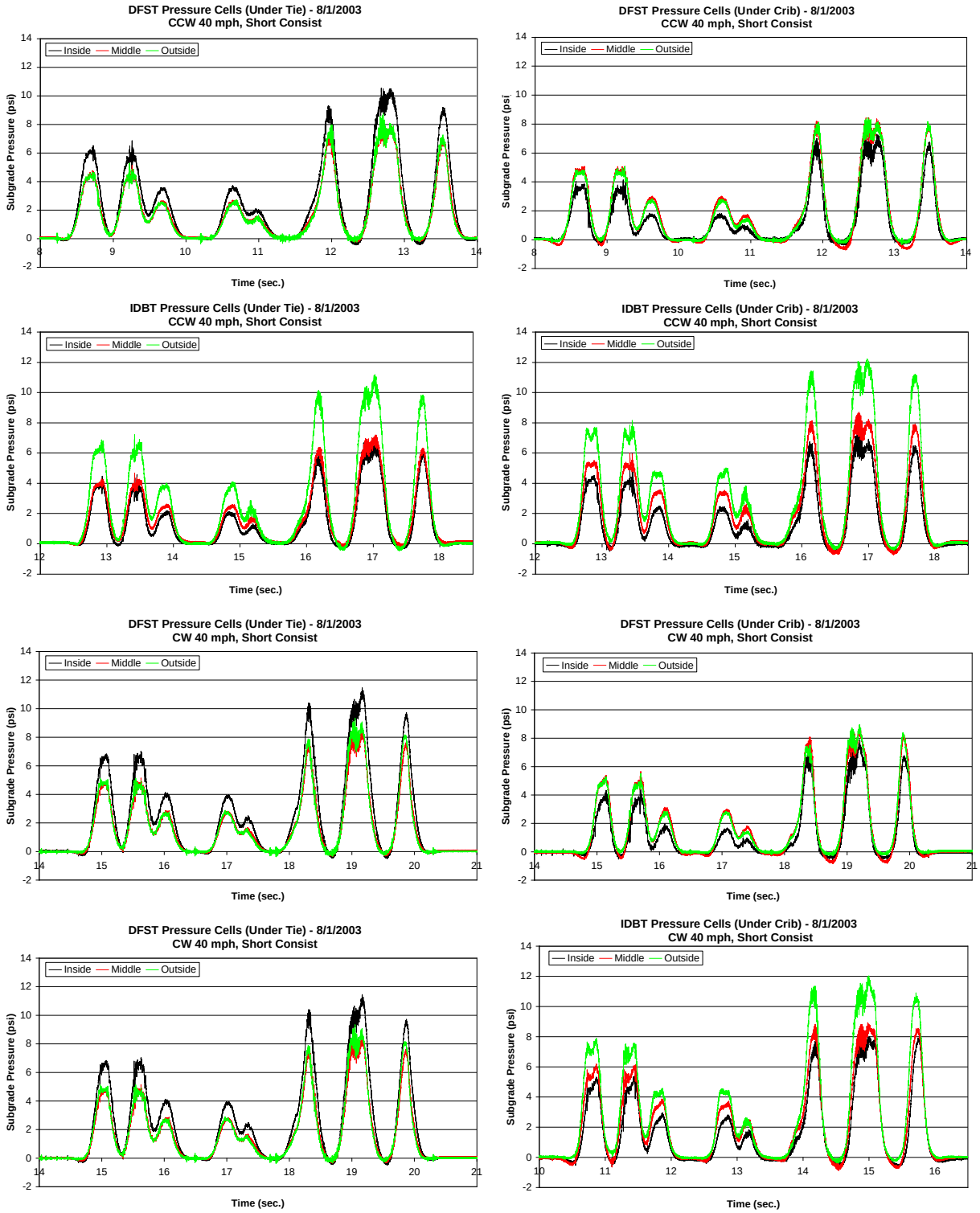

Figure 67. Subgrade Pressure under Short Test Consist

Figure 68 shows the statistical values (minimum, average, maximum, and standard deviation) of subgrade pressures recorded under the train operation at FAST in 2003. Pressures were obtained based on the peak values corresponding to all passing wheels recorded during that test. Again, the maximum subgrade pressure was lower than 12 psi. In addition, subgrade pressure did not vary much from under the tie to under the crib for both the DFST and the IDBT. Across the track, the distribution of subgrade pressure appeared to be affected by the distribution of vertical wheel load between the two rails, particularly for the IDBT; for instance, higher vertical wheel load on the high (outside) rail caused higher subgrade pressure on the high rail side.

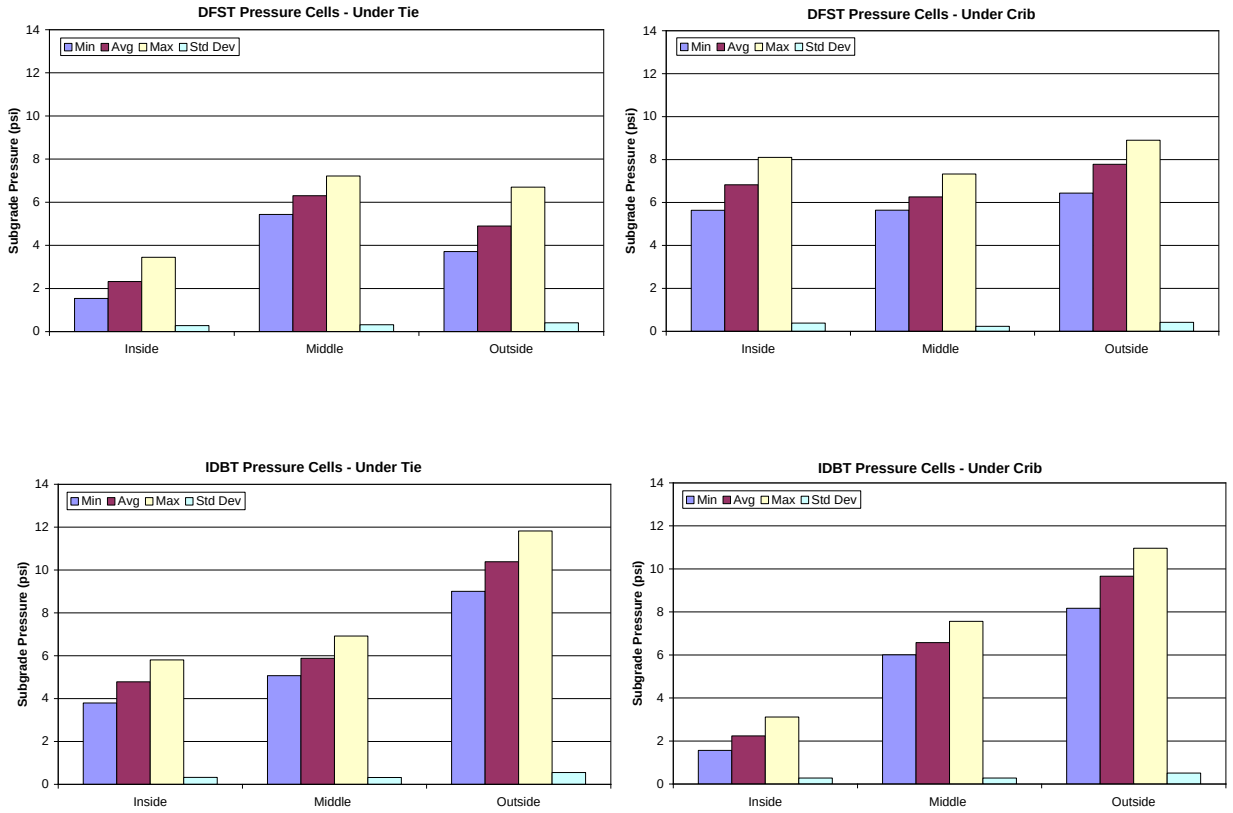

Figure 68. Subgrade Pressure under FAST Train

7.3 Long-Term Use of Subgrade Pressure Cells

Subgrade pressure measurements were also taken under train operations at FAST in January and October 2005. A careful examination of the data recorded by some pressure cells showed significant reductions in subgrade pressure compared with the readings in 2003. As there were no dramatic changes of the slab track or the load environment, which might have explained the large reductions, a decision was made not to use the data recorded from the tests conducted in 2005 to quantify the slab track performance under HAL train operation.

One hypothesis for the reduction of the subgrade pressure readings was the gap development under the concrete slab. The soil cement that was used to cover a pressure cell might not have been compacted to the same stiffness as the soil cement layer installed earlier. Over time, the base of the concrete slab might have bridged over some pressure cells, leading to reduced readings of subgrade pressure by those cells. Another hypothesis focused on questions of the long-term performance of the pressure cells themselves. In fact, no-load (without trains) readings were compared among the three tests from 2003 to 2005, and the comparison indicated significant changes of no-load readings for most of the cells. This indicated a possible long-term performance issue with those cells.

8. Vibration Attenuation of Slab Track

As part of the testing program, vibration measurements were taken to quantify the vibration environment of the slab track test section as well as how much attenuation was achieved from the vibration generated on the rails to the vibration generated on the concrete slab.

Because of the rigid behavior of the concrete slab, slab track designs must provide adequate resilience and damping to attenuate vibration generated at the wheel-rail interface, even though the slab track generates lower dynamic vehicle-track interaction forces than conventional ballasted track (see Section 5).

8.1 Instrumentation for Vibration Measurement

Accelerometers were used to measure vertical vibrations of the rails and the concrete slab. Figure 69 shows the general arrangements of accelerometers installed on each slab track test section. As shown, six accelerometers were used: four at the center of each slab (two for the rails and two for the slab), and two in the transition for the rails. Again, the sampling rate was 2,048 Hz with a 256-hertz low-pass filter.

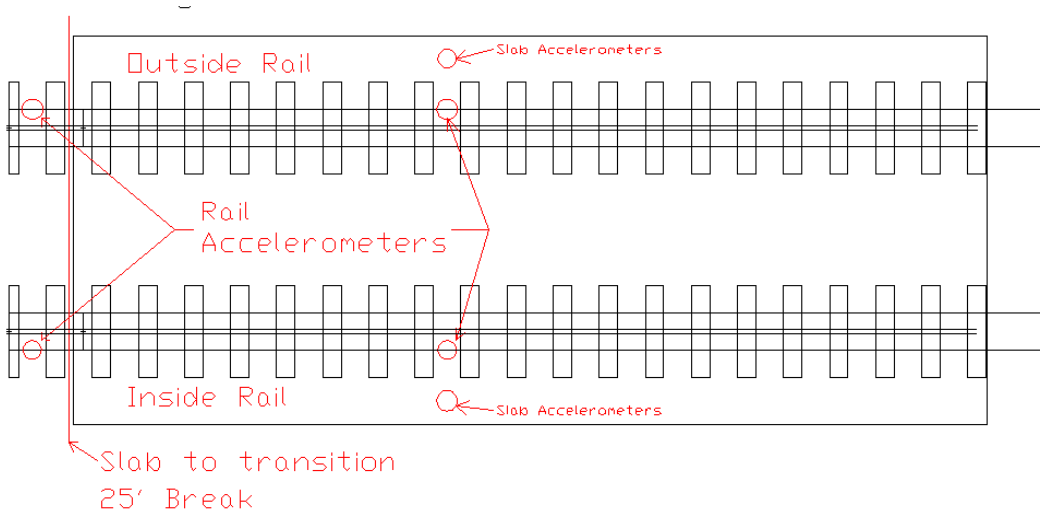

Figure 69. Arrangement of Accelerometers for Vibration Measurement

Figure 70 shows the accelerometers installed on the rail and the slab. On the slab track (IDBT or DFST), the accelerometers (shown next to the arrow pointers) were installed on the rail base and the slab surface near the LVDT transducers used for rail-to-slab deflection measurement (refer to Section 6). Accelerometers were installed on the rail base for rail vibration measurement in the transitions.

Vibration measurements were taken in July and August 2003 following the construction of the slab track.

Figure 70. Accelerometers Installed in Slab Track (arrows) and in Transition

8.2 Test Results

8.2.1 Analysis in Time Domain

In Figure 71, the light gray lines show the accelerations recorded on the rails while the black lines show the accelerations recorded on the slab surface. As illustrated, for either slab (DFST or IDBT), vibration was attenuated greatly from the rails to the concrete slab. Compared with the magnitudes of vibration measured from the rails, vibration measured on the slab surface can be considered insignificant. Attenuation was achieved by installing rubber pads between the rails and the concrete slab in the DFST and installing rubber boots/pads between the block ties and the concrete slab in the IDBT. Figure 71 shows the vibration attenuation test results obtained under the short test consist traveling 40 mph in the CCW direction.

The vibration recorded on the rails was higher for the DFST than for the IDBT. Regardless of the slab track type, no obvious difference can be seen between the vibrations measured on the high and low rails.

Figure 72 shows acceleration test results obtained on the rails in both transition areas. Again, no obvious trend can be seen as far as the difference between the high and low rails. As compared with the rail vibrations measured in the slab areas, transitions did not measure higher vibration in terms of vertical acceleration.

Figure 73 and Figure 74 show the vibration test results obtained when the short consist was traveling at 40 mph in the CW direction. The test results were essentially similar to those obtained when the short test consist was traveling at 40 mph in the CCW direction (Figure 71 and Figure 72). For example, the test results again showed great attenuation of vibration from the rail to the slab by resilient rubber pads (DFST) or rubber boots and pads (IDBT).

Figures 71–74 illustrate that acceleration data was rather noisy, compared with that shown in previous sections. In addition, no obvious peaks could be identified that corresponded to individual passing wheels, unlike the data recorded using other wayside transducers.

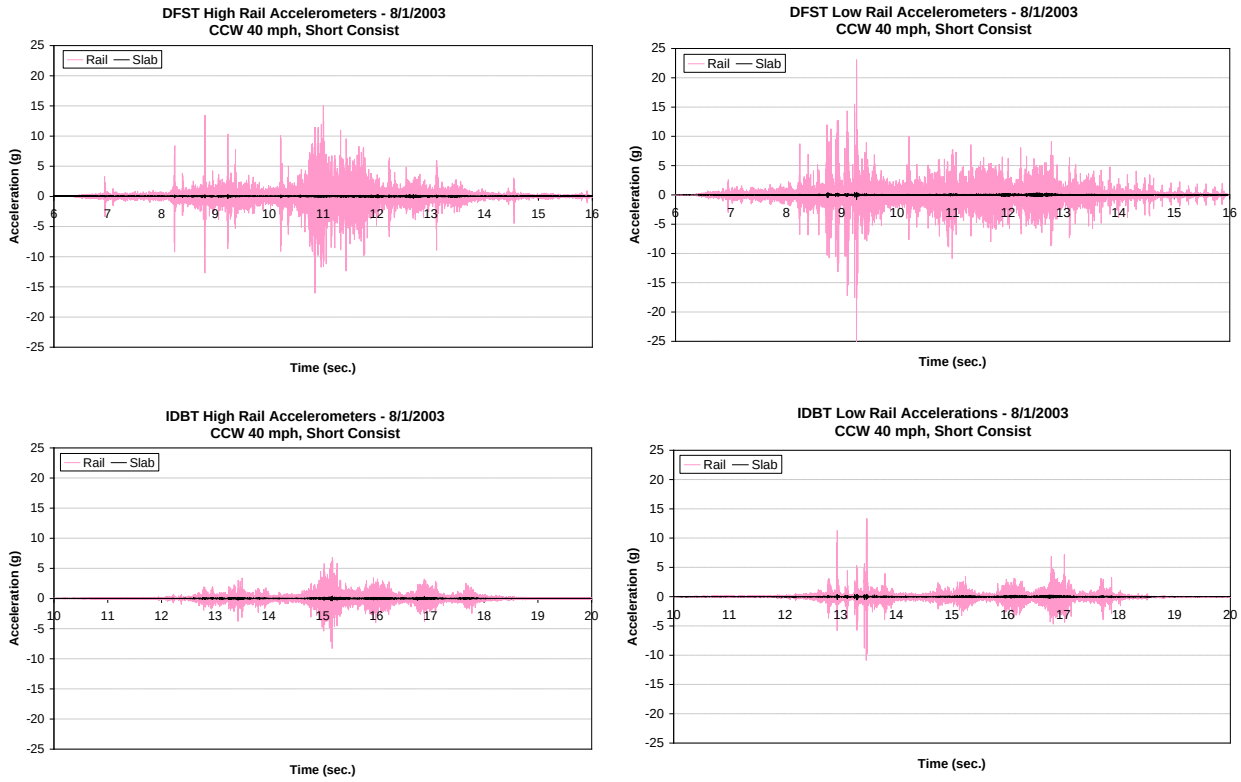

Figure 71. Vibration Attenuation from Rail-to-Slab (Short Consist in CCW Direction)

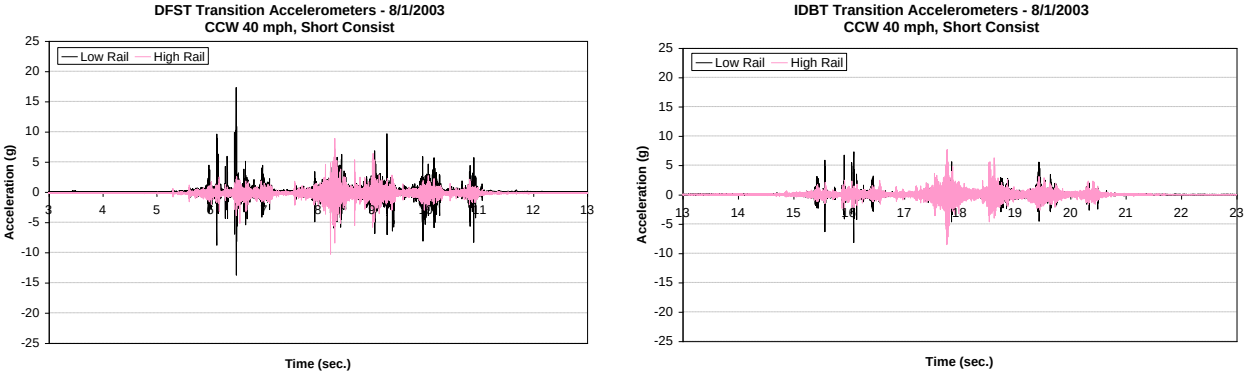

Figure 72. Rail Vibration in Transitions (Short Consist in CCW Direction)

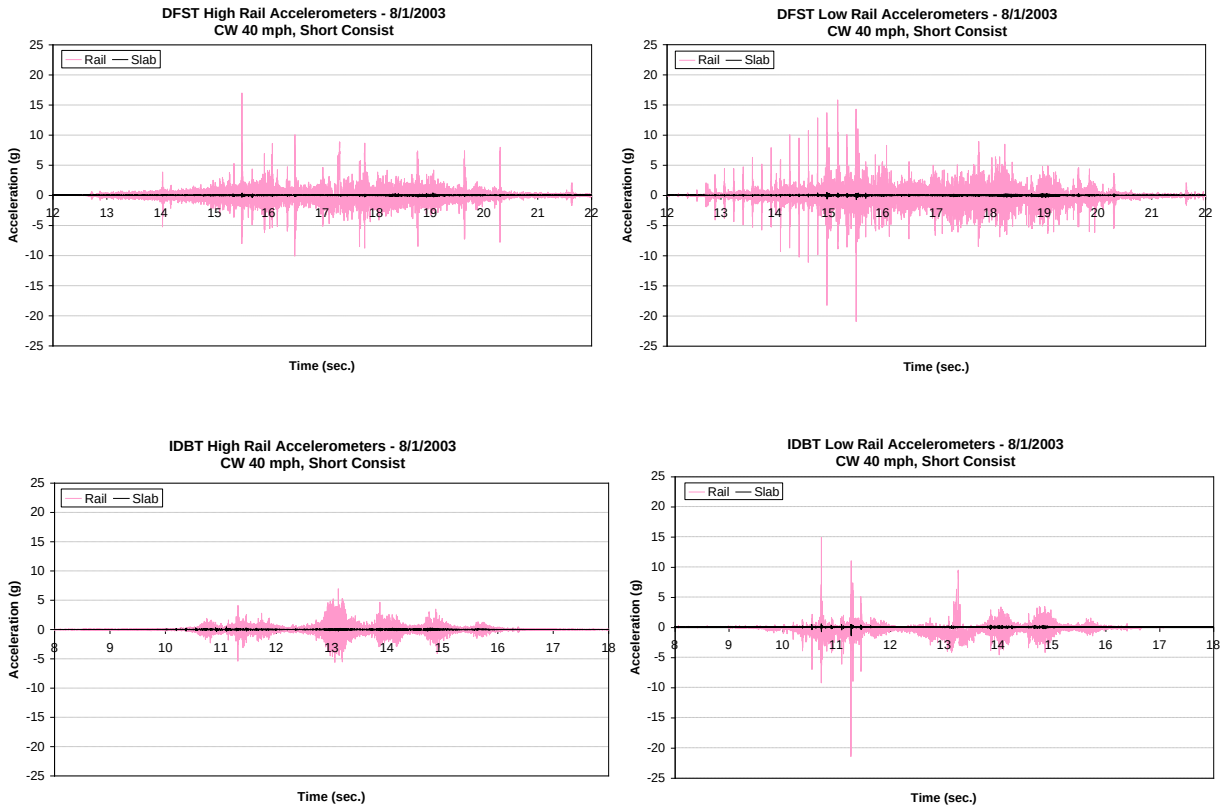

Figure 73. Vibration Attenuation from Rail-to-Slab (Short Consist in CW Direction)

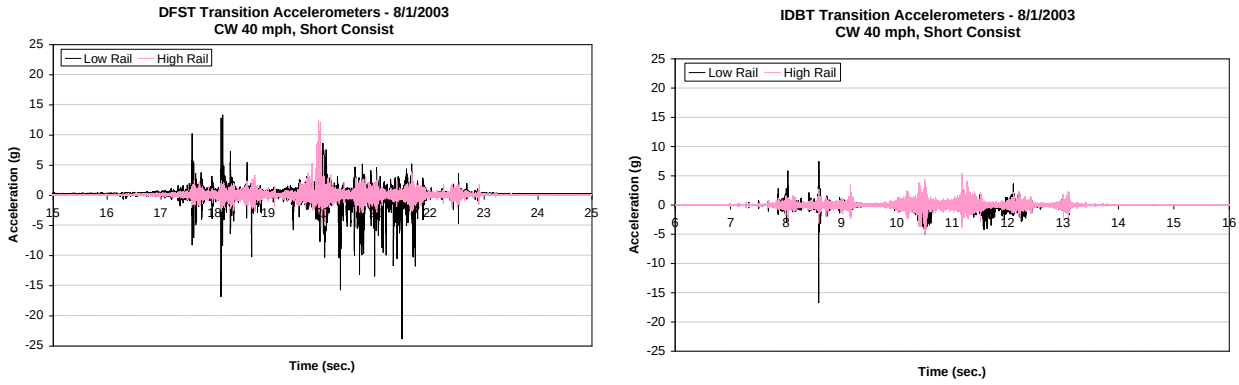

Figure 74. Rail Vibration in Transitions (Short Consist in CW Direction)

Figure 71 through Figure 74 show the acceleration results obtained under the short test consist. Vibration measurements were also taken under the train at FAST. As a result of hundreds of axles under each train, the data recorded were processed to obtain the statistical values. Unlike the statistical values calculated for other wayside data recorded under the train, acceleration responses were processed to obtain values for the following: 95th percentile, 98th percentile and maximum for all positive acceleration data, minimum, 2nd percentile, and 5th percentile for all negative acceleration data (Figure 75). Also unlike the statistical values obtained for other wayside data in which the basis of the statistical values were all peak values corresponding to individual passing wheels, the statistical values for accelerations were calculated based on the entire time histories recorded as it was not possible to identify peak acceleration response values corresponding to individual passing wheels.

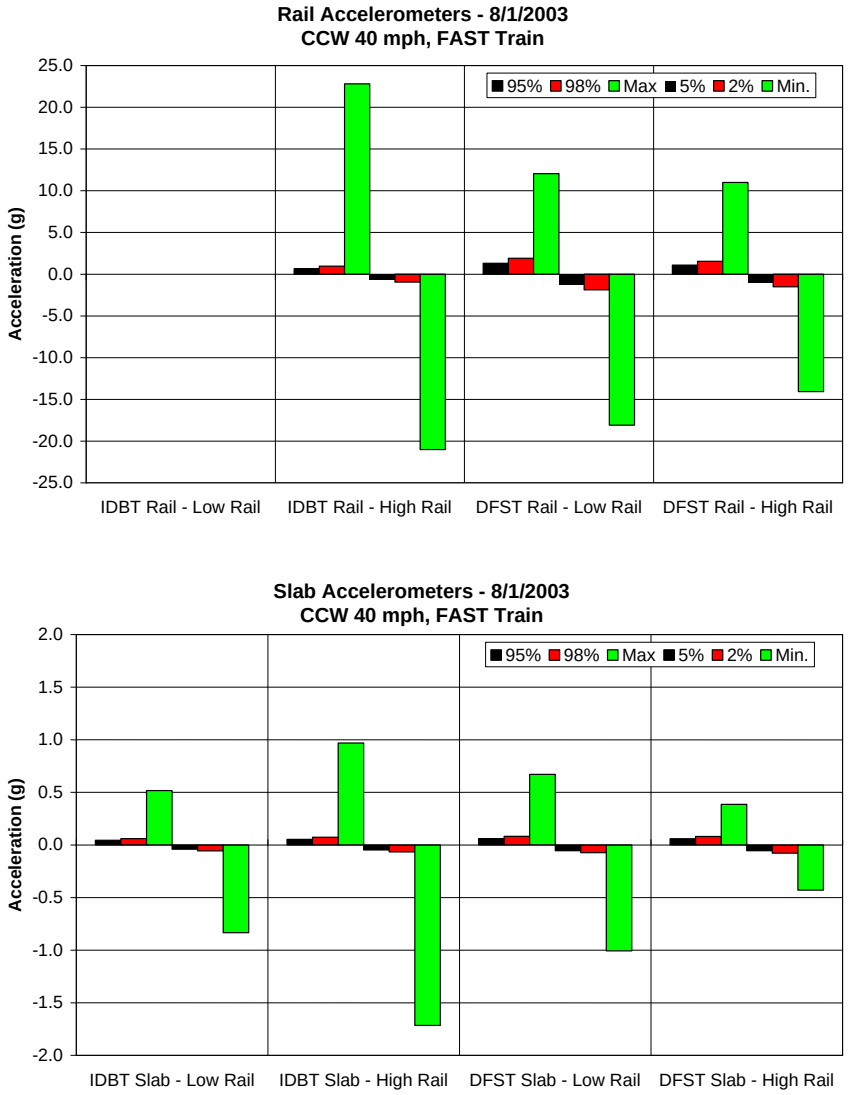

Figure 75. Vibration Attenuation from Rail to Slab

As a result of the use of the entire time history data as the basis for the statistical values shown in Figure 75, a big difference exists between a maximum and a 98th or 95th percentile (e.g., the 98th percentile is a magnitude larger than 98 percent of the data used in the analysis) or between a minimum and a 2nd or 5th percentile.

Nevertheless from the comparisons shown in Figure 75, vibrations, measured on the rails, were reduced greatly when they were measured on the slab track regardless of track type or whether they were obtained from the high or low rail. The maximum or minimum accelerations ranged between 11 and 23g (absolute values) when measured on the rails as compared with between only 0.4 and 1.7g when measured on the slab. On average, it can be estimated that from the rail to the slab attenuation was achieved by a factor of 20.

Figure 76 shows the statistical values of vibration recorded in the transition to the IDBT. As mentioned earlier, magnitude vibrations measured on the rails in the transitions were similar to those measured in the slab.

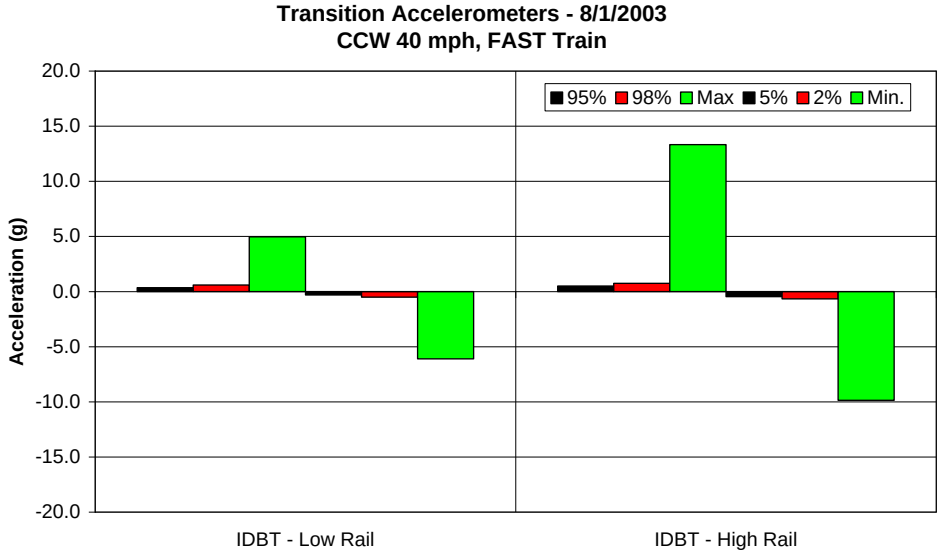

Figure 76. Rail Vibration in Transitions

8.2.2 Analysis in Frequency Domain

Analysis of vibration attenuation was also performed in frequency domain. Figure 77 shows vibration attenuation from the rail to the slab in terms of vibration energy (power spectrum density (PSD)) at various frequencies. As shown, vibration energy was reduced across the entire spectrum from the rail to the slab. In addition, the large vibration energy measured on the rail at higher frequencies (above 100 Hz) was greatly attenuated when it was transmitted to the slab.

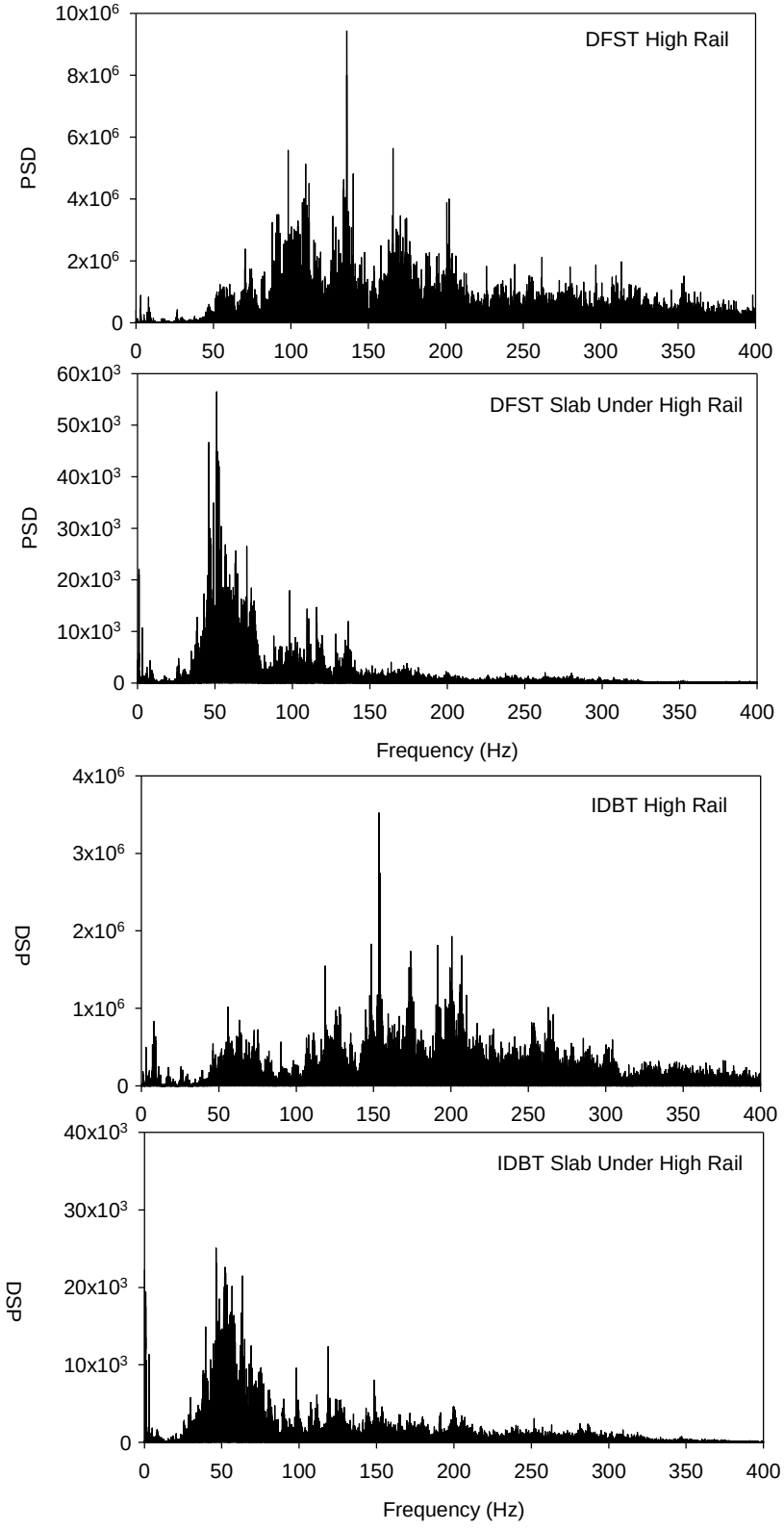

Figure 77. Vibration Attenuation in Frequency Domain from Rail to Slab

9. Other Measurements of Slab Track

Some of the slab track measurements were taken to provide the actual test data to verify the slab track analysis and design procedures developed for shared heavy-freight and high-speed train service (refer to Introduction). As part of the slab track testing program, the following test data were obtained and provided to PCA/CTL for that purpose:

- Rail bending strain at rail base
- Strain of concrete slab surface
- Strain of steel reinforcement bars used in concrete slab

Unlike the test results presented and discussed in previous sections, those presented here were not used directly for quantifying the slab track performance under HAL train operation. Therefore, a brief summary of the data is given but the data are not compared with the test data obtained using the other wayside transducers.

9.1 Instrumentation for Strain Measurement

Strain gages for measuring rail bending were installed at the top of rail bases (see Figure 38). For each slab track (IDBT or DFST), both high and low rails were instrumented for bending strain measurement at the rail base. The rail bending strain gages were installed between two ties and fastener supports but were close to them.

On the concrete slab surface of the IDBT or the DFST, three strain gages were installed in the longitudinal direction: one on the outside, one in the middle, and one on the inside. In addition, one strain gage was installed in the lateral direction in the middle of the slab track. Figure 78 illustrates the locations and orientations of the four strain gages installed on the concrete slab surface. Figure 79 shows a pair of strain gages installed on the concrete slab surface at the middle location.

Strain gages were used on the top and bottom steel bars (see Figure 9 and Figure 11) instead of the steel reinforcement bars used in the concrete slab (Phase 1 slab in the case of the IDBT). As shown in Figure 78, four strain gages were used on the top steel bars: three in the longitudinal direction and one in the lateral direction. For the bottom steel bars, six strain gages were installed: three in the longitudinal direction and three in the lateral direction. Note, the backup strain gages shown in Figure 78 were installed in case some did not work. Figure 79 shows strain gages installed on steel bars before the concrete was poured to form the slab.

Strain measurements under the HAL train operation at FAST were taken in July and August 2003. Again, the sampling rate for collecting data was 2,048 Hz with a 256-hertz low-pass filter. The data were recorded with data collected using the other wayside transducers, as discussed in previous sections.

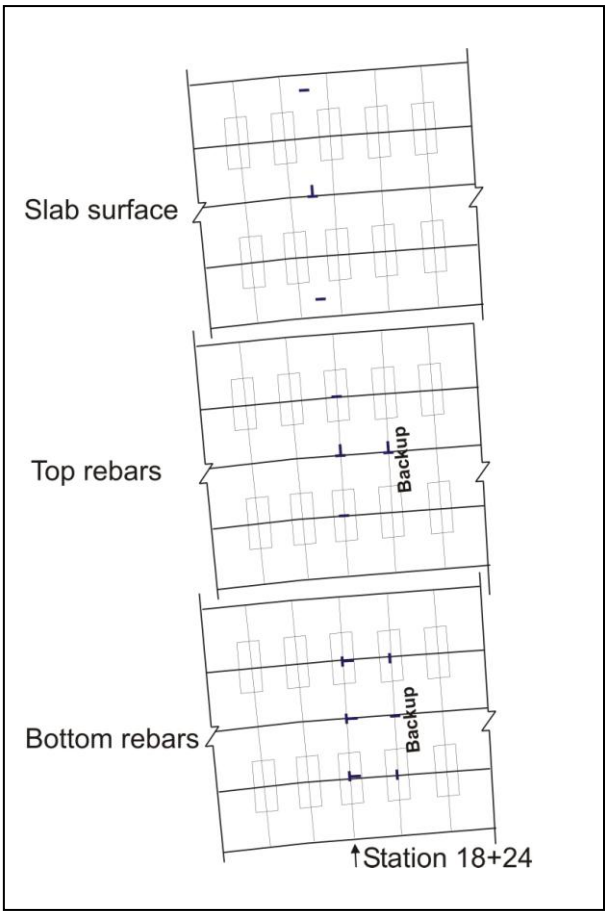

Figure 78. Arrangement of Strain Gages on Slab Surface and Reinforcement Bars

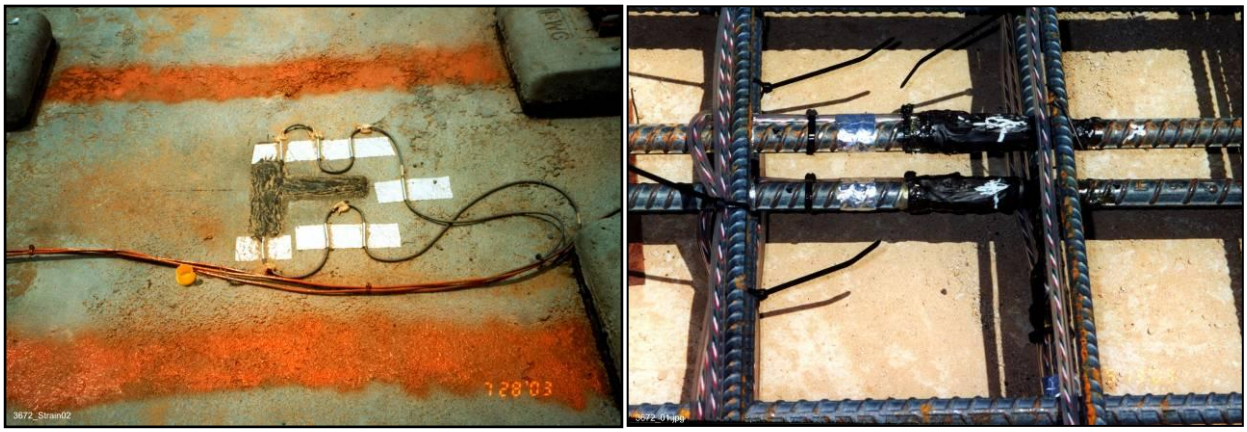

Figure 79. Strain Gages Installed on Slab Surface and Steel Bar

9.2 Test Results

Test results obtained under the short HAL test train are presented in three sections: one for rail bending strains, one for concrete surface strains, and one for steel reinforcement bar strains. A positive value indicates tensile strain and a negative value indicates compressive strain.

Unlike the data signals obtained using the other wayside transducers, the initial offsets of strain signals (if present) were not adjusted to zero for the purpose of showing dynamic responses due to dynamic wheel loads. This is because a negative initial reading for the concrete slabs might indicate a certain amount of compressive stress already applied to the concrete, which would help to prevent crack development resulting from the possible tensile stress caused by dynamic wheel loads.

9.2.1 Rail Base Bending Strain

Figure 80 shows the rail bending strain test results obtained under the short test consist when it was traveling at 40 mph in the CCW direction. The magnitudes of rail bending strain measured on the high and low rails for both the DFST and the IDBT are low as compared with the allowable rail bending strain (i.e., allowable bending stress) for the rail steel. As expected, rail bases are primarily in tension under dynamic wheel loadings.

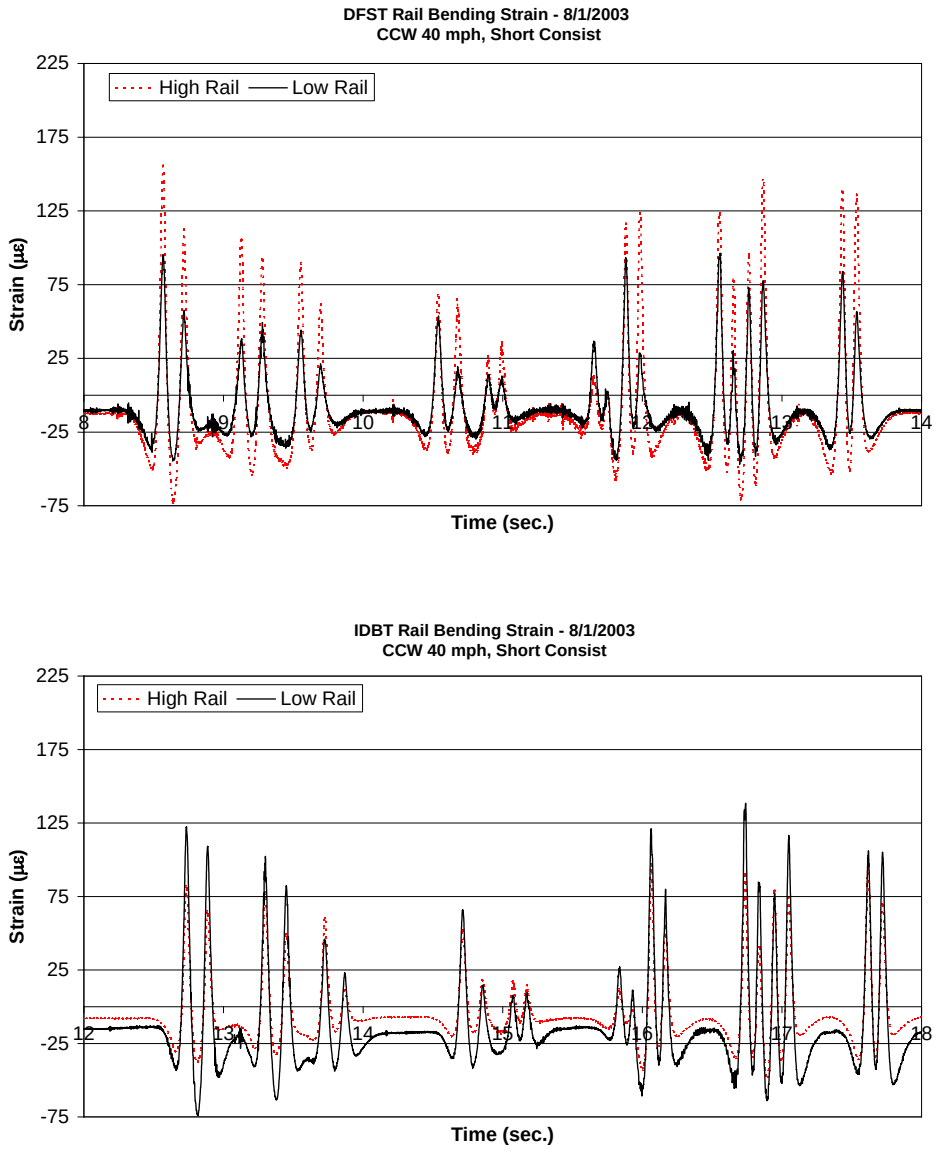

Figure 80. Rail Bending Strain under Short Test Consist in CCW Direction

Figure 81 shows the rail bending strain test results obtained when the short consist was traveling in the CW direction at 40 mph. The results are similar to those shown in Figure 80 for the test run in the CCW direction.

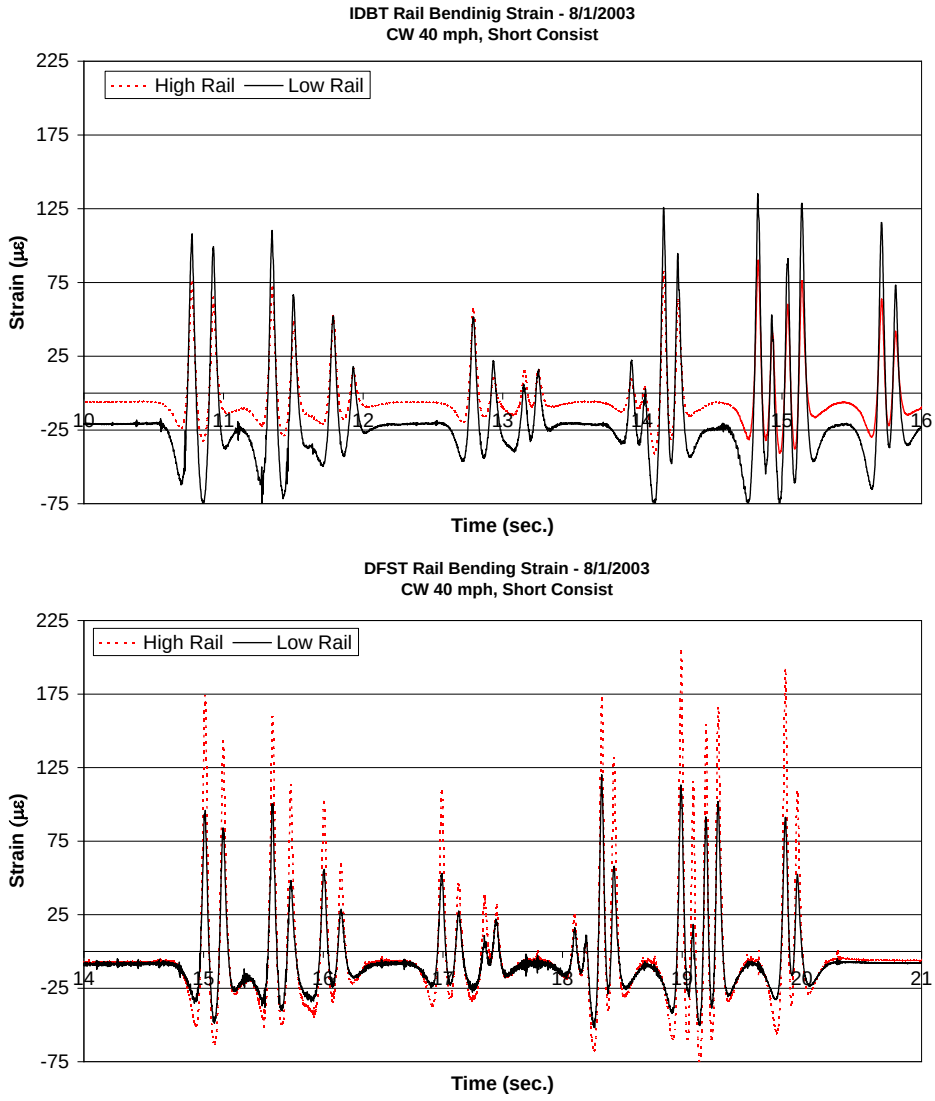

Figure 81. Rail Bending Strain under Short Test Consist in CW Direction (2003)

9.2.2 Concrete Surface Strain

Figure 82 shows the strain measurement results for the eight strain gages installed on the slab surface (four each for the DFST and IDBT). The top two graphs show the longitudinal strains measured on the outside, at the middle, and on the inside for the DFST and IDBT, respectively. The bottom graph shows the lateral strain test results obtained at the middle of the slab track for both the DFST and the IDBT.

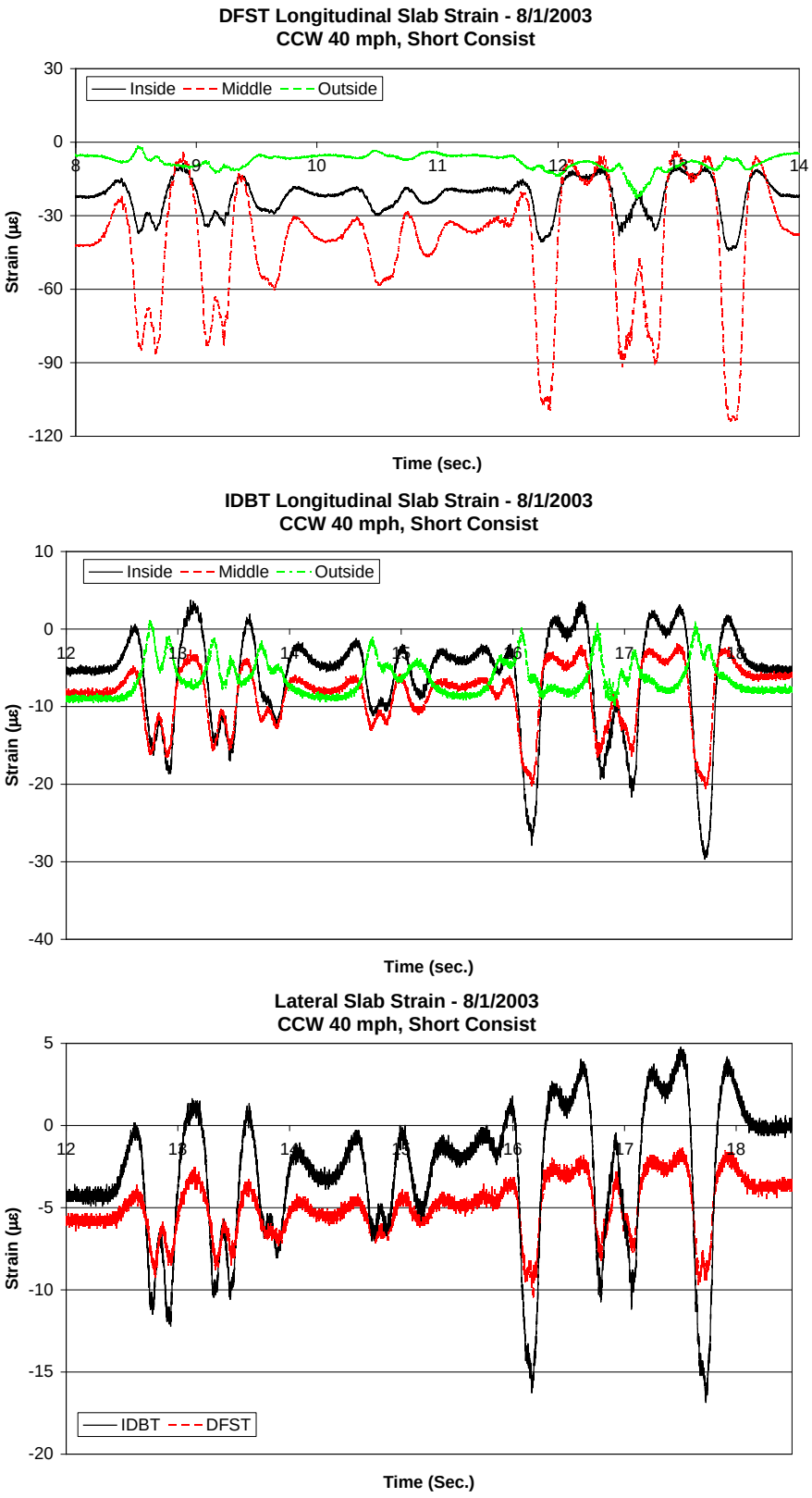

Figure 82. Slab Surface Strains under Short Test Consist in CW Direction

Figure 82 shows that the longitudinal compressive strains were generally larger than the lateral compressive strains, particularly for the DFST slab. On the surface of the DFST slab, no tensile strain in either the longitudinal or the lateral direction was generated under dynamic wheel loads, whereas, the surface of the IDBT slab experienced a small amount of tensile strain in either orientation.

As described in Section 2, the DFST slab was reinforced; the entire slab acts as a main structural layer. For the IDBT, the Phase 1 (base) slab was reinforced; this is the main structural layer supporting dynamic wheel loads. The Phase (top) 2 slab was not reinforced; it is used mainly to hold independent dual block ties. However, the Phase 2 slab is designed for composite action with the roughened Phase 1 slab. The comparison of longitudinal strain test results on the surfaces of the DFST and IDBT slabs appeared to reflect the structural difference between these two slabs. This may be explained by the construction sequence.

9.2.3 Steel Bar Strain

Figure 83 shows the strain measurement results from the eight strain gages installed on the top steel bars (four each for the DFST and the IDBT). The top two graphs show the longitudinal strains measured on the outside (under the high rail), at the middle, and on the inside (under the low rail) for the DFST and IDBT, respectively. The bottom graph shows the lateral strain test results obtained at the middle of the slab track for both the DFST and the IDBT.

Again, longitudinal compressive strains were much larger than lateral compressive strains, particularly for the DFST slab. The DFST slab showed larger compressive strains than the IDBT slab because the top steel bars of the IDBT slab are in Phase 1 concrete and are closer to the neutral axis of the composite section than the top steel bars in the DFST slab. Similarly, in the lateral direction, the measured strain from a top steel bar in the DFST was larger than that measured from a top bar in the IDBT Phase 1 slab.

Top steel bars for either slab were primarily in the compression mode in the longitudinal direction under dynamic wheel loads. For either slab track, the longitudinal direction is the major direction as far as the stress state is concerned. The compressive strain or stress in the longitudinal direction is expected to be higher than in the lateral direction. Also, concrete shrinks during curing, which causes slight compression in the top and bottom longitudinal reinforcement.

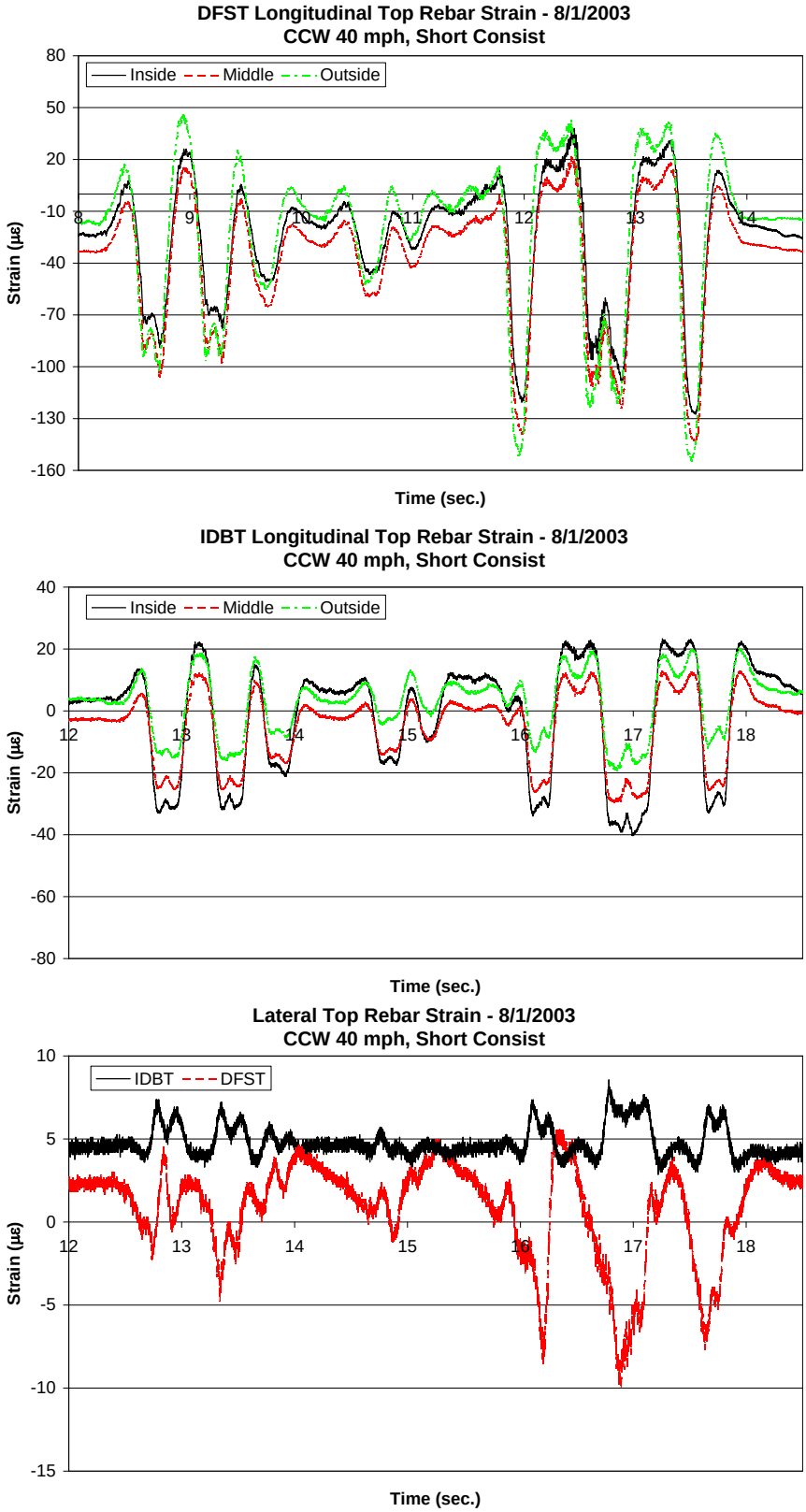

Figure 83. Strains of Top Steel Bars under Short Test Consist in CCW Direction

Figure 84 shows longitudinal strain measurement results for the steel reinforcement bars at the bottom of the concrete slabs. As shown in Figure 78, each slab had six strain gages installed on the bottom steel bars: three on the longitudinal bars and three on the steel bars. In Figure 84, the top graph shows the longitudinal strains measured in the DFST and the bottom graph shows the test results obtained in the IDBT.

As expected, the steel reinforcement bars were primarily in the tension mode regardless of the slab type (DFST or IDBT). Between the two slabs, the magnitudes of tensile strains were basically of the same order.

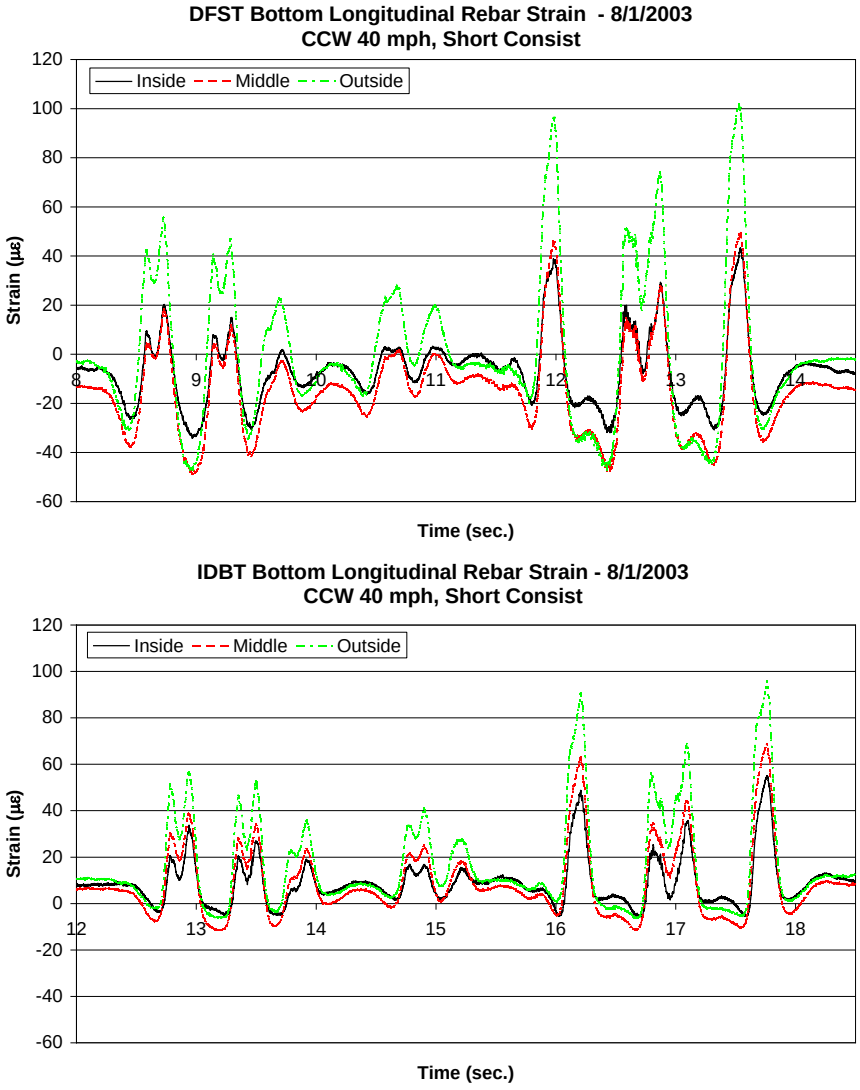

Figure 84. Longitudinal Strains of Bottom Steel Bars

Figure 85 shows lateral strain measurement results for the steel reinforcement bars at the bottom of the concrete slabs. The top graph shows the lateral strains measured in the DFST and the bottom graph shows the lateral strains measured in the IDBT.

As seen with the longitudinal strains measured, steel reinforcement bars installed in the lateral direction were primarily in the tension mode under dynamic wheel loads. Lateral steel bars experienced much lower strain responses than the longitudinal steel bars. As mentioned earlier, the major stress in the concrete slab was in the longitudinal direction.

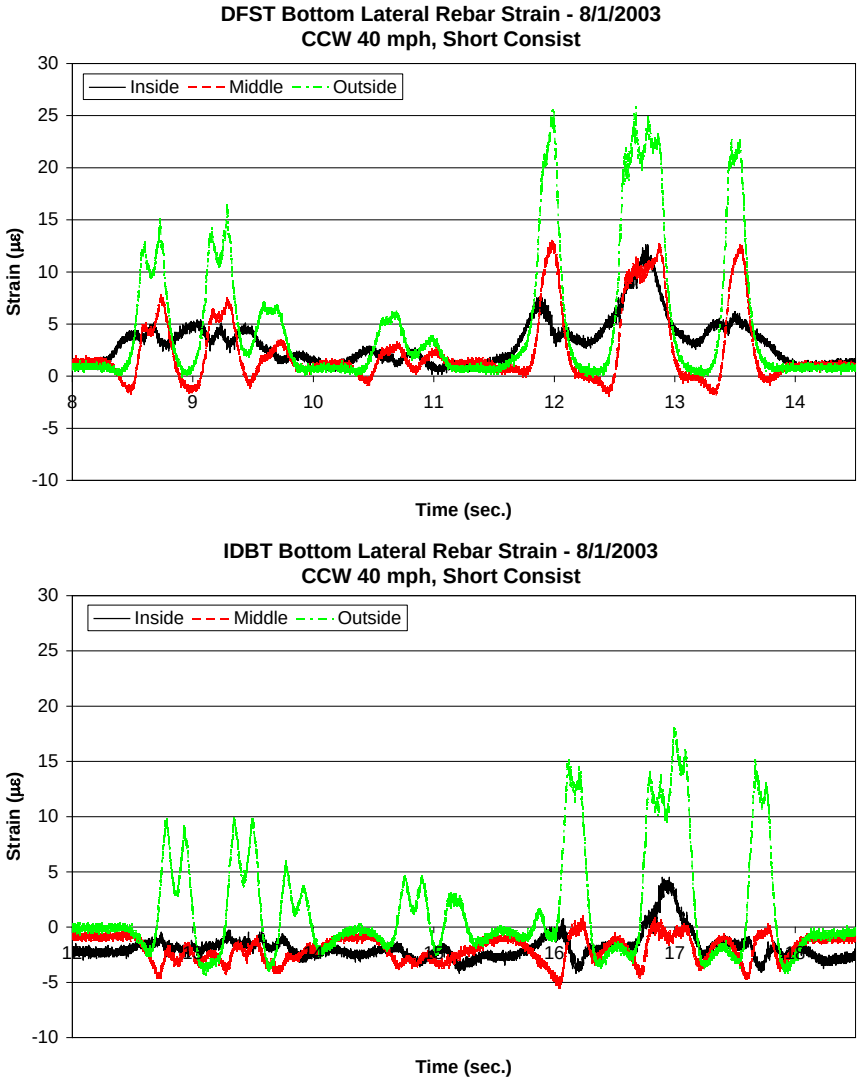

Figure 85. Lateral Strains of Bottom Steel Bars

10. Summary and Conclusions

The Slab Track Field Testing and Demonstration Program for Shared Freight and High-Speed Passenger Service project was completed to demonstrate the durability of the slab track for 39-ton axle loads while maintaining the track geometry conditions for a Class 9 track. More specifically, the program was carried out to characterize slab track stiffness conditions, to quantify slab track dynamic responses and performance under HAL train operation, and to provide test data for validating slab track analysis and design methodologies for shared heavy-freight and high-speed train service.

In July 2003, two types of slab track (DFST and IDBT) were installed on the HTL at TTC. The slab track test section was in a 5-degree curve with 4-inch superelevation. It was 500 ft long and consisted of 250 ft of IDBT and 250 ft of DFST. The transition from each slab to the ballasted track was in a spiral from a 5-degree curve to tangent track.

The testing program concluded in the summer of 2006. Over a period of 3 yr, a total of 170 MGT of HAL traffic was accumulated on the slab track test section, exceeding the target tonnage of 150 MGT. During the period of testing and monitoring, various measurements were conducted to quantify the slab track responses and performance under HAL train operation.

10.1 Track Geometry Performance of Slab Track

The slab track test section in the HTL demonstrated its capability of supporting HAL train operation while maintaining the track geometry conditions for a Class 9 track. During the 3 yr of testing and the 170 MGT of accumulated traffic, little track geometry degradation was measured and no track geometry maintenance was required for surface, alignment, gage, or crosslevel of the slab track test section. From the beginning of the testing program until its completion, there was little cumulative settlement and little lateral movement of the slab track.

An alignment adjustment was done near the end of the DFST slab track following the construction of the slab track test section. The misalignment was due to the severe transition conditions from a Class 9 slab track to a Class 4 ballasted track and a change of curvature from the 5-degree curve to a spiral.

The surface condition of the slab track was superior to that of the adjacent ballasted track. Several spot tamping operations were performed in the transition areas to smooth out differential track settlement accumulated in the ballasted transitions.

10.2 Slab Track Stiffness Characteristics

Both the IDBT and the DFST were built with uniform vertical track stiffness. When measured following the construction of the slab track test section, the IDBT showed an average track modulus of 3,000 lb/in/in and the DFST showed an average track modulus of 2,100 lb/in/in. These values, especially for the DFST, were lower than originally expected and were due to the use of extremely resilient rubber boots and pads.

The installation of 25-foot transitions became unnecessary at least in terms of track stiffness, as the slab track test section (DFST or IDBT) was either more resilient than or resilient as the adjacent ballasted track.

During the 3-year period of testing, the increase in track modulus for the DFST was moderate but the increase for the IDBT was significant. This increase was caused by the gradual deposit of fine windblown sand into spaces between the IDBT components as discovered in November 2006 during the IDBT inspection. This process caused an increase in track modulus by limiting the deflection of the block ties within the rubber boots. Some of the deposited sand was flushed out when combined with rainwater under passing trains. The flushing process had caused the buildup of fine gray material around the block ties. One of the IDBT pads was tested in a laboratory following the inspection, and it was determined that the stiffness of the pad was within the tolerance limits set by the manufacturer of the IDBT block-tie system.

In terms of lateral gage strength, both the IDBT and the DFST tracks showed more uniform lateral gage strength or stiffness than the adjacent ballasted track. For the DFST, there had been a significant decrease in gage strength in terms of delta gage measured by the TLV. From 2 to 169 MGT, delta gage measured under the TLV test loads (33-kilopound vertical wheel load and 18-kilopound lateral wheel load) increased from 0.3 to 0.5 in on the average. Extremely resilient pads, such as those used in the DFST, may be of concern for HAL operation. With the IDBT, there was little gage strength degradation in terms of delta gage, although unloaded track gage increased from 56.8 to 57.1 in on the average, with the maximum being 57.2 in. Compared with the DFST, resilience of rubber boots and pads used in the IDBT had less of an influence on gage strength or stiffness because the boots and pads were installed at the tie-slab interface.

10.3 Dynamic Wheel/Rail Forces on Slab Track

Because of superior track geometry and resilient pads and boots, the slab track test section generated lower dynamic vertical and lateral wheel loads than the ballasted track of the same curvature and superelevation. The maximum vertical load generated in the slab track was 58 kip as compared with 73 kip generated on a ballasted track. The maximum lateral wheel load generated in the slab track was 20 kip as compared with 24 kip in the ballasted track. Note that the slab track test section located in a 5-degree curve with 4-inch superelevation was underbalanced at the nominal train operating speed of 40 mph on the HTL, meaning that higher vertical wheel load was applied on the high rail than on the low rail.

Over the 3 yr of testing, no significant increases were observed in either the vertical or lateral dynamic wheel loads, particularly those generated on the high rail. However, lateral wheel loads generated at the ends of the slab track (transition areas) increased. IWS test results showed a significant increase of lateral wheel load at the ends of the slab test section, particularly when the test train was exiting the slab track. With regard to vertical wheel load, the dynamic responses were also higher (up to 25 percent) in the transitional areas but did not increase during the three tests conducted from 2003 through 2005.

10.4 Slab Track Deflection

Slab track deflection occurred primarily between the rail and the concrete slabs due to resilient pads (DFST) or rubber boots and pads (IDBT). Only a small amount of deformation was recorded from the underlying subbase and subgrade layers.

Vertical and lateral rail-to-slab deflection test results were consistent with dynamic wheel loads and track stiffness test results measured at the same time. Higher dynamic wheel loads and lower track stiffness would correspond to larger rail-to-slab deflections regardless of the slab track type. For the DFST, the maximum vertical rail-to-slab deflection was 0.25 in and the maximum lateral rail-to-slab deflection was 0.1 in, both recorded on the high rail. For the IDBT, the maximum vertical rail-to-slab deflection was 0.15 in and the maximum lateral rail-to-slab deflection was 0.07 in, which was again measured on the high rail.

From 2003 to 2006, little increase measured in vertical rail-to-slab track deflection occurred for the DFTS. There was an increasing trend of lateral rail-to-slab deflection, which appeared consistent with the trend of decreasing gage strength for the DFST. The general trends for vertical and lateral rail-to-slab deflections were decreasing, particularly for the deflections on the high rail for the IDBT. These trends appeared to be consistent with the track stiffness increase for the IDBT slab track.

10.5 Subgrade Pressure and Deformation under Slab Track

The maximum subgrade pressure generated under HAL vehicles was 12 psi, well below the compressive strength of the subgrade soil. The relatively low subgrade pressure with respect to soil strength explains the small amount of subgrade deformation generated under HAL train operation. Under the slab track test section, the maximum deformation recorded in the subbase or subgrade was less than 0.06 in.

10.6 Vibration Attenuation

In the slab track test section, vibration attenuation was achieved through use of rubber pads (DFST) or rubber boots and pads (IDBT). The vibration measurements showed a large amount of vibration attenuation from the rail to the slab regardless of slab track type. Under HAL train operations at 40 mph, the maximum acceleration recorded on the rails ranged between 10 and 25g (absolute value) whereas that on the slab ranged between only 0.4 and 2g (absolute value). On average, attenuation was achieved by a factor of 20.

With regard to vibration measured on the rails, no obvious trends could be identified between the transitions and the slab track or between the high and low rails. Analysis of vibration attenuation in frequency domain showed the attenuation of vibration energy across the entire spectrum. In addition, the large amount of vibrations above 100 Hz was greatly attenuated from that measured on the rails to that measured on the concrete slab.

10.7 Other Performance Parameters

For a total of 170 MGT of HAL traffic, no rail defects were recorded in the slab track test section, nor were any weld defects or failures reported for the 14 thermite welds used in the test

section. For comparison purposes, the average weld life in similar 5-degree curves in the HTL was approximately 80 MGT. In addition, no significant wear of either high or low rails in the test section was observed; nor was rail corrugation development noted. According to the locomotive engineers who operate the trains at FAST, the slab track test section provided the best ride quality of the entire HTL.

10.8 Additional Notes

The results, discussions, and conclusions presented in this report were based on testing of the slab track for a 3-year period (July 2003–July 2006) under a total accumulated traffic of 170 MGT. In September 2006, PCA and FRA gave approval for extending the slab track test for another 2 yr, until September 2008.

In addition to the tests presented and discussed in this report, other tests were done on the slab track test section. PCA and CTL personnel mapped the cracking of the concrete slabs twice throughout the duration of the slab track testing, which showed normal cracking distribution and growth for the concrete slab. Ground-penetrating radar testing done for the slab track in September 2003 showed no voids or loss of support between the base of the slab and the soil cement layer (Smith, 2005).

10.9 Recommendations

As the slab track test section continues to be subjected to HAL train operations at FAST, it is recommended that performance monitoring continue in terms of track geometry conditions. Gage strength testing is also recommended to determine if gage strength of the DFST may further degrade under HAL. For either slab (IDBT or DFST), testing of rubber boots or pads for issues such as possible temperature increase under train operation and change of resilient property over time may provide further insight regarding their eventual life cycle under HAL train operation. Finally, it is recommended that a test section of slab track be installed in revenue service with shared heavy-freight and high-speed train operations.

11. References

Ball, C.G. (2004). Slab Track Laboratory Test Program. PCA R&D, Serial No. 2795. Portland Cement Association, Skokie, IL.

Bilow, D.N., & Li, D. (2005). Concrete Slab Track Test on the High Tonnage Loop at the Transportation Technology Center. In *Proceedings of the AREMA Annual Conference*, Chicago, IL.

Kucera, W.P., Bilow, D.N., Ball, C.G., & Li, D. (2003). Laboratory Test Results and Field Test Status of Heavy Axle Loads on Concrete Slab Track Designed for Shared High-Speed Passenger and Freight Rail Corridors. In *Proceeding of the AREMA Annual Conference*, October 5–8, Chicago, IL.

Li, D., Thompson, R., Marquez, P., & Kalay, S. (2004). Development and Implementation of a Continuous Vertical Track-Support Testing Technique. *Transportation Research Record: Journal of the Transportation Research Board*, U.S. National Academies, no. 1863, pp. 68–73.

Li, D., & Yoshino, D. (2003). Review and Evaluation of Track Designs for Joint High-Speed Rail and Heavy Freight Operations. Final Report to Office of Research and Development, FRA. TTCI, Pueblo, CO.

Lotfi, H.R., & Oesterle, R.G. (2005). Slab Track for 39-Ton Axle Loads, Structural Design. PCA R&D, Serial No. 2832. Portland Cement Association, Skokie, IL.

Selig, E.T., & Li, D. (1994). Track Modulus: Its Meaning and Factors Influencing It. *Transportation Research Record: Journal of The Transportation Research Board*, U.S. National Academies, No. 1470, pp. 47–54.

Selig, E.T., & Waters, J.M. (1994). Track Geotechnology and Substructure Management. Thomas Telford.

Smith, S. (2005). As-Built Survey of Slab Track Using Ground Penetrating Radar at Transportation Technology Center, Pueblo, Colorado. FRA Contract No. DTR-52-02-P-00263, Geo-Recovery Systems, Inc., Golden, CO.

Tayabji, S.D., & Bilow, D.N. (2001). Concrete Slab Track State of the Practice. *Transportation Research Record: Journal of the Transportation Research Board*, U.S. National Academies, No. 1742, pp. 87–96.

Appendix A.
Report of IDBT Inspection on November 20, 2006

Attendees:

David Bilow, Portland Cement Association
Dingqing Li and two to three trackmen, Transportation Technology Center, Inc.

Purpose:

Measurements of the track modulus at 169 MGT indicated that the stiffness of the IDBT test section increased from 3,000 psi to a maximum slightly above 10,000 psi and that the average dynamic rail deflection decreased from 0.13 to 0.07 in during the 3 yr of operation. In addition, when settlement was measured, the IDBT actually rose 0.1–0.3 in during the operation period. It is believed that the increase in track modulus and negative settlement were the results of windblown sand infiltrating the space between the block-tie components. The inspection was conducted to verify this hypothesis and to determine the condition of the elastomeric pad, boots, concrete block tie, and concrete surrounding the block cavity.

Inspection:

1. The temperature at 8 a.m. was 44 °F, and it was sunny with a few clouds. The temperature increased to about 60 °F in the afternoon.
2. Dingqing Li selected low rail tie numbers 190, 191, 192, and 193 for removal and inspection. The track at this location had the highest track modulus, but not much gray material was seen surrounding the blocks ties.
3. The track crew, which consisted of two men and sometimes a third, unclipped the rail's 20 ties each way from the ties to be inspected. The ties to be inspected were not unclipped.
4. Two 15-ton rail jacks were placed on each side of tie numbers 187 and 196. Using the jacks the rail was raised 2 in. Five more ties were unclipped in each direction, and one jack was moved to just west of tie number 191. The rail was than raised a total of 8 in. The boots remained attached to the blocks that were raised.
5. Block numbers 190 and 191 were unclipped and moved from under the rail.
6. During the inspection of the cavity, sand was found on the sides and bottom. Some of the boot, pad, cavity, and block surfaces were wet because the water from earlier rains had not evaporated.
7. The boots were removed from block ties numbers 190 and 191, and more sand was found on the wall of the boots and on the bottom. Also, some sand adhered to the bottom of the concrete block. The sand was removed from the cavity and the block and placed in the boot to be measured later.
8. The concrete in the cavity and the block tie were in good condition. There was no evidence of cracking or spalling. However, the sides of the block ties contained an impression of the ribs of the boots. The impression had a depth of 0.085 in as measured by TTCI. The boots and pads were in good condition and did not show any signs of

wear and tear. The boots and pads from numbers 190 and 191, together with the sand, will be shipped to Clair Ball at CTLGroup.

9. Dingqing Li selected high-rail tie numbers 151 and 152 for removal and inspection. The track at this location also had a high track modulus and, compared with tie numbers 190 and 191, these blocks had much more gray material surrounding them.
10. The track crew unclipped the rails 25 ties each way from the ties to be inspected. The ties to be inspected were not unclipped.
11. Fifteen-ton rail jacks were placed on each side of tie numbers 151 and 152. Using the jacks, the rail was raised a total of 8 in. The boots remained attached to the blocks that were raised.
12. Blocks 151 and 152 were unclipped and moved from under the rail.
13. During the inspection of the cavities, sand 1/8-in thick was found on the sides and bottom.
14. The boots were removed from the block ties, and more sand was found on the wall of the boots and on the bottom. Also, 1/8 to 1/4 inch of sand adhered to the bottom of both concrete blocks. The amount of sand observed at tie numbers 151 and 152 was more than the amount seen at tie numbers 191 and 192. The surfaces of the pads were wet because water from earlier rain had not evaporated.
15. The boot for tie number 151 had a 3-inch-long hole at the corner between the bottom and the long sidewall of the boot. This boot will be sent to CTLGroup.
16. The concrete in the cavity and the block-tie concrete were in good condition. There was no evidence of cracking or spalling. The sides of block numbers 151 and 152, however, contained an impression of the ribs of the boots similar to that found in block tie numbers 190 and 191.
17. The boots and pads from tie numbers 190 and 191 and the boot from number 151 were replaced with new boots and pads from the spare blocks.
18. Each of the four block ties was placed back into the cavity from which it was removed, and the rails were lowered onto the ties. All four replaced blocks did not seat and remained above their correct position by 3 in. A speed crane was used to try and reseat block numbers 190 and 191, which helped somewhat, but the blocks still remained above their correct position.
19. Following the inspection, the track crew used a locomotive to push down the blocks that were raised during the inspection. A tamper was then used to align the rails into proper positions.

Discussion

The sand under the block, both inside and outside the boot, was the cause of the measured rise in the IDBT of 0.1 to 0.3 in. The increase in track modulus was likely caused by the volume of sand around the block inside the boot. (The volume of sand will be measured when the material is inspected at the CTLGroup.) The sand filled up the spaces within the boot, which interfered with the block tie's deflection. Additionally, CTL will test a pad removed during the inspection to determine if there was any change in pad stiffness.

The gray material found around block tie numbers 151 and 152 was caused by a mixture of windblown sand, cement particles, and rainwater being pushed out during train operations. The cement particles were the result of localized abrasion of the block ties as evidenced by the impression of the boot ribs on the sides of the ties. Rainwater mixed with sand and filled any voids that remained between the boot and the block.

Figure A1. IDBT Block Tie Numbers 190 through 193

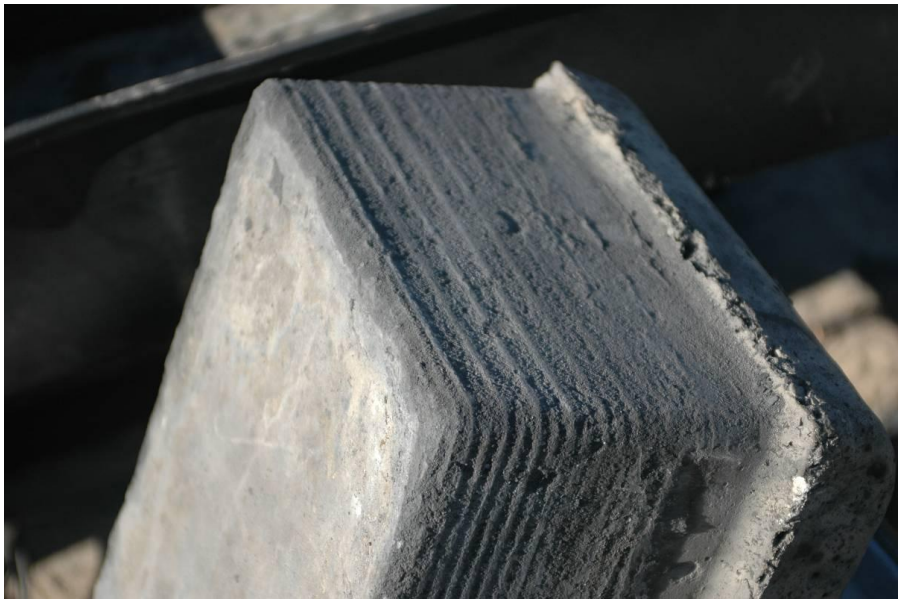

Figure A2. Tie Number 190, Showing Impressions from the Boot Ribs

Figure A3. Cavity of Tie Number 190

Figure A4. Inside of Boot for Tie Number 190

Figure A5. Tie Number 190 Pad

Figure A6. Outside of Boot Tie Number 190

Figure A7. Cavity of Tie Number 151, Showing Sand in the Bottom

Figure A8. Bottom of Tie Number 151

Figure A9. Inside of Boot of Tie Number 151

Figure A10. Pad of Tie Number 151

Figure A11. Bottom of Tie Number 152

Figure A12. Tie Number 151, Placed Back into Cavity and Not Fully Seated

Figure A13. Tie Number 151, Showing Gray Material Discharged from Tie Cavity

Figure A14. Tie Numbers 191, 192, and 193 Not Fully Seated

Appendix B.
Data from January 18, 2007, Test Report

IDBT Microcellular Pad Vertical Load Tests
[redacted]

[redacted]:

As requested and authorized by your January 11, 2007 email, [redacted] has conducted a vertical load-deflection test on one of the IDBT microcellular pads removed from the concrete slab test section in the TTC test track. The microcellular test pad was labeled Tie No. 151 - high rail, outside rail and it was removed from service on November 20, 2006 after approximately 200 MGT of service. Additionally, [redacted] was asked to determine the volume of two soil samples supplied with the test pad.

The pad vertical load-deflection test was conducted similar to pad tests conducted during the original laboratory tests prior to the test track construction. The 10-1/4 X 25-1/4 X 7/16 in. microcellular pad was loaded between two rigid steel plates. The load was applied in 1,000 lb increments to 50,000 lb. Pad deflection readings were taken at each load increment with one-ten thousand increment digital dial gages. The pad was preloaded twice prior to conducting the load-deflection test. As requested, results from this test were compared with the results from a pad test conducted by [redacted] during the original laboratory tests. Results of these tests are presented in attached Table 1 and Fig. 1.

Two samples of material removed from between the rubber boots and concrete ties No. 190 and 191 were measured to determine the total volume of the material removed. Tie No. 190 was 420 ml (25.64 $in.^3$) and Tie No. 191 was 310 ml (18.93 $in.^3$).

If you have any questions or need additional information, please call me.

Sincerely,

Load, kip	Deflection, in.	
	Original	200 MGT
0	0.0000	0.0000
5	0.0315	0.0326
10	0.0502	0.0570
15	0.0668	0.0807
20	0.0814	0.0973
25	0.0927	0.1086
30	0.1011	0.1165
35	0.1066	0.1221
40	0.1100	0.1261
45	0.1122	0.1292
50	0.1136	0.1322
0	0.0021	0.0011

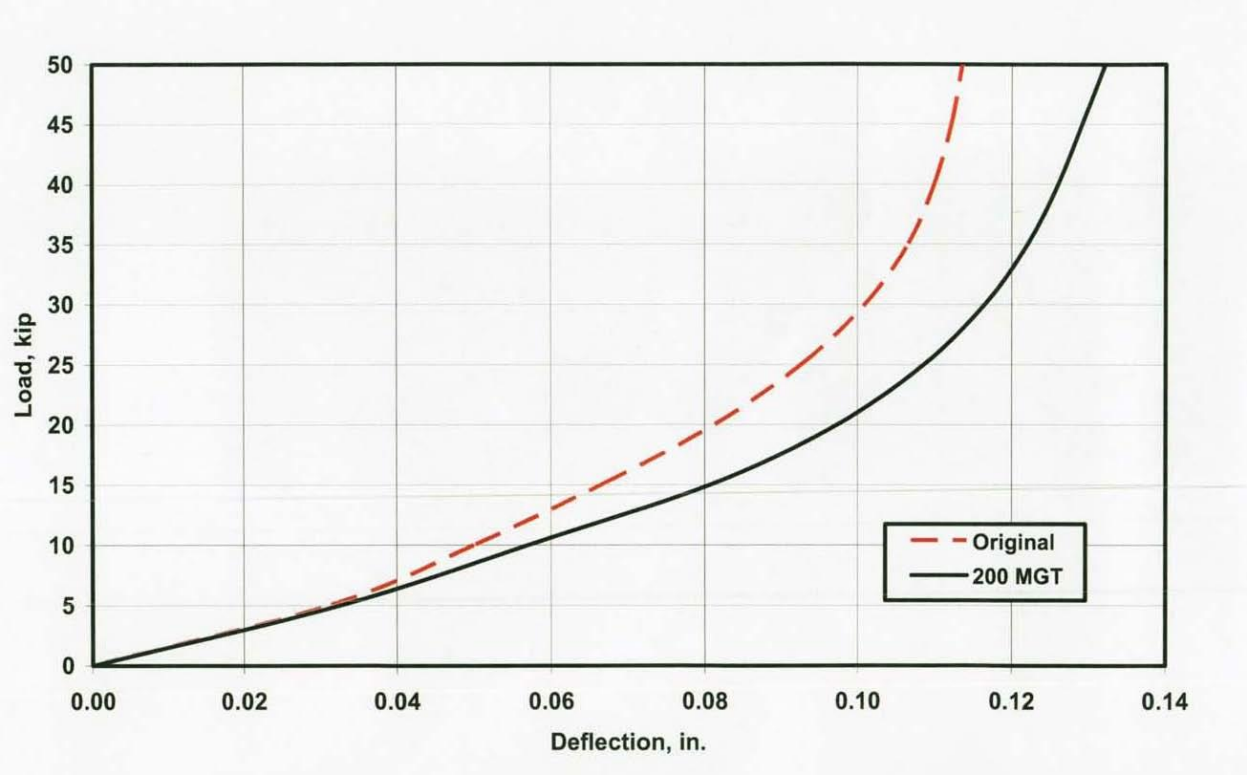

Abbreviations and Acronyms

AAR	Association of American Railroads
CCW	counterclockwise
CTL	Construction Technology Laboratories
CW	clockwise
CWR	continuous welded rail
DFST	direct fixation slab track
FAST	Facility for Accelerated Service Testing
FRA	Federal Railroad Administration
HAL	heavy axle load
HSR	high-speed rail
HTL	High Tonnage Loop
IDBT	independent dual block track
IWS	instrumented wheelsets
LVDT	linear variable differential transformer
MCO	midchord offset
MDD	multidepth deflectometers
MGT	million gross ton
PCA	Portland Cement Association
PSD	power spectrum density
ROW	right-of-way
TGMS	track geometry measurement system
TLV	track loading vehicle
TOR	top-of-rail
TTC	Transportation Technology Center
TTCI	Transportation Technology Center, Inc.